Title
The search for new regulators of remyelination after white matter stroke

Author
DiTullio, David Joseph

Publication Date
2017

Peer reviewed|Thesis/dissertation

UNIVERSITY OF CALIFORNIA

Los Angeles

The search for new regulators of remyelination after white matter stroke

A dissertation submitted in partial satisfaction of the requirements for the degree

Doctor of Philosophy in Neuroscience

by

David DiTullio

2017

ABSTRACT OF THE DISSERTATION

The search for new regulators of remyelination after white matter stroke

by

David DiTullio

Doctor of Philosophy in Neuroscience

University of California, Los Angeles, 2017

Professor Stanley Thomas Carmichael, Chair

White matter stroke comprises up to twenty-five percent of all diagnosed strokes, though up to ten times as many events go undiagnosed until accumulation leads to clinical sequelae such as vascular dementia and gait disturbances. White mater stroke leads to death of oligodendrocytes and demyelination of axons in the peri-infarct area, as well as persistent inflammation and astrogliosis. After injury, oligodendrocyte progenitor cells (OPCs) are unable to differentiate into myelinating oligodendrocytes, leaving axons chronically demyelinated. This pathology is distinct from other demyelinating diseases, but the underlying mechanism remains unknown.

This dissertation presents a series of studies that aim to elucidate genetic mechanisms of the observed OPC differentiation block, with the goal of uncovering regulators that can be manipulated to enhance OPC differentiation, and ultimately, remyelination, after injury. OPCs isolated from control as well as peri-infarct tissue at key time points after stroke are analyzed

using RNA-sequencing to generate an OPC stroke-specific transcriptome. This gene expression dataset is characterized using complementary bioinformatics metrics, and comparisons to previously described transcriptomes show it is specific to OPCs and to the post-stroke context. Using quantitative metrics, ten highly differentially expressed candidate genes are selected for study to identify regulators of OPC differentiation.

First, each candidate gene is overexpressed in primary OPC cultures, and quantitative PCR is used to assess differentiation. Several candidate genes show pro-differentiation effects, but three of the most significant regulators, *Chst10*, *C9orf9*, and *Csrp2*, are selected for study *in vivo*, in a mouse model of white matter stroke. Tissue studies demonstrate that both *Chst10* and *Csrp2* induce significant differentiation of OPCs in post-stroke as well as stroke-naïve tissue, suggesting that these genes are involved in pathways that respond to white matter stroke, but may be applicable in oligodendrocyte biology more broadly.

A final set of experiments returns to the OPC stroke transcriptome to explore ways to apply this knowledge of OPC differentiation regulators. Small molecule regulators identified through additional transcriptome analyses are found to promote OPC differentiation both *in vitro* and *in vivo*, underscoring the power of the combined bioinformatics and cell-level approaches taken in this study.

The dissertation of David DiTullio is approved.

Jean S. de Vellis

Baljit S. Khakh

Harley I. Kornblum

Carlos Portera-Cailliau

Stanley Thomas Carmichael, Committee Chair

University of California, Los Angeles

2017

For my parents, in eternal gratitude for their love and support.

Every day I marvel at how lucky I am.

TABLE OF CONTENTS

LIST OF FIGURES

LIST OF FIGURES
(cont.)

LIST OF TABLES

ACKNOWLEDGMENTS

This journey has been one of immense personal and professional growth, and I cannot begin to thank everyone who has contributed their guidance and support to make it possible. Nonetheless, I am compelled to recognize a few people in particular.

Tom has been an inspiration. From the beginning of my time in the lab, when his patience and determination to let me make and learn from my own mistakes; to today, when our scientific discussions always leave me with a broader, deeper perspective and excited to delve into new studies – he has exceeded anything I could have expected from a mentor. That he maintains his commitment to strong science, and more importantly, mentorship on all levels, is awe-inspiring. I hope to someday be able to reach such earnest success in whatever career path I end up pursuing.

None of this would be possible without the members of the Carmichael laboratory. Everyone, from post-bac to post-doc, has informed, guided, and questioned my research and made me a better scientist. I have to especially thank a few people: Esther patiently guided me through the first weeks of my rotation, when I had never worked with a mouse model before. Harriett's passion for science while still seeing the balance in life kept me grounded. Amy's constant support (and love of glia) is I'm sure appreciated by all in the lab, but certainly by me. Irene, Andrew, Catherine, and more have been friends as well as teachers in their own time. And Michal has been a wonderful colleague and friend whose love of teaching is a joy to see.

My thesis committee has guided me throughout this entire journey. To Dr. de Vellis, thank you for opening your lab to me early on as I learned about oligodendrocyte biology – and to Araceli, for your guidance and continued support. Dr. Kornblum, thank you for offering your ideas, but also always ending meetings asking about my future plans and other interests – this is something not all graduate students are fortunate enough to have. Dr. Khakh: your scientific mind is second to none; thank you for being a strong champion of glia at UCLA. And Carlos, thank you for your guidance throughout this process, but also for the tireless work you have put into the MSTP. Though your work is often done behind the scenes, seeing the program grow and flourish in so many ways since I've been here, I know you deserve many more thanks than you sometimes get. We are lucky to have you, and Leanne, at the helm.

I hope this dissertation will speak to the quality of scientific mentorship I have received. But it will not do justice to all of the friends who have guided me along the way. To the members of SRBPC, thank you for being the best friends I could imagine, and I am so glad to see so many of you even after you've begun your careers all across the country. To Preservation Society, thank you for opening my eyes to new perspectives and ideas, and for being my family in the dust and in adventures all across the world. And all the people I've met along the way: Ryan, Jen, Alex, Elaine, Leah: you have made every day better. Jaya, at this point you feel more like family. Lizzie, you have been a pillar of support for the past ten years and I look forward to the next ten and more.

Finally, my parents and family have done more to help me than I think I will ever know. I will continue to strive to make you proud.

CURRICULUM VITAE OF

DAVID DITULLIO

EDUCATION

2011 – present **DAVID GEFFEN SCHOOL OF MEDICINE AT UCLA** Los Angeles, CA
M.D., Ph.D. Anticipated 2020
- Ph.D. Research Advisor: S. Thomas Carmichael, M.D., Ph.D.
  "Molecular Mechanisms of Remyelination and Repair after White Matter Stroke"

2007 – 2011 **POMONA COLLEGE** Claremont, CA
B.A., Molecular Biology, Mathematics, magna cum laude
- Molecular Biology Thesis Advisor: Lenny Seligman, Ph.D.
  "Biochemical characterization of two novel homing endonucleases"
- Mathematics Thesis Advisor: Ami Radunskaya, Ph.D.
  "Classification of embryonic spinal neurons using wavelet analysis"

RESEARCH

2013 – present **NEUROSCIENCE PH.D. THESIS RESEARCH** Los Angeles, CA
Advisor: S. Thomas Carmichael, M.D., Ph.D.
- Identify and characterize novel genes that promote oligodendrocyte differentiation and remyelination after white matter stroke

2013 **MEDICAL EDUCATION RESEARCH** Los Angeles, CA
Advisor: Lee T. Miller, M.D.
- Develop and assess new education and peer tutoring initiatives to support medical students throughout the four-year curriculum

Summer 2011 **RESEARCH ROTATION** Los Angeles, CA
Advisor: X. William Yang, M.D., Ph.D.
- Examine the relationship between damage to glial cells and impact on neurodegeneration in Huntington's Disease using a mouse model

2008 – 2011 **MOLECULAR BIOLOGY UNDERGRADUATE THESIS RESEARCH** Claremont, CA
Advisor: Lenny M. Seligman, Ph.D.
- Biochemical characterization of two novel homing endonucleases

2010 – 2011 **MATHEMATICS UNDERGRADUATE THESIS RESEARCH** Claremont, CA
Advisor: Ami Radunskaya, Ph.D.
- Classification of embryonic spinal neurons using wavelet analysis"

TEACHING EXPERIENCE

2014 – present **HEAD TUTOR, DGSOM PEER TUTORING PROGRAM** Los Angeles, CA
Contact: Sue Nahm
- Work closely with the Learning Skills Office to coordinate the peer tutoring program

Winter 2014 **COURSE CO-INSTRUCTOR, NEUROSCIENTIFIC METHODS** Los Angeles, CA
Contact: Anne M. Andrews, Ph.D.
- Co-led a student-taught course on neuroscience methods taken by all incoming neuroscience graduate students as part of the teaching requirement for the Neuroscience Graduate Program

PUBLICATIONS

- Sozmen EG, Rosenzweig S, Llorente IL, **DiTullio DJ**, Machnicki M, Vinters HV, Giger RJ, Hinman JD, Carmichael ST. Nogo receptor blockade overcomes remyelination failure after white matter stroke and stimulates functional recovery in mice. *Proc Nat Acad Sci*. 2016: epub ahead of print. DOI 10.1073/pnas.1615322113.

PRESENTATIONS

- **DiTullio DJ**, Carmichael ST. The search for new regulators of remyelination after white matter stroke. International Stroke Conference; February 2017; Houston, TX.
- **DiTullio DJ**, Carmichael ST. A stroke-specific oligodendrocyte progenitor cell transcriptome reveals novel genes impacting recovery after white matter stroke. American Heart Association-Bugher Foundation Member Meeting; October 2016; Miami, FL.

SELECTED POSTERS

- **DiTullio DJ**, Sozmen EG, Carmichael ST. A stroke-specific oligodendrocyte progenitor cell transcriptome reveals *Csrp2* as a novel regulator of OPC differentiation. Neurology Science Day; April 2017; UCLA, Los Angeles, CA. *Awarded 1st place graduate student prize.*
- **DiTullio DJ**, Sozmen EG, Carmichael ST. A stroke-specific oligodendrocyte progenitor cell transcriptome reveals *Csrp2* as a novel regulator of OPC differentiation. Glial Biology: Functional Interactions Among Glia & Neurons (Gordon Research Conference); March 2017; Ventura, CA.
- **DiTullio DJ**, Sozmen EG, Carmichael ST. A stroke-specific oligodendrocyte progenitor cell transcriptome reveals novel genes impacting recovery after white matter stroke. Society for Neuroscience Annual Conference; November 2016; San Diego, CA.
- **DiTullio DJ**, Sozmen EG, Carmichael ST. A stroke-specific oligodendrocyte progenitor cell transcriptome reveals novel genes impacting recovery after white matter stroke. Poster presented at: Glia in Health and Disease; July 2016; Cold Spring Harbor Laboratory, NY.
- **DiTullio DJ**, Sozmen EG, Carmichael ST. An oligodendrocyte progenitor cell transcriptome specific to white matter stroke reveals unique gene expression patterns. Poster presented at: 9th Annual SoCal Symposium on Glial-Neuronal Interactions in Health and Disease; January 2016; Riverside, CA.

SELECTED LEADERSHIP EXPERIENCES

2017 – present	**Coordinating Committee on Graduate Affairs**	Oakland, CA
2016 – present	**UC Student Health Insurance Program Executive Oversight Board**	Oakland, CA
2016 – present	**Graduate Council**	Los Angeles, CA

SELECTED HONORS

2017	**Brain Research Institute Knaub Fellowship in Multiple Sclerosis Research**	
2015 – present	**ARCS Foundation Scholar**	
2015 – 2016	**American Heart Association WSA Predoctoral Fellowship**	(15PRE22580000)
2011	**Phi Beta Kappa**, Pomona College Chapter	
2011	**Michael H. Rosen Memorial Premedical Award**	

Chapter 1

Introduction

1.1 Stroke: a major health challenge

In an age of rapid advances in health sciences research and innovation, stroke remains a major medical challenge. It is the second leading cause of death worldwide, accounting for 11% of all deaths globally in 2015 (World Health Organization, 2017a, 2017b). In the United States, the annual incidence of strokes is 795,000, meaning that on average, someone has a stroke every 40 seconds (Benjamin et al., 2017). Thus, stroke is a pervasive and serious disease. Complicating this issue beyond its simple mortality statistics, however, are the major challenges and costs associated with stroke survival. Multiple reports point to a gradual but steady decrease in death rates worldwide, as imaging techniques and education regarding early signs improve (Carandang et al., 2006; Ovbiagele et al., 2011). Evidence suggests that this trend will continue over the coming decades as well: one study estimates that stroke incidence will increase more than twofold by 2050, while survival increases in most groups (Howard & Goff, 2012). With increased survival comes an increasing need to support patients in recovery: rehabilitation strategies are limited, and the toll of living with sensorimotor and cognitive deficits secondary to chronic injury can be both functionally and emotionally devastating (Carod-Artal & Egido, 2009). Furthermore, although there is a wealth of research into rehabilitation strategies effective in stroke, recovery is often incomplete, and complementary interventions targeting post-stroke biology that enhance efficacy of current strategies would greatly improve patient well-being (Dobkin, 2005; Langhorne et al., 2011). Finally, the impact of these trends extends beyond the toll it takes on patients and their families: cost of stroke treatment from 2005 to 2050 is estimated to exceed $2.2 trillion, with over 80% of these costs due to post-hospitalization care,

rehabilitation, and lost earnings (Brown et al., 2006). To this end, research into the pathophysiology of stroke is of paramount importance. By understanding the specific mechanisms underlying injury after stroke, through both acute and chronic phases, we can then identify interventions to minimize negative consequences, as well as enhance and expedite recovery. New discoveries in this area have the potential not only to reduce mortality, but also to give survivors back control over their lives.

This dissertation attempts to answer this challenge in one of the most understudied but pervasive subtypes of stroke: white matter stroke. Ischemia in the white matter is an especially exciting area of neuroscientific research due to its unique and complex biology, which integrates responses between well-known neurons and their lesser-known neighbors: the oligodendrocytes. This project takes a systems-to-cells approach to explore oligodendrocyte biology, with a specific eye towards stroke pathology. Its foundation is a novel toolkit: a transcriptomic dataset describing oligodendrocyte progenitor gene expression following white matter stroke. Bioinformatics analysis identifies a highly promising subset of differentially expressed genes upon which *in vitro* screening techniques are focused to explore novel pathways in oligodendrocyte differentiation. From this screen, three particularly promising genes are extracted for detailed *in vivo* study. The remainder of the dissertation explores these *in vivo* studies, with a particular focus on how findings using an animal model of injury can both enhance our understanding of oligodendrocyte biology generally, as well as identify promising new treatment targets, and specific pharmacologic interventions, that have the potential to augment the clinician's toolkit in the fight against this serious and widespread disease.

1.2 White matter ischemia is a pervasive stroke subtype

As with many diseases, "stroke" is a fairly broad term that encompasses a host of different pathologies sharing central characteristics. The most common of these is ischemic stroke, which arises from an interruption in blood flow to a brain region and comprises 85% of diagnosed strokes (Moskowitz et al., 2010). Intracerebral hemorrhage induces stroke via mechanical disruption of brain architecture and makes up much of the remaining diagnoses (Barratt et al., 2014; Qureshi et al., 2009). Finally, stroke can also arise secondary to other severe systemic conditions, such as cardiac arrest (Moskowitz et al., 2010). Thus, even at the highest level, stroke involves a constellation of mechanisms, each with its own research challenges.

Divisions between stroke subtypes continue beyond the ischemic/hemorrhagic categorization; specifically, the brain region in which stroke occurs can have a marked effect on symptomatology, severity, and cellular mechanism of injury (Bamford et al., 1991; Sacco et al., 2013). To this end, one particularly understudied category of ischemic injury is white matter stroke (WMS). These arise subsequent to interruptions in blood flow to the small penetrating arterioles that supply subcortical structures of the brain, and, in particular, axonal tracts that are highly structured but poorly perfused (Prins & Scheltens, 2015). Prevalence of WMS is high: it is estimated to comprise at least 15-25% of all stroke diagnoses (Bamford et al., 1991; Schneider et al., 2004). This figure almost certainly underestimates the pervasiveness of WMS, however, as one study notes presence of white matter lesions in 70% of participants aged 50-75 (Schmidt et al., 2003). Furthermore, its clinical presentation is variable, and in many cases, white matter injury is detected well into the chronic phase of the disease, as small infarcts build up in sequence until a threshold of clinical symptoms develops (Wright et al., 2008). Thus, treatment

of WMS by its nature requires attention to the post-acute and chronic phases of injury, with an eye towards enhancing recovery and rehabilitative mechanisms.

Challenges in clinical treatment of white matter stroke

Although WMS often progresses subclinically, it is a debilitating disease and can lead to serious sequelae. First, even undetected white matter lesions are associated with significant cognitive impairment, accounting for what patients and their families may brush off as "normal aging" (Wright et al., 2008). WMS can also impair motor function and has been associated with increased risk of falls due to gait impairment (Chui, 2007; Srikanth et al., 2009). More serious effects of WMS can arise with aggregation of multiple lesions; this underlies the pathology of vascular dementia, the second-leading cause of dementia after Alzheimer's disease (Prins & Scheltens, 2015; Schmidt et al., 2003). **Figure 1-1** demonstrates the pathology of WMS in patients and the wide spectrum of injury seen across patients.

A survey of the clinical understanding of white matter stroke, as summarized above, indeed demonstrates the serious impact of this disease on health, particularly in elderly populations. Unfortunately, it also highlights distinct gaps in our knowledge of this disease. For example, in some cases, white matter lesions accumulate in a predictable, progressive fashion; in others, lesions are apparently benign and remain silent throughout life. The use of magnetic resonance imaging (MRI) has greatly improved detection rates of white matter injury, but the correlation between imaging results and clinical effects is imperfect (Grueter & Schulz, 2012; Longstreth et al., 1996; Manolio et al., 1994; Schmidt et al., 2003). As a result, it is difficult to offer patients specific interventions before symptoms present, because we lack the tools to determine who will most benefit.

A final challenge in the clinical practice of stroke treatment, particularly white matter stroke, is a severe lack of tools. Tissue plasminogen activator (tPA) is the only approved pharmacologic intervention for acute ischemic stroke but is used only within the first 4.5 hours after stroke onset, including travel time to the hospital (Prabhakaran et al., 2015; Saver et al., 2013). White matter stroke, due to its insidious nature, is not typically treated in the acute stage. No pharmacologic interventions are available for subacute or chronic phases of injury (Teasell et al., 2013).

Successes in stroke rehabilitation

It is well known, however, that the brain possesses the capacity for repair, even after serious injuries. Neuroplasticity in the context of stroke has been identified as a major mechanism of recovery and is enhanced by therapeutic intervention (Teasell et al., 2013). One of the most impressive examples of this phenomenon is the advent of constraint-induced movement therapy, in which the stroke-unaffected limb is restrained to force use of the affected side (Kunkel et al., 1999; Liepert et al., 2000). Because of its efficacy, it is no surprise that constraint-induced therapy has been carefully refined to maximize benefit, and it is now one of the mainstays of stroke rehabilitation (Uswatte et al., 2005). Importantly, research into the biological basis of this recovery suggest that there is a close interplay between behavioral intervention and cell-level mechanisms of repair (Nie, 2016). In short, recovery in the subacute and chronic phases of injury is made possible by specific gene expression changes, along with cellular growth and differentiation on a region- and circuit-specific level.

This interplay between biology and rehabilitative therapy is especially promising when considering white matter stroke. Because this disease is in large part a chronic condition, with

symptoms slowly building up over time, interventions must be efficacious even well after the initial ischemic insult. Thus, identifying endogenous repair mechanisms that already exist and using biological treatment to enhance these pathways offers patients with WMS the best hope for successful therapy. Research into the basic biology of WMS must thus focus on two major areas: first, what repair mechanisms exist to repair damage at different phases post-ischemia; and second, what features of disease are preventing the brain from undergoing full recovery.

As will be discussed below, research into white matter stroke is, even now, at relatively early stages. The basic pathology has been described as death of myelinating oligodendrocytes and subsequent inflammation (Sozmen et al., 2012). However, the specific challenges of repair in the context of WMS are only just now coming to light, and much remains to be discovered. Regardless, any discussion of white matter injury must first begin with an understanding of the development and function of a fascinating glial cell type: the oligodendrocyte.

1.3 Oligodendrocytes in the white matter

The concept of neuroglia was first presented to the neuroscience community over 150 years ago, by Rudolf Virchow at a lecture in Berlin (Kettenmann & Verkhratsky, 2008). At that time, the term referred to neuroglia as an element totally distinct from any "nervous" function, instead identifying them as providing structure to the brain. Over the next several decades, neuroscience slowly began to understand the diversity of glial cells present in the brain, beginning with the astrocyte and its regionally-defined protoplasmic and fibrous populations. It was not until 1919 and the work of Pío del Río-Hortega, a colleague of Pedro Ramón y Cajal, that the oligodendrocyte was identified (Pérez-Cerdá et al., 2015). His work provided the first

insight into how oligodendrocytes function in the white matter milieu, integrated with neurons, but also astrocytes, microglia, and vasculature (**Figure 1-2**).

Early understanding of oligodendrocytes centered on their role as myelinating cells of the central nervous system, as seen in del Río-Hortega's drawings, and indeed, they were long thought to serve this purpose almost exclusively (Pfeiffer et al., 1993). As a result, much of the research into oligodendrocyte biology in the twentieth century focused on developmental pathways surrounding myelin formation (Baumann & Pham-Dinh, 2001). Our understanding of these cells has since expanded considerably, and it is clear that oligodendrocytes do a great deal within the brain beyond producing myelin. Nonetheless, this is undoubtedly one of their most important roles and is important to understand in some detail.

Development of oligodendrocytes as myelin-producing cells

Oligodendrocytes are initially generated from neuroepithelial sources during neural tube formation, and arise in multiple waves from different regions along the developing nervous system (Kessaris et al., 2006; Zuchero & Barres, 2013). The committed progenitor population, the oligodendrocyte progenitor cell (OPC), is self-renewing and resident throughout the brain, comprising approximately 5% of all cells (Dawson et al., 2003). The classic view is that OPC differentiation is induced primarily by transcription factors Olig1 and Olig2 (Meijer et al., 2012). How this switch from progenitor to committed state occurs is complicated. Experiments *in vitro* identified a number of signals that induce the differentiation pathway, including transforming growth factor β (TGF-β), triiodothyronine (T_3) (Baumann & Pham-Dinh, 2001). However, the differentiation process *in vivo* is more complicated and likely involves a combination of

paracrine signaling (both cytokines and growth factors), epigenetic changes, and responses to neuronal activity (Zuchero & Barres, 2013).

Upon initiating the differentiation process, OPCs proceed through a series of intermediate stages, which have been defined by gene expression profiles. Markers characteristic of each stage are summarized in **Figure 1-3**, and are helpful to facilitate study of this process in the laboratory setting (Espinosa-Jeffrey et al., 2009; Nishiyama et al., 2009). In general, OPCs are, at their earliest stages, small, bipolar cells approximately 20 μm in diameter (Dumas et al., 2015). Receipt of differentiation signals induces changes that include increased cell process number and cell size, though expression characteristic of OPCs; these cells are often referred to as new oligodendrocytes (new OLs) or immature OLs (Nishiyama et al., 2009). Expression of the proteoglycan NG2 disappears, while PDGFRα expression is maintained (Espinosa-Jeffrey et al., 2009). Of note, the surface marker O4 appears in this stage (Espinosa-Jeffrey et al., 2009).

Further differentiation to the mature OL stage brings the expression of myelin basic protein (MBP) and dramatic increases in the cell size and number and complexity of processes. Cells at this stage can be 100 μm or more in diameter (Bakiri et al., 2011; Michalski & Kothary, 2015). In addition to expression of MBP, cells also express mature markers including CC1, GSTπ, and O1 (Mei et al., 2016; Nishiyama et al., 2009). From this stage, further signaling pathways induce oligodendrocyte process extension towards axons and myelination, leading to the myelinating OL stage of development. Cell morphology changes as processes extend myelin wrapping around axons in a stereotyped fashion, generally aligning in parallel processes especially in the white matter. A single myelinating OL can interact with fifty or more axons, with each process covering a length of 200 μm, suggesting a potential role for oligodendrocytes in co-regulating networks of axons (Simons & Nave, 2016). Thus, as described above, a great

deal of research has focused on characterizing the oligodendrocyte differentiation pathway from progenitor to myelin-producing cell integrated into an axonal network. It is important to note, however, that while stages have been described here as distinct and are often treated as such in the literature, cells almost certainly proceed along a continuous spectrum of differentiation.

There is a clear pathway from OPC to myelinating oligodendrocyte, and ample research demonstrates the importance of this pathway in development (Tripathi et al., 2011; Zuchero & Barres, 2013). OPCs also generate oligodendrocytes in the adult brain, as part of the normal process of cell turnover. Recent work has used carbon dating in human tissue, combined with modeling, to show that white matter oligodendrocyte turnover is approximately 0.33% annually, or one of every 300 oligodendrocytes (Bercury & Macklin, 2015; Yeung et al., 2014). This is both much slower than the myelin turnover rate, highlighting the dynamism of oligodendrocytes; and of oligodendrocytes in the cortex, which have a turnover rate of 2.5%. This suggests region-specific behavior, but also highlights that mechanisms for oligodendrocyte replacement are established parts of normal physiology.

Myelination of axons by oligodendrocytes

While the process of oligodendrocyte differentiation has been characterized over decades, the actual process by which axons are myelinated, and the signals that indicate to oligodendrocytes which axons to myelinate and to what degree, have only recently begun to be elucidated. OPCs possess synapses, allowing them to directly sense neuronal activity (Bergles et al., 2000). Optogenetic experiments have since directly tested this hypothesis and shown that increased neuronal activity induces both oligodendrocyte differentiation and myelination, confirming that oligodendrocytes participate in signaling pathways and can play a role in

network plasticity (Gibson et al., 2014). Axons can release additional signals specific to oligodendrocytes, as well, providing additional control over selective myelination, and additional features like axon size may play a role (Simons & Lyons, 2013). Nonetheless, the exact mechanisms by which oligodendrocytes identify which axons to myelinate, and conversely, what systems prevent myelination of others, remain mysterious.

Just as new insights are being made into neuron-oligodendrocyte interactions in the decision to myelinate, new work by Brad Zuchero and Ben Barres has elucidated the physical mechanism of myelination (Zuchero et al., 2015). They report that actin assembly promotes initial oligodendrocyte-axon interaction, while wrapping of the axon relies on actin disassembly. Actin in oligodendrocytes is also important for assembling key protein complexes that regulate the formation of nodes of Ranvier (Brivio et al., 2017). Taken together, this research makes clear the diversity of proteins and genes important for oligodendrocyte function. In addition to the classically-studied myelin genes, systems and structures from the nucleus to the cytoskeleton play key roles in oligodendrocyte differentiation and function.

Non-myelinating functions of the oligodendrocyte lineage

Oligodendrocytes have been suspected to function as more than just myelinating cells since the 1980s, when culture experiments suggested that OPCs could differentiate into astrocytes or oligodendrocytes depending on culture conditions, suggesting that OPCs existed for reasons beyond producing new myelin-making cells (Barres et al., 1990; Raff et al., 1983). Although these specific results were not recapitulated *in vivo* for many years, it opened the door to the perspective that oligodendrocytes may have additional functions in the brain, both at the progenitor stage and upon differentiation (L. Zhang et al., 2016). As it stands now, the field is

actively working to expand our understanding of these additional functions, and much will surely be presented in the coming years. Already, however, recent research suggests important additional roles of these cells that contribute to normal physiology and, importantly, could contribute to pathology.

Oligodendrocytes themselves are poised to play an important role in axonal support due to their close physical relationship to the axons themselves. NMDA receptors present on oligodendrocytes, in addition to being a pro-myelination signal, continue to facilitate neuron-oligodendrocyte signaling once myelination is complete. Glutamatergic signaling via these receptors induces glucose transporter 1 (GLUT1) translocation to the oligodendrocyte membrane, increasing glucose uptake and subsequent release of glycolysis products to the axon, providing long-term reliable metabolic support (Saab et al., 2016). Furthermore, electrophysiology experiments suggest that oligodendrocytes have electrical activity, and that their depolarization directly affects latency of action potential in nearby neurons (Fields, 2008). Both the metabolic and electrical properties of oligodendrocytes are areas of active research in the field, and these initial findings suggest that there is more to be discovered about the role of oligodendrocytes within the brain.

Perhaps the most exciting debate in the oligodendrocyte field currently focuses on the OPC. Thought to exist as a progenitor, resident in the brain to replenish oligodendrocytes when needed, researchers began to question the utility of 5% of the brain's cells serving such a quiescent purpose. Indeed, it appears that cells previously grouped into the category of OPCs are likely a diverse cluster of cells serving many roles in the brain. OPCs, generally defined as $PDGFR\alpha^{+}$ $NG2^{+}$ cells, were initially treated purely as progenitor cells, but given their abundant

functions beyond this, they are starting to earn a place as a distinct glial cell type[1] (Hill & Nishiyama, 2014).

In addition to forming synapses with neurons, as described above, OPCs express a variety of membrane ion channels that, like oligodendrocytes, confer unique electrophysiological properties (Hill & Nishiyama, 2014). In particular, OPCs express AMPA receptors, which respond to activity from nearby neurons in a way similar to classical long-term potentiation (Ge et al., 2006). This leads to long-term changes in calcium permeability in the cell. Though the downstream effects of this are still not understood, it may relate to differentiation signaling and/or communication with neurons (Hoffmann et al., 2010). Another feature suggesting OPCs play unique roles in the brain is that many OPCs never differentiate into oligodendrocytes at all, suggesting that such a large number of cells would not be necessary for their differentiation capacity alone.

Finally, there has recently been work to revisit the early culture experiments of OPCs, in which alterations to culture medium (namely, an increase in serum concentration) induced differentiation of cells into astrocytes rather than oligodendrocytes. This multipotency was not observed *in vivo*, though true fate mapping of cells was difficult due to the transient nature of receptor expression and limited technologies by which to trace cell fate (Nishiyama et al., 2009). However, application of bacterial artificial chromosome (BAC) genetic manipulation enabled researchers to trace $NG2^+$ cells during development. In this process, researchers identified a small population of $NG2^+$ OPCs that differentiated into protoplasmic gray matter astrocytes, sometimes comprising 40% of the astrocytes in the area (Hill & Nishiyama, 2014; Zhu et al., 2007). Research by Q. Richard Lu's lab has shown that histone modification can induce

[1] For clarity, these $PDGFR\alpha^+$ $NG2^+$ cells will continue to be referred to as oligodendrocyte progenitor cells (OPCs), consistent with the majority of the relevant literature on this topic.

astrocyte differentiation of OPCs, providing a potential mechanism for this phenomenon (L. Zhang et al., 2016). It is worth noting that astrocyte differentiation of OPCs has not been seen in normal physiology outside of early developmental stages, and even in development, only protoplasmic astrocytes were derived, while all white matter-localized OPCs appeared to differentiate into oligodendrocytes (Zhu et al., 2007). Still, this suggests that cellular mechanisms for this switch exist within OPCs, again showing that these cells play many roles within the brain, many of which have yet to be identified.

1.4 Oligodendrocytes in disease

Much is known about the development of oligodendrocytes and their function in normal physiology. Not surprisingly, they also play central roles in disease, particularly those involving significant white matter pathology (**Table 1-1**). In each case, oligodendrocyte loss leads to demyelination of axons, which directly impairs saltatory conduction and thus communication between brain regions (Crawford, Mangiardi, & Tiwari-Woodruff, 2009). Pathology extends beyond impaired conduction of demyelinated axons, however, as axons that remain chronically demyelinated can degenerate, leading to permanent neuronal loss (Crawford, Mangiardi, Xia, et al., 2009; Nave, 2010). Additionally, in most cases, injury to the white matter leads to inflammation. This involves CNS-native cells such as microglia and astrocytes, but also macrophages that infiltrate following transient disruption of the blood-brain barrier (BBB) (Popescu & Lucchinetti, 2012; Ransohoff, 2012). How oligodendrocytes, and the white matter as a whole, respond to injury thus depends on the degree and duration of injury, as well as associated secondary effects.

Multiple sclerosis as a model of demyelination

Although many diseases involve sustained demyelination as a primary pathology, much of the research in this area has focused on multiple sclerosis (MS) as a model (Deshmukh et al., 2013; Ransohoff, 2012). MS is a chronic disease that is at the core autoinflammatory, similar to rheumatoid arthritis, in which T cells become autoreactive against antigens specific to myelinated axons; this could be myelin proteins or other proteins in the axon-oligodendrocyte network (Gold & Wolinsky, 2011) (**Figure 1-4**). These activated immune cells then cross the BBB via expression of inflammatory markers that permit passage through the vasculature and into the CNS. There, the abundance of myelin proteins activates an immune response, and myelin is attacked and broken down, releasing even more antigen that exacerbates the response. Thus, inflammation is a key feature of MS; however, it should be noted that mechanism is such that a specific subset of immune cells, Th17 cells, are primary drivers of this. This makes the core mechanism different from ischemic injury like WMS, where necrosis and subsequent release of cellular contents drives an immune response (Sozmen et al., 2012).

There are two main animal models of MS, each of which targets a different pathologic mechanism to assess disease (Ransohoff, 2012). First, cuprizone, a copper chelator, can be given to rodents with food for a period of weeks to induce mitochondrial defects selectively in oligodendrocytes, leading to apoptosis and thus demyelination. After cuprizone is removed, myelination recovers, making this method effective to study remyelination typical of relapsing-remitting MS. On the other hand, experimental autoimmune encephalomyelitis (EAE) is a model based on the immune response and subsequent inflammation seen in MS. Here, a preparation of proteins from the CNS is injected peripherally to induce immune activation, leading to pathology

that has shown to be similar to MS, and has actually led directly to the approval of a new treatment for the disease (Polman et al., 2006; Yednock et al., 1992).

Models of white matter stroke

Despite the wealth of research into MS, there are few similar studies looking at the pathology of WMS. What is known is that the underlying pathology of WMS is unique, and not accurately modeled by the same systems as outlined above (Souza-Rodrigues et al., 2008; Tanaka et al., 2008). In WMS, the primary pathology is ischemia, which leads to necrosis of oligodendrocytes, but can also affect other cell types. As with other stroke types, there are also multiple zones of injury, as in most stroke injuries: the center of ischemia is termed the infarct core, in which there is total destruction of axons and glia alike (Sozmen et al., 2009). The peri-infarct region is generally defined as 200-300 μm from the stroke border, and has disordered axonal architecture as well as significant demyelination (Hinman et al., 2013; Sozmen et al., 2009). Furthermore, such changes have been correlated to human MRI findings of white matter hyperintensities and then to post-mortem tissue, suggesting that these pathological studies of ischemia in animal models accurately depicts the condition in humans (Hinman et al., 2015; Jones et al., 1999).

Given its unique pathology, it is clear that specific models for white matter stroke are needed to study the pathophysiology and interrogate novel treatments for this disease. In fact, a handful of such models have been developed, broadly classified as either mechanical vascular occlusion (generally the common carotid), or of direct stereotactic injection of a vasoconstrictor (Sozmen et al., 2012). Both have utility, but in general, the stereotactic injection model more closely models the type of age-related white matter stroke seen in elderly patients (Rosenzweig

& Carmichael, 2013; Sozmen et al., 2009). The development of such models has expanded the potential for careful study of pathophysiology of WMS using genetically tractable animal models such as the mouse.

Oligodendrocyte differentiation in stroke

In most MS models, the principle demyelination injury is followed by OPC proliferation and subsequent differentiation of oligodendrocytes and remyelination of axons, which matches the pathology seen in relapsing-remitting MS (Deshmukh et al., 2013). This has recently been identified as a key difference between MS and WMS: in the latter, OPCs proliferate, but differentiation into mature oligodendrocytes is significantly inhibited, leading to sustained demyelination (Sozmen et al., 2016). One interesting mechanism that may account for this is that a subset of OPCs seem to differentiate into astrocytes in the context of WMS, recapitulating a behavior previously seen only in development or in cell culture experiments (Sozmen et al., 2016; Zhu et al., 2007). In other words, WMS displays a unique pathophysiology as compared to other demyelinating diseases.

Given the central role oligodendrocytes play in both MS and white matter stroke, and the key differences in their response, it follows that identifying novel factors that affect OPC differentiation would be a central question in the field. Finding pathways specific to oligodendrocyte differentiation in pathology is especially enticing as it would open the door to therapeutic targets that minimize unwanted side effects. Indeed, a wide number of pathways have been identified as playing a role in oligodendrocyte differentiation, and new ones are reported regularly. **Figure 1-5** shows a selection of these factors, along with key pieces of their associated

pathways (Back et al., 2005; Patel et al., 2010; Sloane et al., 2010; Sozmen et al., 2016; Ueno et al., 2012; Yu et al., 2013; Yuen et al., 2013; Ziabreva et al., 2010).

At the same time, although the cast of characters involved in this process has greatly expanded, two main gaps in our understanding of the disease remain. First, with so many pathways identified, there is a lack of a unifying model or understanding of oligodendrocytes in disease that makes sense of the multitude of contributing factors. Second, this research has not as of yet led to the development of clinically relevant therapeutics that can alleviate disease in patients. There is reason to be hopeful, however: with the advent of modern bioinformatics, analysis of groups of genes and pathways is now possible. Characterization of gene expression in other stroke subtypes has been described and led to promising therapeutic targets (Li et al., 2010, 2015; Zamanian et al., 2012). RNA-sequencing of multiple glial cell types has also been reported, providing foundational datasets on which to compare disease-specific gene profiles (Y. Zhang et al., 2014).

1.5 Summary and motivation for the dissertation

In summary, a basic pathologic picture of white matter stroke has emerged in recent years. Ischemia in axon-rich white matter leads to death of oligodendrocytes and destruction of axons in the stroke core (Rosenzweig & Carmichael, 2013; Sozmen et al., 2016). In the peri-infarct region, axon fibers are intact, though they are demyelinated and lack proper nodal architecture and function as a result (Hinman et al., 2015; Sozmen et al., 2016). The injury response involves accumulation of microglia and then astrocytes, adding inflammation to the post-stroke milieu (Rosenzweig & Carmichael, 2013). Over the following days, as the injury enters the post-acute period, OPCs proliferate at the site of injury, but fail to differentiate or

replenish the cells lost in the initial injury (Sozmen et al., 2016). The result is sustained demyelination. Accumulation of these injuries has behavioral consequences and, in humans, can accumulate undetected for years until such conditions as vascular dementia develop (Rosenzweig & Carmichael, 2013; Wright et al., 2008).

At the same time, abundant research in the field has uncovered dozens of novel regulators and pathways involved in OPC differentiation, but it remains challenging to put together a complete picture of OPC behavior, particularly in pathology and especially in WMS. This dissertation builds upon the most promising tools available to address this challenge: transcriptomic analysis of OPCs specific to stroke provides an unbiased approach to identifying regulators of oligodendrocyte differentiation in WMS. The goal is to increase our understanding of these crucial cells within the stroke context through a combination of bioinformatics analysis, *in vitro* screens, and *in vivo* manipulation. This is the first such dataset available for this disease, and it attempts to expand our understanding of oligodendrocyte differentiation in general by bringing promising results forward to treatment as well as back to understand the biochemical processes underlying any positive effects.

1.6 Figures

Figure 1-1

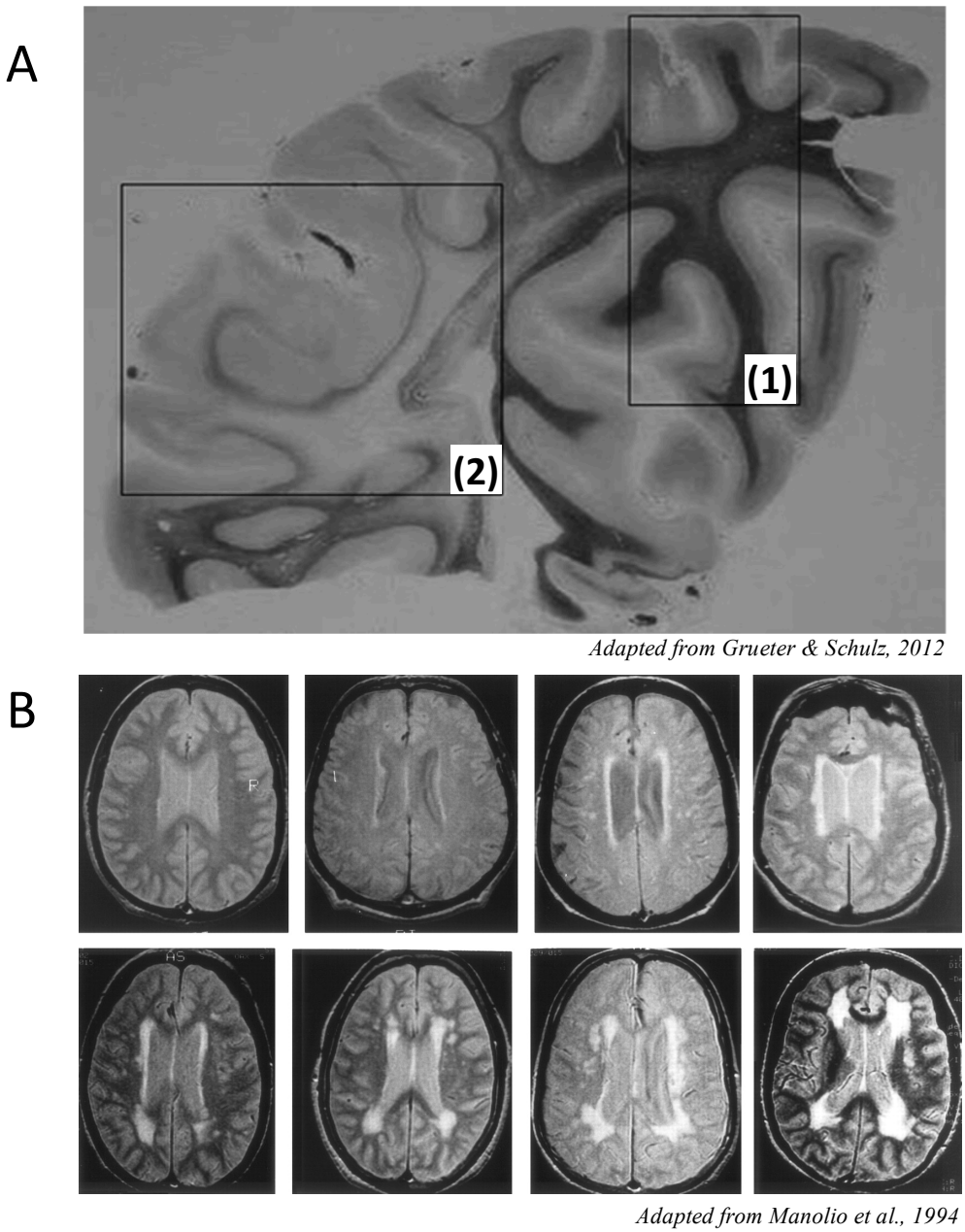

Adapted from Grueter & Schulz, 2012

Adapted from Manolio et al., 1994

Figure 1-1. Pathology of white matter stroke
(A) Coronal human brain stained with luxol fast blue, in which myelin appears dark. Area (1) shows an area of normal myelination, while multiple white matter (lacunar) infarcts have left white matter in area (2) nearly devoid of myelin. In contrast, grey matter is normal. **(B)** Proton density-weighted magnetic resonance imaging (MRI) scans suppress fat signal and highlight white matter injury via hyperintensity. This series demonstrates progressively worsening white matter disease in patients 65 years and older, from grade 1 (top left; barely detectable) to grade 8 (bottom right; confluent damage).

Figure 1-2

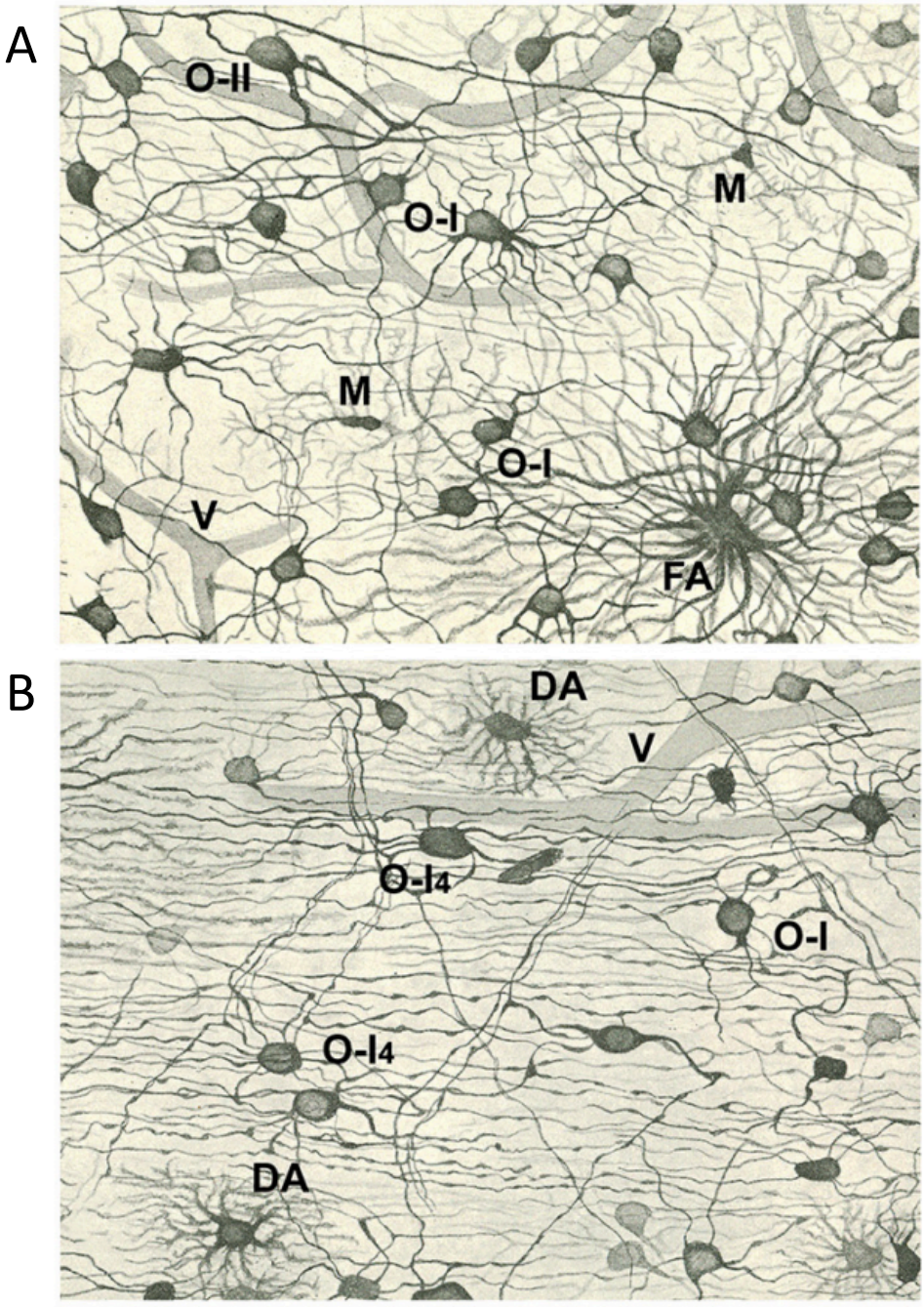

Adapted from Perez-Cerda et al, 2012

Figure 1-2. Early drawings of oligodendrocytes
Drawings by Pío del Río-Hortega show oligodendrocytes in the white matter milieu. **(A)** oligodendrocytes (O) shown in context vessels (V), microglia (M), and fibrous astrocytes (FA). **(B)** Oligodendrocytes arranged along axon tracts, which proceed along the horizontal axis. DA, dwarf astrocyte.

Figure 1-3

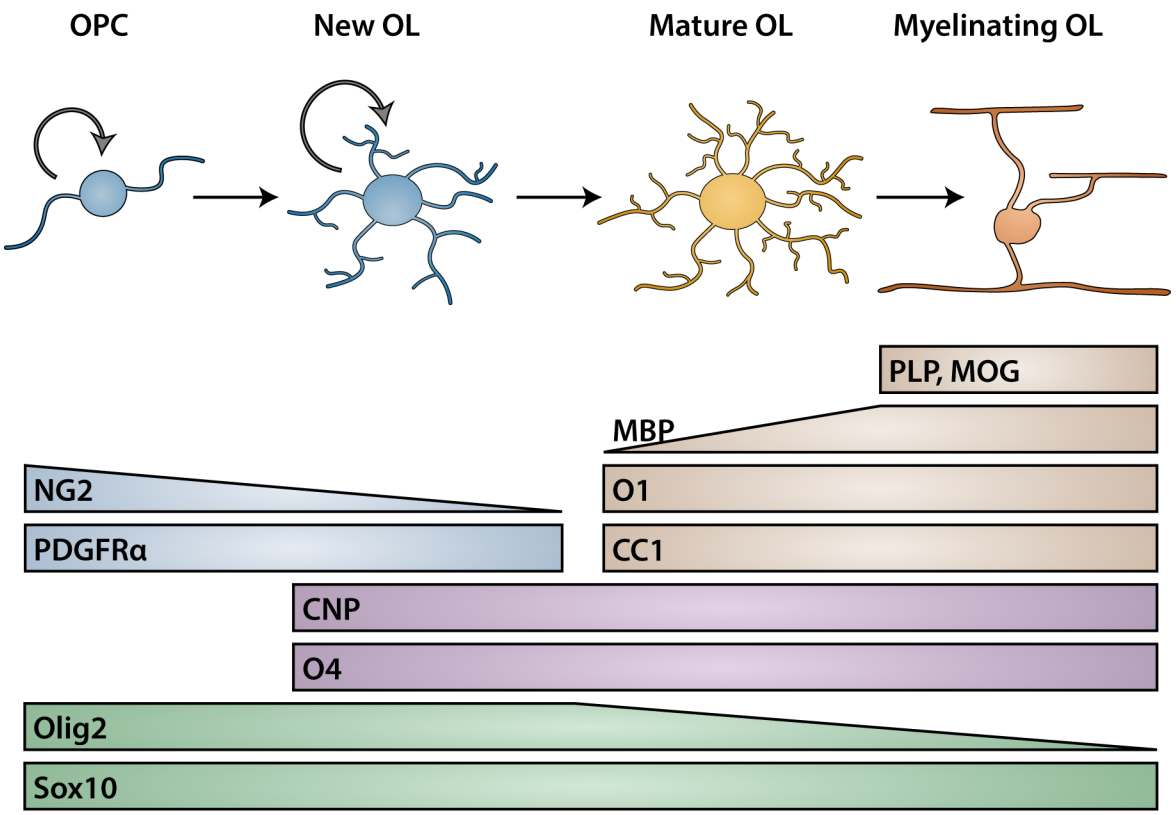

Adapted from: Espinosa-Jeffrey et al. 2009
Nishiyama et al. 2009

Figure 1-3. Oligodendrocyte lineage markers
A selection of cell markers can be used to identify oligodendrocyte (OL) lineage cells at key stages of development and differentiation. Cartoon cells demonstrate important morphologic features at each stage and are color coded for immature (blue) or mature (orange) subtypes. Marker proteins are identified similarly, or as a combination (purple) or pan-lineage (green). Relative levels of markers across stages are demonstrated by slope when applicable. OPC: oligodendrocyte progenitor cell.

Figure 1-4

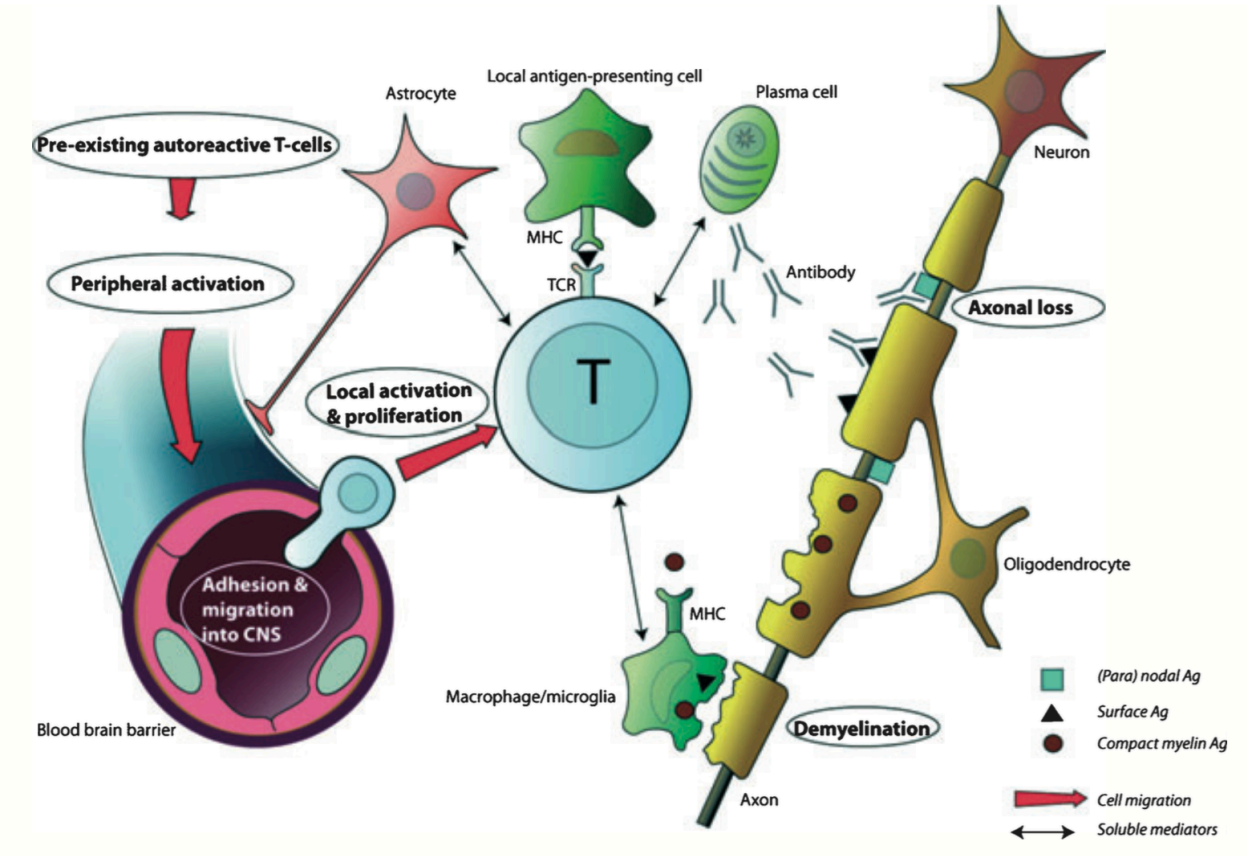

Adapted from: Gold & Wolinsky, 2011

Figure 1-4. Pathogenesis of multiple sclerosis
This model, from Gold & Wolinsky (2011) in their review of multiple sclerosis pathophysiology, depicts the key pathologic mechanisms of the disease. At the core is peripheral immune cell activation, in particular T cells, which recognize myelin proteins, or other proteins at the oligodendrocyte-axon junction. Activation leads to T cell extravasation into the CNS where it targets myelinated axons for destruction, leading to demyelination and death of oligodendrocytes, though it can also lead to direct axonal damage as well.

Figure 1-5

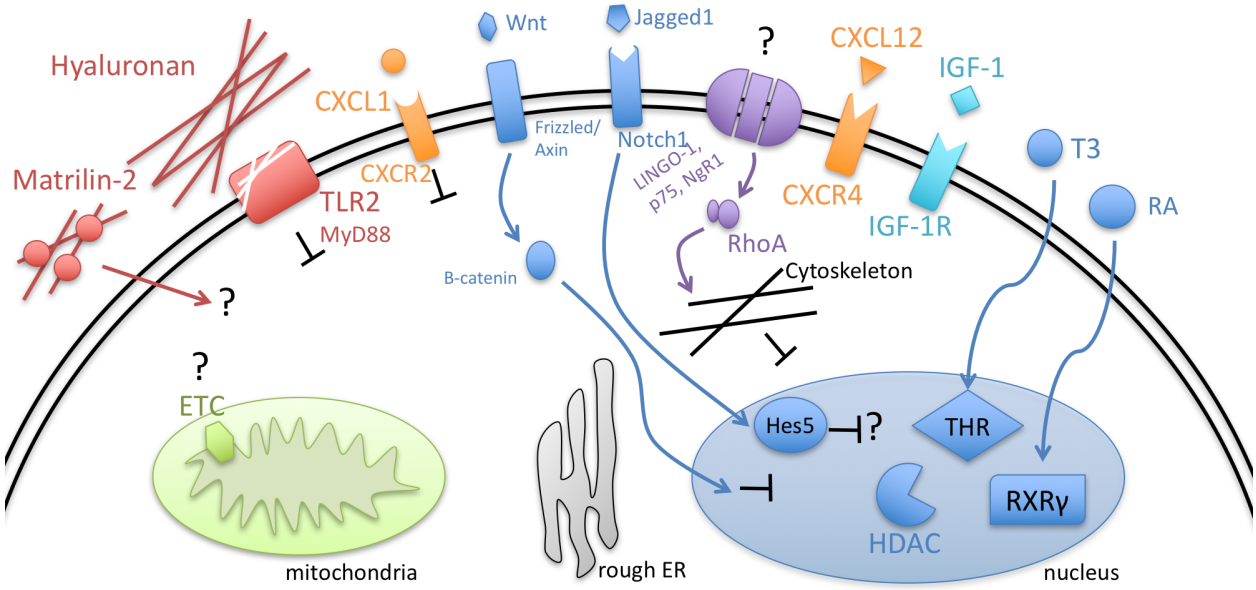

Figure 1-5. Selected pathways implicated in oligodendrocyte differentiation
A wealth of research has identified numerous factors and pathways that promote or inhibit differentiation of oligodendrocytes. This schematic highlights a selection of these, along with key targets or steps in the pathway. Note the diversity of factors, from cell surface receptors to extracellular matrix proteins. *See text for full citations.*

Table 1-1

White matter injury models

Disease	Mechanism of white matter injury	Example animal model(s)	Citation
White matter stroke	Ischemic cell death	• Vasoconstrictor injection • Common carotid stenosis	Fern et al., 2014 Sozmen et al., 2012
Multiple sclerosis	T-cell mediated damage to myelin and axons	• Experimental autoimmune encephalomyelitis • Toxic injury (cuprizone)	Ransohoff, 2012
Traumatic brain injury	Shear forces on axons and vessels	• Fluid percussion injury	Flygt et al., 2013
Leukodystrophies	Genetic defect in myelin synthesis	• Genetic mouse models	Nave, 2010 Pouwels et al., 2014
Alzheimer's disease	Oligodendrocyte damage from beta-amyloid and neurofibrillary tangles	• Genetic mouse models	Cai & Xiao, 2016 Desai et al., 2009

1.7 References

Back, S. A., Tuohy, T. M. F., Chen, H., Wallingford, N., Craig, A., Struve, J., … Sherman, L. S. (2005). Hyaluronan accumulates in demyelinated lesions and inhibits oligodendrocyte progenitor maturation. *Nature Medicine*, *11*(9), 966–72. https://doi.org/10.1038/nm1279

Bakiri, Y., Káradóttir, R., Cossell, L., & Attwell, D. (2011). Morphological and electrical properties of oligodendrocytes in the white matter of the corpus callosum and cerebellum. *The Journal of Physiology*, *589*(3), 559–573. https://doi.org/10.1113/jphysiol.2010.201376

Bamford, J., Sandercock, P., Dennis, M., Burn, J., & Warlow, C. (1991). Classification and natural history of clinically identifiable subtypes of cerebral infarction. *The Lancet*, *337*, 1521–1526.

Barratt, H. E., Lanman, T. a, & Carmichael, S. T. (2014). Mouse intracerebral hemorrhage models produce different degrees of initial and delayed damage, axonal sprouting, and recovery. *Journal of Cerebral Blood Flow and Metabolism*, *34*(May), 1–9. https://doi.org/10.1038/jcbfm.2014.107

Barres, B. A., Koroshetz, W. J., Swartz, K. J., Chun, L. L. Y., & Corey, D. P. (1990). Ion channel expression by white matter glia: the O-2A glial progenitor cell. *Neuron*, *4*(4), 507–24. https://doi.org/10.1016/0896-6273(90)90109-S

Baumann, N., & Pham-Dinh, D. (2001). Biology of oligodendrocyte and myelin in the mammalian central nervous system. *Physiological Reviews*, *81*(2), 871–927. https://doi.org/10.1111/j.1365-2427.2009.02340.x

Benjamin, E. J., Blaha, M. J., Chiuve, S. E., Cushman, M., Das, S. R., Deo, R., … Muntner, P. (2017). *Heart Disease and Stroke Statistics—2017 Update: A Report from the American Heart Association*. *Circulation* (Vol. 135). https://doi.org/10.1161/CIR.0000000000000485

Bercury, K. K., & Macklin, W. B. (2015). Dynamics and mechanisms of CNS myelination. *Developmental Cell*, *32*(4), 447–458. https://doi.org/10.1016/j.devcel.2015.01.016

Bergles, D. E., Roberts, J. D. B., Somogyi, P., & Jahr, C. E. (2000). Glutamatergic synapses on oligodendrocyte precursor cells in the hippocampus. *Nature*, *405*(6783), 187–191. https://doi.org/10.1038/35012083

Brivio, V., Faivre-Sarrailh, C., Peles, E., Sherman, D. L., & Brophy, P. J. (2017). Assembly of CNS Nodes of Ranvier in Myelinated Nerves Is Promoted by the Axon Cytoskeleton. *Current Biology*, *27*(7), 1068–1073. https://doi.org/10.1016/j.cub.2017.01.025

Brown, D. L., Boden-Albala, B., Langa, K. M., Lisabeth, L. D., Fair, M., Smith, M. A., … Morgenstern, L. B. (2006). Projected costs of ischemic stroke in the United States. *Neurology*, *67*(8), 1390–1395. https://doi.org/10.1212/01.wnl.0000237024.16438.20

Cai, Z., & Xiao, M. (2016). Oligodendrocytes and Alzheimer's disease. *International Journal of Neuroscience*, *126*(2), 97–104. https://doi.org/10.3109/00207454.2015.1025778

Carandang, R., Seshadri, S., Beiser, A., Kelly-Hayes, M., Kase, C. S., Kannel, W. B., & Wolf, P. A. (2006). Trends in Incidence, Lifetime Risk, Severity, and 30-Day Mortality of Stroke Over the Past 50 Years. *JAMA*, *296*(24), 2939–2946.

Carod-Artal, F. J., & Egido, J. A. (2009). Quality of life after stroke: The importance of a good recovery. *Cerebrovascular Diseases*, *27*(SUPPL. 1), 204–214. https://doi.org/10.1159/000200461

Chui, H. C. (2007). Subcortical Ischemic Vascular Dementia. *Neurologic Clinics*, *25*(3), 717–740. https://doi.org/10.1016/j.ncl.2007.04.003

Crawford, D. K., Mangiardi, M., & Tiwari-Woodruff, S. K. (2009). Assaying the functional effects of demyelination and remyelination: Revisiting field potential recordings. *Journal of*

Neuroscience Methods, *182*(1), 25–33. https://doi.org/10.1016/j.jneumeth.2009.05.013

Crawford, D. K., Mangiardi, M., Xia, X., López-Valdés, H. E., & Tiwari-Woodruff, S. K. (2009). Functional recovery of callosal axons following demyelination: a critical window. *Neuroscience*, *164*(4), 1407–1421. https://doi.org/10.1016/j.neuroscience.2009.09.069

Dawson, M. R. L., Polito, A., Levine, J. M., & Reynolds, R. (2003). NG2-expressing glial progenitor cells: An abundant and widespread population of cycling cells in the adult rat CNS. *Molecular and Cellular Neuroscience*, *24*(2), 476–488. https://doi.org/10.1016/S1044-7431(03)00210-0

Desai, M. K., Sudol, K. L., Janelsins, M. C., Mastrangelo, M. A., Frazer, M. E., & Bowers, W. J. (2009). Triple-transgenic Alzheimer's disease mice exhibit region-specific abnormalities in brain myelination patterns prior to appearance of amyloid and tau pathology. *Glia*, *57*(1), 54–65. https://doi.org/10.1002/glia.20734

Deshmukh, V. A., Tardif, V., Lyssiotis, C. A., Green, C. C., Kerman, B., Kim, H. J., … Lairson, L. L. (2013). A regenerative approach to the treatment of multiple sclerosis. *Nature*, *502*(7471), 327–32. https://doi.org/10.1038/nature12647

Dobkin, B. (2005). Rehabilitation after stroke. *New England Journal of Medicine*, *352*(16), 1677–1684. Retrieved from http://www.nejm.org/doi/full/10.1056/NEJMcp043511

Dumas, L., Heitz-Marchaland, C., Fouquet, S., Suter, U., Livet, J., Moreau-Fauvarque, C., & Chédotal, A. (2015). Multicolor analysis of oligodendrocyte morphology, interactions, and development with brainbow. *Glia*, *63*(4), 699–717. https://doi.org/10.1002/glia.22779

Espinosa-Jeffrey, A., Wakeman, D. R., Kim, S. U., Snyder, E. Y., & de Vellis, J. (2009). Culture system for rodent and human oligodendrocyte specification, lineage progression, and maturation. *Current Protocols in Stem Cell Biology*, *Chapter 2*(September), Unit 2D.4.

https://doi.org/10.1002/9780470151808.sc02d04s10

Fern, R. F., Matute, C., & Stys, P. K. (2014). White matter injury: Ischemic and nonischemic. *Glia*, *62*(11), 1780–9. https://doi.org/10.1002/glia.22722

Fields, R. D. (2008). Oligodendrocytes Changing the Rules: Action Potentials in Glia and Oligodendrocytes Controlling Action Potentials. *The Neuroscientist*, *14*(6), 540–543. https://doi.org/10.1177/1073858408320294

Flygt, J., Djupsjö, A., Lenne, F., & Marklund, N. (2013). Myelin loss and oligodendrocyte pathology in white matter tracts following traumatic brain injury in the rat. *European Journal of Neuroscience*, *38*(1), 2153–2165. https://doi.org/10.1111/ejn.12179

Ge, W.-P., Yang, X.-J., Zhang, Z., Wang, H.-K., Shen, W., Deng, Q.-D., & Duan, S. (2006). Long-term potentiation of neuron-glia synapses mediated by Ca2+-permeable AMPA receptors. *Science*, *312*, 1533–1537. https://doi.org/10.1126/science.1124669

Gibson, E. M., Purger, D., Mount, C. W., Goldstein, A. K., Lin, G. L., Wood, L. S., … Monje, M. (2014). Neuronal activity promotes oligodendrogenesis and adaptive myelination in the mammalian brain. *Science*, *344*(6183), 480–481. https://doi.org/10.1126/science.1254446

Gold, R., & Wolinsky, J. S. (2011). Pathophysiology of multiple sclerosis and the place of teriflunomide. *Acta Neurologica Scandinavica*, *124*(2), 75–84. https://doi.org/10.1111/j.1600-0404.2010.01444.x

Grueter, B. E., & Schulz, U. G. (2012). Age-related cerebral white matter disease (leukoaraiosis): a review. *Postgraduate Medical Journal*, *88*(1036), 79–87. https://doi.org/10.1136/postgradmedj-2011-130307

Hill, R. A., & Nishiyama, A. (2014). NG2 cells (polydendrocytes): Listeners to the neural network with diverse properties. *Glia*, *62*, 1195–1210. https://doi.org/10.1002/glia.22664

Hinman, J. D., Lee, M. D., Tung, S., Vinters, H. V., & Carmichael, S. T. (2015). Molecular disorganization of axons adjacent to human lacunar infarcts. *Brain*, 1–10. https://doi.org/10.1093/brain/awu398

Hinman, J. D., Rasband, M. N., & Carmichael, S. T. (2013). Remodeling of the axon initial segment after focal cortical and white matter stroke. *Stroke; a Journal of Cerebral Circulation*, *44*(1), 182–9. https://doi.org/10.1161/STROKEAHA.112.668749

Hoffmann, A., Grimm, C., Kraft, R., Goldbaum, O., Wrede, A., Nolte, C., … Harteneck, C. (2010). TRPM3 is expressed in sphingosine-responsive myelinating oligodendrocytes. *Journal of Neurochemistry*, *114*(3), 654–665. https://doi.org/10.1111/j.1471-4159.2010.06644.x

Howard, G., & Goff, D. C. (2012). Population shifts and the future of stroke: Forecasts of the future burden of stroke. *Annals of the New York Academy of Sciences*, *1268*(1), 14–20. https://doi.org/10.1111/j.1749-6632.2012.06665.x

Jones, D. K., Lythgoe, D., Horsfield, M. a, Simmons, A., Williams, S. C., & Markus, H. S. (1999). Characterization of white matter damage in ischemic leukoaraiosis with diffusion tensor MRI. *Stroke; a Journal of Cerebral Circulation*, *30*(2), 393–7. https://doi.org/10.1161/01.STR.30.2.393

Kessaris, N., Fogarty, M., Iannarelli, P., Grist, M., Wegner, M., & Richardson, W. D. (2006). Competing waves of oligodendrocytes in the forebrain and postnatal elimination of an embryonic lineage. *Nature Neuroscience*, *9*(2), 173–179. https://doi.org/10.1038/nn1620

Kettenmann, H., & Verkhratsky, A. (2008). Neuroglia: the 150 years after. *Trends in Neurosciences*, *31*(12), 653–659. https://doi.org/10.1016/j.tins.2008.09.003

Kunkel, A., Kopp, B., Müller, G., Villringer, K., Villringer, A., Taub, E., & Flor, H. (1999).

Constraint-induced movement therapy for motor recovery in chronic stroke patients. *Archives of Physical Medicine and Rehabilitation*, *80*(6), 624–628. https://doi.org/10.1016/S0003-9993(99)90163-6

Langhorne, P., Bernhardt, J., & Kwakkel, G. (2011). Stroke rehabilitation. *The Lancet*, *377*(9778), 1693–1702. https://doi.org/10.1016/S0140-6736(11)60325-5

Li, S., Nie, E. H., Yin, Y., Benowitz, L. I., Tung, S., Vinters, H. V, … Carmichael, S. T. (2015). GDF10 is a signal for axonal sprouting and functional recovery after stroke. *Nature Neuroscience*, *18*(12), 1737–1745. https://doi.org/10.1038/nn.4146

Li, S., Overman, J. J., Katsman, D., Kozlov, S. V, Donnelly, C. J., Twiss, J. L., … Carmichael, S. T. (2010). An age-related sprouting transcriptome provides molecular control of axonal sprouting after stroke. *Nature Neuroscience*, *13*(12), 1496–504. https://doi.org/10.1038/nn.2674

Liepert, J., Bauder, H., Miltner, W. H. R., Taub, E., & Weiller, C. (2000). Treatment-Induced Cortical Reorganization After Stroke in Humans. *Stroke*, *31*(6), 1210–1216. https://doi.org/10.1161/01.STR.31.6.1210

Longstreth, W. T., Manolio, T. A., Arnold, A., Burke, G. L., Bryan, N., Jungreis, C. A., … Fried, L. (1996). Clinical Correlates of White Matter Findings on Cranial Magnetic Resonance Imaging of 3301 Elderly People. *Stroke*, *27*(8), 1274 LP-1282. Retrieved from http://stroke.ahajournals.org/content/27/8/1274.abstract

Manolio, T. A., Kronmal, R. A., Burke, G. L., Poirier, V., O'Leary, D. H., Gardin, J. M., … Bryan, R. N. (1994). Magnetic resonance abnormalities and cardiovascular disease in older adults. The Cardiovascular Health Study. *Stroke*, *25*(2), 318–327. https://doi.org/10.1161/01.STR.25.2.318

Mei, F., Mayoral, X. S. R., Nobuta, H., Wang, X. F., Desponts, X. C., Lorrain, D. S., … Chan, X. J. R. (2016). Identification of the Kappa-Opioid Receptor as a Therapeutic Target for Oligodendrocyte Remyelination. *The Journal of Neuroscience*, *36*(30), 7925–7935. https://doi.org/10.1523/JNEUROSCI.1493-16.2016

Meijer, D. H., Kane, M. F., Mehta, S., Liu, H., Harrington, E., Taylor, C. M., … Rowitch, D. H. (2012). Separated at birth? The functional and molecular divergence of OLIG1 and OLIG2. *Nature Reviews Neuroscience*, *13*(12), 819–831. https://doi.org/10.1038/nrn3386

Michalski, J.-P., & Kothary, R. (2015). Oligodendrocytes in a Nutshell. *Frontiers in Cellular Neuroscience*, *9*(September), 1–11. https://doi.org/10.3389/fncel.2015.00340

Moskowitz, M. A., Lo, E. H., & Iadecola, C. (2010). The science of stroke: mechanisms in search of treatments. *Neuron*, *67*(2), 181–98. https://doi.org/10.1016/j.neuron.2010.07.002

Nave, K.-A. (2010). Myelination and support of axonal integrity by glia. *Nature*, *468*(7321), 244–252. https://doi.org/10.1038/nature09614

Nie, E. H. (2016). *Axonal sprouting in a novel intracortical connection formed upon limb overuse after stroke: A circuit-specific transcriptomic study*. University of California, Los Angeles.

Nishiyama, A., Komitova, M., Suzuki, R., & Zhu, X. (2009). Polydendrocytes (NG2 cells): multifunctional cells with lineage plasticity. *Nature Reviews Neuroscience*, *10*(1), 9–22. https://doi.org/10.1038/nrn2495

Ovbiagele, B., Markovic, D., & Towfighi, A. (2011). Recent age- and gender-specific trends in mortality during stroke hospitalization in the United States. *International Journal of Stroke*, *6*(5), 379–387. https://doi.org/10.1111/j.1747-4949.2011.00590.x

Patel, J. R., McCandless, E. E., Dorsey, D., & Klein, R. S. (2010). CXCR4 promotes

differentiation of oligodendrocyte progenitors and remyelination. *Proceedings of the National Academy of Sciences*, *107*(24), 11062–11067. https://doi.org/10.1073/pnas.1006301107/-/DCSupplemental.www.pnas.org/cgi/doi/10.1073/pnas.1006301107

Pérez-Cerdá, F., Sánchez-Gómez, M. V., & Matute, C. (2015). Pío del Río Hortega and the discovery of the oligodendrocytes. *Frontiers in Neuroanatomy*, *9*(July), 7–12. https://doi.org/10.3389/fnana.2015.00092

Pfeiffer, S. E., Warrington, A. E., & Bansal, R. (1993). The oligodendrocyte and its many cellular processes. *Trends in Cell Biology*, *3*(6), 191–197. https://doi.org/10.1016/0962-8924(93)90213-K

Polman, C. H., O'Connor, P. W., Havrdova, E., Hutchinson, M., Kappos, L., Miller, D. H., … Sandrock, A. W. (2006). A Randomized, Placebo-Controlled Trial of Natalizumab for Relapsing Multiple Sclerosis. *New England Journal of Medicine*, *354*(9), 899–910. https://doi.org/10.1056/NEJMoa044397

Popescu, B. F. G., & Lucchinetti, C. F. (2012). Pathology of Demyelinating Diseases. *Annual Review of Pathology: Mechanisms of Disease*, *7*(1), 185–217. https://doi.org/10.1146/annurev-pathol-011811-132443

Pouwels, P. J. W., Vanderver, A., Bernard, G., Wolf, N. I., Dreha-Kulczewksi, S. F., Deoni, S. C. L., … Barkovich, A. J. (2014). Hypomyelinating leukodystrophies: Translational research progress and prospects. *Annals of Neurology*, *76*(1), 5–19. https://doi.org/10.1002/ana.24194

Prabhakaran, S., Ruff, I., & Bernstein, R. A. (2015). Acute stroke intervention: A systematic review. *JAMA*, *313*(14), 1451–1462. https://doi.org/10.1002/9781118504499.ch34

Prins, N. D., & Scheltens, P. (2015). White matter hyperintensities, cognitive impairment and dementia: an update. *Nature Reviews Neurology*, *11*(3), 157–165. https://doi.org/10.1038/nrneurol.2015.10

Qureshi, A. I., Mendelow, A. D., & Hanley, D. F. (2009). Intracerebral haemorrhage. *The Lancet*, *373*(9675), 1632–1644. https://doi.org/10.1016/S0140-6736(09)60371-8

Raff, M. C., Miller, R. H., & Noble, M. (1983). A glial progenitor cell that develops in vitro into an astrocyte or an oligodendrocyte depending on culture medium. *Nature*, *303*(5916), 390–396. https://doi.org/10.1038/303390a0

Ransohoff, R. M. (2012). Animal models of multiple sclerosis: the good, the bad and the bottom line. *Nature Neuroscience*, *15*(8), 1074–1077. https://doi.org/10.1038/nn.3168

Rosenzweig, S., & Carmichael, S. T. (2013). Age-dependent exacerbation of white matter stroke outcomes: a role for oxidative damage and inflammatory mediators. *Stroke; a Journal of Cerebral Circulation*, *44*(9), 2579–86. https://doi.org/10.1161/STROKEAHA.113.001796

Saab, A. S., Tzvetavona, I. D., Trevisiol, A., Baltan, S., Dibaj, P., Kusch, K., … Nave, K. A. (2016). Oligodendroglial NMDA Receptors Regulate Glucose Import and Axonal Energy Metabolism. *Neuron*, *91*(1), 119–132. https://doi.org/10.1016/j.neuron.2016.05.016

Sacco, R. L., Kasner, S. E., Broderick, J. P., Caplan, L. R., Connors, J. J., Culebras, A., … Vinters, H. V. (2013). An updated definition of stroke for the 21st century: A statement for healthcare professionals from the American heart association/American stroke association. *Stroke*, *44*(7), 2064–2089. https://doi.org/10.1161/STR.0b013e318296aeca

Saver, J. L., Fonarow, G. C., Smith, E. E., Reeves, M. J., Grau-Sepulveda, M. V, Hernandez, A. F., … Schwamm, L. H. (2013). Time to treatment with intravenous tissue plasminogen activator and outcome from acute ischemic stroke. *JAMA*, *309*(23), 2480–2488.

Schmidt, R., Enzinger, C., Ropele, S., Schmidt, H., & Fazekas, F. (2003). Progression of cerebral white matter lesions: 6-Year results of the Austrian Stroke Prevention Study. *Lancet*, *361*(9374), 2046–2048. https://doi.org/10.1016/S0140-6736(03)13616-1

Schneider, A. T., Kissela, B., Woo, D., Kleindorfer, D., Alwell, K., Miller, R., … Broderick, J. (2004). Ischemic stroke subtypes: A population-based study of incidence rates among blacks and whites. *Stroke*, *35*(7), 1552–1556. https://doi.org/10.1161/01.STR.0000129335.28301.f5

Simons, M., & Lyons, D. A. (2013). Axonal selection and myelin sheath generation in the central nervous system. *Current Opinion in Cell Biology*, *25*(4), 512–519. https://doi.org/10.1016/j.ceb.2013.04.007

Simons, M., & Nave, K.-A. (2016). Oligodendrocytes: Myelination and axonal support. *Cold Spring Harbor Perspectives in Biology*, *8*(a020479), 1–16. https://doi.org/10.1101/cshperspect.a020479

Sloane, J. A., Batt, C., Ma, Y., Harris, Z. M., Trapp, B., & Vartanian, T. (2010). Hyaluronan blocks oligodendrocyte progenitor maturation and remyelination through TLR2. *Proceedings of the National Academy of Sciences of the United States of America*, *107*(25), 11555–60. https://doi.org/10.1073/pnas.1006496107

Souza-Rodrigues, R. D., Costa, A. M. R., Lima, R. R., Dos Santos, C. D., Picanço-Diniz, C. W., & Gomes-Leal, W. (2008). Inflammatory response and white matter damage after microinjections of endothelin-1 into the rat striatum. *Brain Research*, *1200*, 78–88. https://doi.org/10.1016/j.brainres.2007.11.025

Sozmen, E. G., Hinman, J. D., & Carmichael, S. T. (2012). Models that matter: white matter stroke models. *Neurotherapeutics : The Journal of the American Society for Experimental*

NeuroTherapeutics, *9*(2), 349–58. https://doi.org/10.1007/s13311-012-0106-0

Sozmen, E. G., Kolekar, A., Havton, L. A., & Carmichael, S. T. (2009). A white matter stroke model in the mouse: axonal damage, progenitor responses and MRI correlates. *Journal of Neuroscience Methods*, *180*(2), 261–72. https://doi.org/10.1016/j.jneumeth.2009.03.017

Sozmen, E. G., Rosenzweig, S., Llorente, I. L., DiTullio, D. J., Machnicki, M., Vinters, H. V., … Carmichael, S. T. (2016). Nogo receptor blockade overcomes remyelination failure after white matter stroke and stimulates functional recovery in aged mice. *Proceedings of the National Academy of Sciences*, *113*(52), E8453–E8462. https://doi.org/10.1073/pnas.1615322113

Srikanth, V., Beare, R., Blizzard, L., Phan, T., Stapleton, J., Chen, J., … Reutens, D. (2009). Cerebral white matter lesions, gait, and the risk of incident falls: a prospective population-based study. *Stroke; a Journal of Cerebral Circulation*, *40*(1), 175–80. https://doi.org/10.1161/STROKEAHA.108.524355

Tanaka, Y., Imai, H., Konno, K., Miyagishima, T., Kubota, C., Puentes, S., … Saito, N. (2008). Experimental model of lacunar infarction in the gyrencephalic brain of the miniature pig: neurological assessment and histological, immunohistochemical, and physiological evaluation of dynamic corticospinal tract deformation. *Stroke; a Journal of Cerebral Circulation*, *39*(1), 205–12. https://doi.org/10.1161/STROKEAHA.107.489906

Teasell, R., Foley, N., Hussein, N., & Speechley, M. (2013). The Elements of Stroke Rehabilitation. *Evidence-Based Review of Stroke Rehabilitation*, 1–54.

Tripathi, R. B., Clarke, L. E., Burzomato, V., Kessaris, N., Anderson, P. N., Attwell, D., & Richardson, W. D. (2011). Dorsally and Ventrally Derived Oligodendrocytes Have Similar Electrical Properties but Myelinate Preferred Tracts. *Journal of Neuroscience*, *31*(18),

6809–6819. https://doi.org/10.1523/JNEUROSCI.6474-10.2011

Ueno, T., Ito, J., Hoshikawa, S., Ohori, Y., Fujiwara, S., Yamamoto, S., … Ogata, T. (2012). The identification of transcriptional targets of Ascl1 in oligodendrocyte development. *Glia*, *60*(10), 1495–505. https://doi.org/10.1002/glia.22369

Uswatte, G., Foo, W. L., Olmstead, H., Lopez, K., Holand, A., & Simms, L. B. (2005). Ambulatory monitoring of arm movement using accelerometry: An objective measure of upper-extremity rehabilitation in persons with chronic stroke. *Archives of Physical Medicine and Rehabilitation*, *86*(7), 1498–1501. https://doi.org/10.1016/j.apmr.2005.01.010

World Health Organization. (2017a). Cardiovascular diseases (CVDs). Retrieved November 10, 2017, from http://www.who.int/mediacentre/factsheets/fs317/en/

World Health Organization. (2017b). Global Health Observatory (GHO) data. Retrieved November 10, 2017, from http://www.who.int/gho/mortality_burden_disease/causes_death/top_10/en/

Wright, C. B., Festa, J. R., Paik, M. C., Schmiedigen, A., Brown, T. R., Yoshita, M., … Stern, Y. (2008). White matter hyperintensities and subclinical infarction: Associations with psychomotor speed and cognitive flexibility. *Stroke*, *39*(3), 800–805. https://doi.org/10.1161/STROKEAHA.107.484147

Yednock, T., Cannon, C., Fritz, L., Sanchez-Madrid, F., Steinman, L., & Karin, N. (1992). Prevention of experimental autoimmune encephalomyelitis by antibodies against alpha 4 beta 1 integrin. *Nature*, *356*(6364), 63–66. https://doi.org/10.1038/356063a0

Yeung, M. S. Y., Zdunek, S., Bergmann, O., Bernard, S., Salehpour, M., Alkass, K., … Fris??n, J. (2014). Dynamics of oligodendrocyte generation and myelination in the human brain. *Cell*, *159*(4), 766–774. https://doi.org/10.1016/j.cell.2014.10.011

Yu, Y., Chen, Y., Kim, B., Wang, H., Zhao, C., He, X., … Lu, Q. R. (2013). Olig2 targets chromatin remodelers to enhancers to initiate oligodendrocyte differentiation. *Cell*, *152*(1–2), 248–61. https://doi.org/10.1016/j.cell.2012.12.006

Yuen, T. J., Johnson, K. R., Miron, V. E., Zhao, C., Quandt, J., Harrisingh, M. C., … Ffrench-Constant, C. (2013). Identification of endothelin 2 as an inflammatory factor that promotes central nervous system remyelination. *Brain : A Journal of Neurology*, *136*(Pt 4), 1035–47. https://doi.org/10.1093/brain/awt024

Zamanian, J. L., Xu, L., Foo, L. C., Nouri, N., Zhou, L., Giffard, R. G., & Barres, B. A. (2012). Genomic Analysis of Reactive Astrogliosis. *Journal of Neuroscience*, *32*(18), 6391–6410. https://doi.org/10.1523/JNEUROSCI.6221-11.2012

Zhang, L., He, X., Liu, L., Jiang, M., Zhao, C., Wang, H., … Lu, Q. R. (2016). Hdac3 interaction with p300 histone acetyltransferase regulates the oligodendrocyte and astrocyte lineage fate switch. *Developmental Cell*, *36*, 316–330. https://doi.org/10.1016/j.devcel.2016.06.004

Zhang, Y., Chen, K., Sloan, S. A., Bennett, M. L., Scholze, A. R., Keeffe, S. O., … Wu, X. J. Q. (2014). An RNA-Sequencing Transcriptome and Splicing Database of Glia, Neurons, and Vascular Cells of the Cerebral Cortex. *The Journal of Neuroscience : The Official Journal of the Society for Neuroscience*, *34*(36), 1–19. https://doi.org/10.1523/JNEUROSCI.1860-14.2014

Zhu, X., Bergles, D. E., & Nishiyama, A. (2007). NG2 cells generate both oligodendrocytes and gray matter astrocytes. *Development*, *135*(1), 145–157. https://doi.org/10.1242/dev.004895

Ziabreva, I., Campbell, G., Rist, J., Zambonin, J., Rorbach, J., Wydro, M. M., … Mahad, D. (2010). Injury and differentiation following inhibition of mitochondrial respiratory chain complex IV in rat oligodendrocytes. *Glia*, *58*(15), 1827–1837.

https://doi.org/10.1002/glia.21052

Zuchero, J. B., & Barres, B. a. (2013). Intrinsic and extrinsic control of oligodendrocyte development. *Current Opinion in Neurobiology*, *23*(6), 914–920. https://doi.org/10.1016/j.conb.2013.06.005

Zuchero, J. B., Fu, M., Sloan, S. A., Ibrahim, A., Olson, A., Zaremba, A., … Barres, B. A. (2015). CNS Myelin Wrapping Is Driven by Actin Disassembly. *Developmental Cell*, *34*(2), 152–167. https://doi.org/10.1016/j.devcel.2015.06.011

Chapter 2

The oligodendrocyte progenitor stroke transcriptome is a unique resource to assess white matter stroke pathology

2.1 Introduction

Over the past several years, advances in research and computational technologies have made large genome studies accessible to academic research groups (Ozsolak & Milos, 2011; Wang et al., 2009). In particular, RNA-sequencing (RNAseq) takes advantage of high-throughput sequencing to enable unbiased interrogation of gene expression profiles of cells or tissues. After reverse transcribing purified RNA into cDNA, massively parallel sequencing allows for not only whole-exome sequencing, but also additional tools, such as characterization of microRNAs and other small noncoding RNAs, as well as alternative splicing quantification. Given that such features are thought to play a role in many diseases in neurology and beyond, this offers a valuable tool to identify key biological regulators at both the genetic and epigenetic level (He et al., 2016; T. W. Yu et al., 2013; Zhao et al., 2010).

RNAseq also offers immense benefits when studying complex biological questions such as the behavior of OPCs in a novel disease context. Assessing expression of every gene gives researchers an unbiased assessment of cell behavior in the system. That is, with the correct bioinformatics analysis tools, transcriptomic datasets identify genes that quantifiably play a significant role in disease. Such an approach is needed in white matter stroke: many regulators of OPC differentiation have been identified but in different diseases models; transcriptomic analysis

of OPCs in the stroke context offers the chance to filter these for only those that are most impactful in an ischemic pathology.

Generation of the OPC stroke transcriptome

An OPC-specific stroke transcriptome has been generated as outlined previously (Sozmen, 2013). Briefly, *in vivo* studies using an NG2::CreERT2/Rosa-YFP reporter mouse identified significantly heightened proliferation of OPCs following ischemic WMS, but very limited differentiation into maturing oligodendrocytes as assessed by cytoplasmic translocation of Olig1 (**Figure 2-1**) (Arnett et al., 2004; Sozmen et al., 2016). The mouse model of WMS used is summarized in **Figure 2-2** (Paxinos & Watson, 2001). To assess the observed differentiation block, OPCs were isolated from peri-infarct tissue at two time points after induction of WMS as well as control tissue (n = 5-6 animals per group). The first stroke time point, 5 days, was identified as the peak of OPC proliferation, while the second, at 15 days, showed limited differentiation and decreases in OPCs suggestive of terminal cell fate. Importantly, OPCs were labeled with a PDGFRα/lckGFP lentivirus, as recent reports suggest that $NG2^+$ cells may not strictly be oligodendrocyte progenitors, while PDGFRα represents a more selective marker for OPCs (Nishiyama et al., 2009). Pairwise comparisons between the three groups of OPCs allows for tracking of stroke-specific genes as well as alterations in gene expression over time.

In this chapter, analysis of the RNAseq data is described, in several stages. First, bioinformatics analysis is performed to identify the most significantly differentially expressed genes between each group. This approach combines several methods to ensure stringency and minimize false positives. Next, it is important to validate the dataset as OPC specific. This is done through several metrics, including tracking of significant genes compared to well-known

markers, as well as comparison of the dataset as a whole to published transcriptome datasets from other groups. Finally, a quantitative methodology is developed to identifying genes of particular interest for their novelty, either in OPC biology or in white matter stroke injury. Additional promising genes novel to white matter stroke are also selected, concurrent with truly novel genes. These studies will form the basis for the mechanistic studies to follow using an *in vitro* screen (Chapter 3) and *in vivo* studies (Chapter 4).

2.2 Results

Bioinformatic analysis of the transcriptome

The first step in analyzing the OPC stroke transcriptome was to determine appropriate significance thresholds to minimize false positive hits. There are a number of metrics commonly assessed in RNAseq data, and these were combined to form a stringent paradigm to filter the gene lists. The first and most common of these is the false discovery rate (FDR). This method, in short, provides a significance measure (calculated using but distinct from the *P*-value) that is adjusted for the large number of pairwise comparisons made on the data (Benjamini & Hochberg, 1995; J. Li et al., 2012). Given that there are over 20,000 genes analyzed in each of the three treatment groups, controlling for the large number of comparisons is crucial, but not sufficient, as even selecting a very stringent FDR would still lead to hundreds or thousands of false positives.

Unfortunately, there is no consensus regarding appropriate FDR cutoffs. Some reports even use different cutoffs for different comparisons within the same experiment (Zamanian et al., 2012). Because FDR is never used on its own, a cutoff within reasonable bounds that provides an acceptable level of stringency and a manageable dataset for further analysis was deemed

appropriate. In a survey of similar studies using RNAseq data in neuroscience, an FDR cutoff of 0.1 was most common (Anderson et al., 2016; S. Li et al., 2015; Novarino et al., 2014). To verify the selection of this cutoff for this dataset, a total of three comparisons per gene were made: (1) 5 day post-WMS vs. control, (2) 15 day post-WMS vs. control, and (3) 15 day vs. 5 day post-WMS. The number of genes below a variety of FDR thresholds is shown in **Figure 2-3**. Of note, regardless of FDR cutoff, day 15 vs. control led to a higher number of genes passing the cutoff compared to day 5 and day 15 vs. 5; in each case, at least four times as many genes were significant in the day 15 dataset, suggesting many expression changes occur at this sub-acute time point compared to resting OPCs.

Because several additional thresholds were to be set prior to selecting genes for further study, a cutoff of FDR < 0.1 was selected. The next measurement examined was fold change, or the relative difference in gene expression levels between conditions. At this point, it was observed that a large number of genes in each group had fold change values of essentially "infinity." Upon further examination of these occurrences, it became clear that when a gene product was not detected in one of the groups, the fold change would be coded as the maximum. To address this, an additional threshold that represented some semi-quantitative number of RNA transcripts in the sample was necessary. The metric selected is the fragments per kilobase of transcript per million reads mapped (FPKM). Briefly, FPKM uses the number of reads of a given gene obtained in each condition (Garber et al., 2011). However, it normalizes this number to the length of the transcript, as longer transcripts are more likely to be sequenced more often. Thus, although FPKM is not an absolute measure of mRNA content per condition, it does allow for comparison within a given experiment when all samples were prepared and sequenced together.

FPKM values were obtained for each gene within each sample and averaged per condition. Thresholds were discussed and selected based on a survey of the literature, as well as the ultimate goals of the study to identify pathways and potential therapeutic targets. FPKM thresholds in the literature, used to select genes based on having detectable expression, vary greatly, but generally fall within the range of 1 – 100 (Anderson et al., 2016; Bennett et al., 2016; Zhang et al., 2014). For this study, we did not want to exclude genes whose expression change was "on-off," but rather those genes for which very small changes led to outsized fold change values. As a result, genes were included as long as one of the conditions being compared had FPKM > 1. This led to exclusion of 10-20% of genes in each group (**Fig. 2-3B**).

Validating specificity of the transcriptome

Thus, through the combination of FDR and FPKM thresholds, the dataset has been refined into a set of genes most likely to have a statistically and biologically significant impact on OPC differentiation in white matter stroke. The next step was to validate the specificity of the dataset. Because cells were individually isolated using laser capture microdissection, it was important to verify that gene expression was specific to OPCs and not skewed by inadvertent capture of additional cell types. Two approaches were taken to accomplish this. First, individual genes known to be specific for non-oligodendrocyte lineage cell types were assessed examined for expression within the dataset. We used the Brain RNA-Seq tool available from the Barres lab (https://web.stanford.edu/group/barres_lab/brain_rnaseq.html). This database is developed from an elegant set of transcriptomic profiling studies conducted on every major cell type in the brain, isolated from tissues using FACS as well as the immunopanning technique (Zhang et al., 2014). Thus, it is an ideal set of baseline data, procured from control tissue, against which to compare

our disease-specific OPC transcriptome data. The online tool provides the option to compare FPKM values between combinations of cell types to determine cell type enrichment for each gene.

The cell type enrichment tool was used to generate enrichment profiles for key non-oligodendrocyte lineage cells: astrocytes, microglia, and neurons. For each cell type, enrichment was calculated relative to OPCs. A set of OPC-specific genes was included by calculating enrichment in OPCs relative to non-oligodendrocyte lineage cells. For each gene, average FPKM values were examined within each group of OPCs in our transcriptome. Results are shown in **Figure 2-4**. Of note, only one gene of the top 5 from each group stands out: *Slfn2*, encoding Schlafen-2, first identified in immune cells of the lymph node and thought to play several roles in injury, including cell differentiation (Mavrommatis et al., 2013). Of note, it has been shown to be active in other tissue gene expression studies of demyelinating disease models (Matejuk & Hopke, 2003). It has not been described in oligodendrocytes, and could potentially represent some microglial contamination; however, it was the only microglial gene to show high FPKM values, even when the analysis was extended to 10 microglial-specific genes. The remainder of the cell-specific genes validate observations seen in the mouse model of WMS: first, there is enrichment of multiple OPC-specific genes; and excluding *Slfn2*, the cell type with the highest overall FPKM values are astrocytes (see **Fig. 2-4B**). This is potentially consistent with the observation that a subpopulation of OPCs may shunt to astrocyte fate in the context of WMS, though this was not statistically validated.

This result was further validated by examining the FDR values for each of the cell-type specific genes, using each of the pairwise comparisons. None of these cell-type specific genes reached the FDR < 0.1 threshold set to include genes in further analyses (**Figure 2-5**). In

contrast, genes that were selected for further study based on bioinformatics described later in this chapter all reached high levels of significance based on FDR.

Comparisons of the OPC stroke transcriptome to small sets of cell-type specific genes provides an effective initial validation and is helpful to visualize the degree of specificity of the data. However, it does not take advantage of the great power of these large datasets, wherein it is possible to compare the entire datasets against one another. In order to assess on a large scale the similarities between our data the Barres lab dataset, we consulted with bioinformatic scientists at the UCLA Informatics Center for Neurogenetics and Neurogenomics. To best correlate data from these two independently-run datasets, the recommendation was to compare log-transformed FPKM values, using a threshold in the Barres dataset to specifically analyze expression in our dataset to enriched genes of each cell type, similar to the process used in the gene-specific correlations. Log transformation achieves two goals: first, it reduces the power of a small number of highly-expressed genes to skew the data. Second, it enables comparison of magnitude of expression rather than specific FPKM values, which would be inappropriate given that these two datasets were prepared at different times.

The results of this analysis are shown in a series of figures based on cell type compared in the Barres dataset: **Figure 2-6** (astrocytes), **Figure 2-7** (neurons), **Figure 2-8** (microglia), and **Figure 2-9** (OPCs). Statistical comparison of each dataset was performed by using linear regression analysis to compare slopes of pairs of regressions. For example, in **Fig. 2-6**, the regression of Zhang OPCs vs. astrocytes is compared to control OPCs from our dataset vs. Zhang astrocytes. A significantly higher (more positive) slope would indicate higher similarity in expression patterns within a given comparison pair. Results for each analysis are indicated on the legend of each figure. The results indicate that there is either no significant difference in

correlation between OPCs from the Zhang dataset and OPCs from the stroke dataset presented here; or, in some cases, a lower correlation within the stroke dataset OPCs. Given the differences in sample preparation, this lower correlation is not unexpected, but still provides evidence against significant contamination of the dataset from non-oligodendrocyte lineage cells. Furthermore, when comparing Zhang OPCs to OPCs from each group of our dataset (**Fig. 2-9**), statistical analysis demonstrated a significantly higher correlation to control OPCs than to OPCs in either post-stroke group, providing evidence of stroke-specific expression patterns in OPCs in our test conditions. In total, correlation analyses provide further validation that the OPC stroke transcriptome is oligodendrocyte-lineage specific.

Disease specificity of the OPC stroke transcriptome

Correlation testing of OPCs in control vs. stroke conditions against OPCs within the Zhang dataset provided initial evidence that our dataset identified genes unique to stroke. However, additional analysis was undertaken to examine whether and to what extent the data was stroke-specific and thus represented a truly novel tool to examine pathology of this disease. Again, we went to the Barres RNA-seq dataset. This time, we examined expression patterns in the two WMS conditions (5 day and 15 day) against Barres lab data for each oligodendrocyte lineage stage: OPCs, new OLs, and myelinating OLs. Because the online database only provides FPKM, we were not able to use statistical methods to pull curated lists of genes for each cell type. Instead, we calculated fold enrichment as was done in **Fig. 2-4** above, with one adjustment: the cell of interest was compared to the average of all other cell types, as in this case differentiating between OPCs and new OLs is central to the objective of the analysis. This was compared to the number of significantly overexpressed genes at each time point relative to

control OPCs. A number of fold enrichment cutoffs in the Barres dataset were examined, and ultimately a fold enrichment of two was chosen. This led to approximately similar numbers of genes identified between our dataset and the Barres data. Note, however, that proportions largely did not change when using higher fold cutoffs.

Four-way Venn diagrams for these analyses are shown in **Figure 2-10**. Of note, over 80% of genes in each condition are unique to the OPC stroke transcriptome, while the rest are split relatively evenly between the three stages of OPCs identified in the Barres dataset. This indicates that our RNA-seq data represents a novel resource specific to the disease condition.

To assess whether our transcriptome is truly unique to WMS, comparison to other disease-specific datasets would be ideal. Unfortunately, at the time of writing, there is a dearth of such datasets available in the literature. The closest correlate to our model is a study of reactive astrogliosis using microarray technology (Zamanian et al., 2012). A different stroke model was used in this case, known as transient middle cerebral artery occlusion (MCAo). This induces a large ischemic stroke that crosses multiple brain regions, and in this study, cortex, corpus callosum, hippocampus, and striatum were collected and pooled before FACS sorting of astrocytes. Given the different platform of this study, only fold change values were available for 1 day, 3 day, and 7 days post-stroke. Comparisons were made to 1 day and 7 day time points, again using correlation of the log-transformed data. When plotting log-fold change values for each pair of post-stroke time points within the two datasets, slopes of regression lines of best fit did not differ from zero; however, the range of fold change values was limited in the microarray dataset, and given the differences in preparation and expression testing done for each of these studies, comparisons were not pursued beyond these initial tests.

Selecting genes of interest for further study

Having validated the OPC stroke transcriptome as OPC- and white matter stroke-specific, we next developed a process by which to identify promising genes worthy of further study. Two metrics had already been introduced: FDR and FPKM thresholds ensured that only genes with significant differential expression between time points were selected and that these differences involved substantial changes in absolute transcription. To select genes for study, we aimed for a process that was (1) unbiased, and (2) provided room for genetic manipulation and mechanistic studies. We also had to consider whether genes would be studied from each condition, or whether to focus on one specific set.

The second challenge was addressed first. The transcriptome arose out of the observation that there was a failure to switch OPC behavior from proliferation to differentiation, and this switch occurred between 5 days and 15 days post-injury. Thus, the 15 day vs. 5 day subset of genes was prioritized for further study. Though there is undoubtedly much to be gleaned from the other comparisons as well, this gene list offers a window into how OPC behavior changes over time in response to injury.

To generate an unbiased rank list of genes of interest, we took a straightforward approach: in each dataset, genes were sorted by log-fold change expression, and those with the highest differential expression were identified as potential targets. Of note, although we did not specifically look for genes overexpressed in one time point versus another, the day 15 vs. 5 time point consisted of 309 genes overexpressed at day 15 as compared to day 5, and only 48 genes overexpressed at day 5 relative to day 15. Thus, the majority of genes selected were overexpressed at day 15 compared to day 5.

A final consideration was made prior to initiating in vitro studies. Given the novelty of the dataset and the fact that some of the genes identified have not been studied in any system previously, we elected to include a subset of genes for which there was evidence in the literature providing support for a role in oligodendrocyte differentiation. This may involve differentiation of cells in another system, or a known role in CNS disease. The motivation was thus to provide a foundation of genes with likely positive effects and with more tools (such as antibodies) available to study molecular pathways.

The proposed list of genes of interest destined for further study is shown in **Table 2-1** along with putative functions and key data for each. Of note, additional genes appear as novel genes unstudied in OPC differentiation since, as studied continued, additional genes were added for a variety of reasons (see Chapter 3 for a discussion of this process). Thus, every gene examined throughout the screening process is included in this table. From here, additional validation is done on a per-gene basis, prior to analyzing capacity to promote or inhibit differentiation *in vitro*. These studies are outlined in Chapter 3.

2.3 Discussion

Analysis of the OPC stroke transcriptome involves three statistical metrics

In this chapter, the OPC stroke transcriptome is analyzed using a variety of techniques to assess its specificity to WMS and to OPCs. First, an FDR threshold was used based on the desire to retain a comfortable number of genes for further analysis, but also to reduce false positive rates to acceptable levels. Next, FPKM was introduced as a method of focusing only on genes with a baseline level of expression in at least one condition. Finally, comparisons to existing

gene expression datasets allowed us to assess specificity of our dataset to OPCs and oligodendrocyte lineage cells and to white matter stroke.

The methods presented here highlight a challenge in the analysis of large datasets like those produced by RNA-seq: what is the best method for analyzing these data in a logical way, that balances likelihood of success while still allowing for novel discoveries. In particular, statistics has become a crucial aspect of any bioinformatics analysis. Our selection of an FDR threshold of 0.1 is based on a survey of other RNA-seq experiments in the field, as well as our own experience (Anderson et al., 2016; S. Li et al., 2010, 2015). Nonetheless, this is on the less stringent end of the spectrum when it comes to analyzing genomic expression data (Novarino et al., 2014; Zamanian et al., 2012). However, this was done with the knowledge that additional criteria would be introduced to further refine the dataset prior to selection of genes of interest.

The use of FPKM as one way to refine the dataset was selected both for statistical and biological reasons. Specifically, it was noted that in the dataset, looking only at FDR and log fold change, some fold change values were coded as >100 million. This is the result of one sample set not detecting any RNA transcripts for that gene; then, any number of reads in another condition would be impossible to calculate. Though mathematically accurate, the downside of this is the loss of the ability to compare fold change between different genes. For example, a theoretical gene for which absolute number of mRNA transcripts went from zero to 100 would be very different than one for which number of transcripts increased from zero to 100,000, even though both would read as an infinite fold change increase. Thus, it was important to find a way to further assess each of these occurrences and to develop a way to ascertain any differences between them.

The most effective way to address this is to introduce a threshold requirement for absolute number of mRNA molecules. Unfortunately, due to the technical needs of the experimental setup, absolute number of transcripts cannot be measured. This is a common challenge throughout the transcriptomics field, and as a result, various semi-absolute metrics have been developed (Garber et al., 2011). Based on the sequencing technique used for this experiment, the most appropriate of these is the FPKM method.

Multiple methods of thresholding using FPKM were considered. As with FDR, there is not a single accepted limit in the field (Anderson et al., 2016; Zhang et al., 2014). We thus considered the biological implications of various approaches. First, we reasoned that a gene need not be detectable in every condition to be worth investigating; for example, a gene that is undetectable in control OPCs that then has an FPKM of 5 in the 15 day OPC condition represents a potentially novel pathway to OPCs turned on specifically in the context of WMS. Thus, we required specific thresholds to be met in at least one condition in each pairwise comparison, an approach that has been successfully used in other studies (Jiang et al., 2015; Toung et al., 2011). Second, as with FDR, we knew further analyses were to be carried out on these data, so we wanted to set a lower limit on FPKM that would not exclude any potentially novel or interesting genes, but rather exclude those for which biological relevance would be difficult to assess. That is, manipulation of a gene both in the research setting as well as through any potential therapeutics developed would ideally be able to induce changes to expression that relatively accurately modeled biologically relevant changes seen *in vivo*. For these reasons, an FPKM value was selected, a value 10-fold higher than the lowest limits in the literature of 0.1, but still low enough that no more than 20% of genes from any condition were excluded in our study (**Fig. 2-3B**). It should be noted, however, that specific processes have been developed to

objectively identify "unreliable" FPKM reads and thus exclude them from analysis (Trapnell et al., 2010). Such an approach could be used in the future if further analysis or refinement of the data is necessary.

The final step in refining the gene list was ordering the by log fold change. Because log fold change is closely correlated with FDR (when considering absolute value of fold change, that is), inclusion of this final statistic increased the statistical stringency of our selection process. As a result, all of the *novel* genes selected for further study have FDR < 0.001, 100-fold lower than the initial threshold. It should be noted that the list of non-novel genes in some cases had FDRs greater than 0.01 but still matched the FDR < 0.1 threshold. This was acceptable for the purposes of this study because such genes were chosen to have a strong foundation for an effect on oligodendrocytes based on the literature, so only genes with such a background were chosen for this group. In essence, this further highlights the novelty of this dataset, as most of the highest-priority genes were truly novel to oligodendrocyte biology.

Regardless of the final FDR or log fold-change expression values for the genes selected for further study, it will be important to further validate each gene individually. For example, immunohistochemistry should be used to verify expression of the associated proteins in OPCs and in the context of WMS. There is also an argument for testing the effects of each gene in a small-scale system prior to initiating mechanistic studies in the WMS mouse model. Indeed, this was a major motivation for the *in vitro* screening studies that will be conducted in the following chapter. In summary, though the combination of three different bioinformatics measures led to a list of genes that minimized risk of false positives, the experimental setup going forward was designed to identify and exclude any such genes that made it through this statistical screening process.

The transcriptome is specific to OPCs and to white matter stroke

Comparison of our dataset to published gene expression databases allowed us to assess both its cell-type and disease specificity. First, we compared our data to that of various cell types reported in Zhang et al. (2014). This dataset has proven extremely valuable to the field of glial biology, and for this study, it allowed us to run several validation steps to assess uniqueness of our dataset. However, some caveats should be raised to use of these data prior to drawing conclusions from the analysis. First, neonatal mice were used for this study, a time at which OPCs and oligodendrocytes are still developing (Franklin & ffrench-Constant, 2017; Nave, 2010). Additionally, cells were put through a series of culture steps prior to running RNA-seq, as opposed to laser capture directly from tissue as described from here. Thus, differences between the two datasets are inevitable. Nonetheless, this provides an excellent dataset to run initial comparisons to assess quality of our RNA-seq data.

As shown in **Fig. 2-4** and **Fig. 2-5**, examining the top enriched genes in astrocytes, microglia, and neurons indicates that our cells appear to be largely OPC-specific. Two caveats to this, as noted previously, are worth discussing. First, the microglial gene *Slfn2* showed high FPKM values in our dataset. This was unexpected, and *Slfn2* has not been described in oligodendrocytes or any other non-immune cell previously. Further interrogation of the Barres data indicated that this was the only one of the ten most microglia-enriched genes to show high levels of expression when calculating FPKM; additionally, this gene did not meet the FDR threshold in our data and was excluded from further analysis regardless. Thus, it may be an outlier, the result of expected deviations in sequencing in our amplified dataset that led to an

unexpected high reading. It does further highlight the importance of downstream validation, and especially validating expression of genes in OPCs whenever possible.

Comparison of the entire datasets as shown from **Fig. 2-6** to **Fig. 2-9** again highlights that (1) there does not appear to be non-oligodendrocyte lineage contamination in the dataset, and (2) our datasets are in many cases dissimilar from other published datasets. Comparisons to individual cell types within the Zhang dataset suggested that correlation between OPCs within the stroke transcriptome were no more, and often significantly less, correlated to non-oligodendrocyte cell types than the OPCs derived within that study. On the other hand, control OPCs from our dataset were more highly correlated to Zhang OPCs than either of our post-stroke OPC groups, providing validation of the control OPCs as a baseline dataset against which to compare the post-stroke OPC groups.

The result that OPCs from our study were often less correlated to a given cell type than Zhang OPCs highlights a limitation of this approach to analysis. It is challenging to compare FPKM values of datasets derived separately, given the measure still is relative to the sample preparation within a given study (Ozsolak & Milos, 2011). In addition, the Zhang dataset itself has significant limitations: cells were derived from culture purification, meaning they spent hours *ex vivo* prior to RNA extraction. In addition, all tissue was derived from P7 mice, rather than adult animals as were used in this study. Finally, cells from gray and white matter were combined into a single pool, ignoring important regional differences between cell types (Chai et al., 2017; Marques et al., 2016). Nonetheless, as the field of glial biology grows, this represents one of the early and comprehensive datasets available for comparison; additional such comparisons will likely become more powerful and informative as transcriptomic analysis of glial cells in health and disease becomes more prolific.

Finally, the stroke-specificity of the dataset is assessed via further comparisons shown in **Fig. 2-10**. Although additional comparisons were made to the only other available post-stroke gene expression dataset available, the ability to compare between datasets using vastly different techniques was extremely limited. However, although global analyses were not informative, one avenue that may provide interesting insight is to identify genes that show significant expression changes across both datasets. Such an experiment may begin to uncover common stroke pathways and new mechanisms of communication between oligodendrocytes and astrocytes. In any case, that was not the purpose of the present experiment, and thus these data will be set aside in favor of a closer look into the genes arising from the OPC stroke transcriptome.

Future directions

Having provided a thorough analysis of the transcriptome and finishing with a list of genes of interest for further study, gene-by-gene experiments can begin. The next steps are to first validate expression of genes of interest in WMS and in oligodendrocyte lineage cells. Next, a screening method to assess each of the genes individually will be necessary in order to identify any effect on oligodendrocyte survival, differentiation, or myelination. Such experiments will be outlined in the next chapter.

2.4 Methods

Generation and analysis of the transcriptome

Isolation of OPCs was carried out prior to this study, as described elsewhere (Sozmen, 2013). Briefly, stroke was induced in mice 2.5 months or older. Animals were then injected with an OPC-specific PDGFRα/lckGFP lentivirus 4 days prior to sacrifice at the given time point: either 5 days or 15 days post-stroke. (For a description of the stroke model see Chapter 3 methods.) Laser capture microdissection was performed as described elsewhere (Overman et al., 2012). Isolated total RNA was amplified and sequence libraries were prepared using the NuGEN Ovation UltraLow library preparation kit (NuGEN Technologies, Inc.) and sequenced using paired-end 2x100 bp reads. Analysis of the sequencing data, including FPKM calculations per animal, were performed by the UCLA Informatics Center for Neurogenetics and Neurogenomics.

Additional analyses of the transcriptome dataset

Further analyses of the RNA-seq data were performed using Excel. FPKM values were averaged per treatment condition (n = 8-10 per group). Comparisons to the Barres dataset was done using both publicly available raw data, as well as the Brain-RNAseq website available at https://web.stanford.edu/group/barres_lab/brain_rnaseq.html. The online tool was used to identify top cell-type enriched genes shown in Figs. 2-4 and 2-5. Correlation graphs shown in Figs. 2-6 through 2-9 were generated by aligning the raw FPKM data downloaded from the Barres lab to our dataset using the Excel "vlookup" function. Log-transformed data was then graphed, selecting only the genes of which $\log_2(\text{FPKM}) > 2$ for that cell type in the Barres dataset. No thresholds were set based on our data so as not to bias the analysis.

To assess stroke specificity, comparisons between conditions in the OPC stroke transcriptome were used, precluding the continued use of FPKM values for comparisons to the Barres dataset. Thus, a comparable enrichment value had to be calculated based on the Barres FPKM data. To do this, the FPKM value of each gene for the cell type of interest was divided by the average FPKM of all other cell types, generating a "fold enrichment" value. This was then compared to the list of genes matching our previously determined metrics for our data, including FDR < 0.1 and FPKM > 1 for at least one of the paired conditions. Different thresholds for the fold enrichment of the Barres data were selected, and ultimately the two-fold condition was selected to provide relatively equivalent numbers of genes between the Barres data and our groups.

Finally, to compare to the reactive astrocyte gene expression data in Zamanian et al. (2012), only log fold change was available. Thus, we directly compared $\log_2$ fold change values between datasets. Because our data had a number of entries with fold change >100 million, even after FPKM thresholding, we normalized all of these very high values to a value of ±20 as appropriate, which was 2^5-fold (32×) higher than any other fold change value in the dataset.

2.5 Figures

Figure 2-1

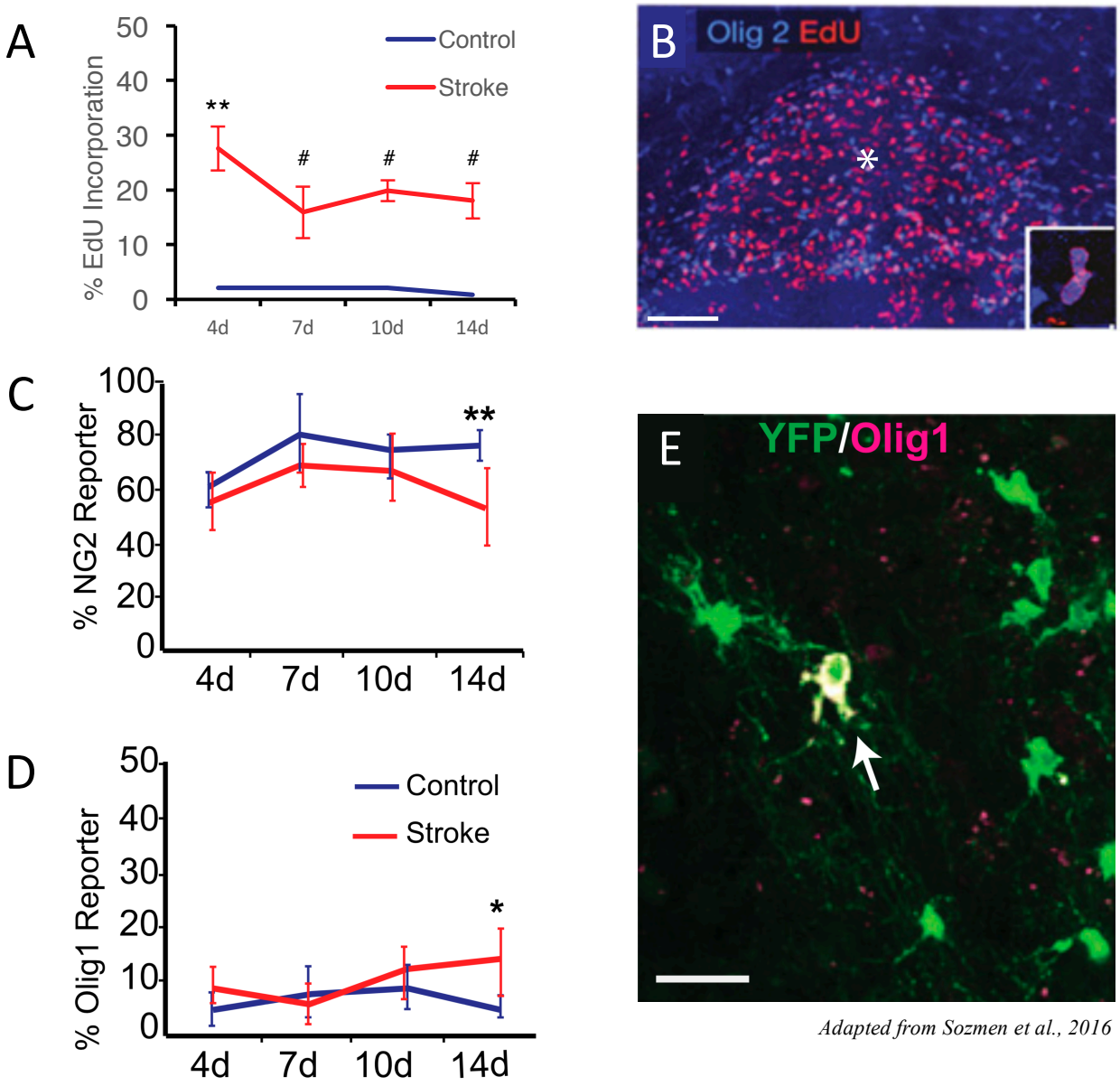

Adapted from Sozmen et al., 2016

Figure 2-1. Failure of OPC differentiation after white matter stroke
(A) Cell fate mapping using EdU shows increased proliferation in stroke animals (red line) vs. control (blue line), highest in days immediately following injury but continuing up to two weeks. *n* = 5 per group. # $P < 0.0001$, ** $P < 0.001$ 4d vs. other stroke time points. **(B)** Example image shows stroke core (*) with Olig2/EdU positive cells. Inset: double positive cell. **(C)** Percentage of YFP^+ reporter cells that are $NG2^+$ identifies proportion of OPCs that remain in progenitor stage following stroke. **(D)** Percentage of YFP^+ cells that exhibit cytoplasmic Olig1 signal indicate indicates that only a small proportion of OPCs differentiate. *n* = 5-6 per group. ** $P < 0.001$ in (C) and (D). **(E)** Example stain shows cytoplasmic expression of Olig1. Scale bars: 30 µm.

Figure 2-2

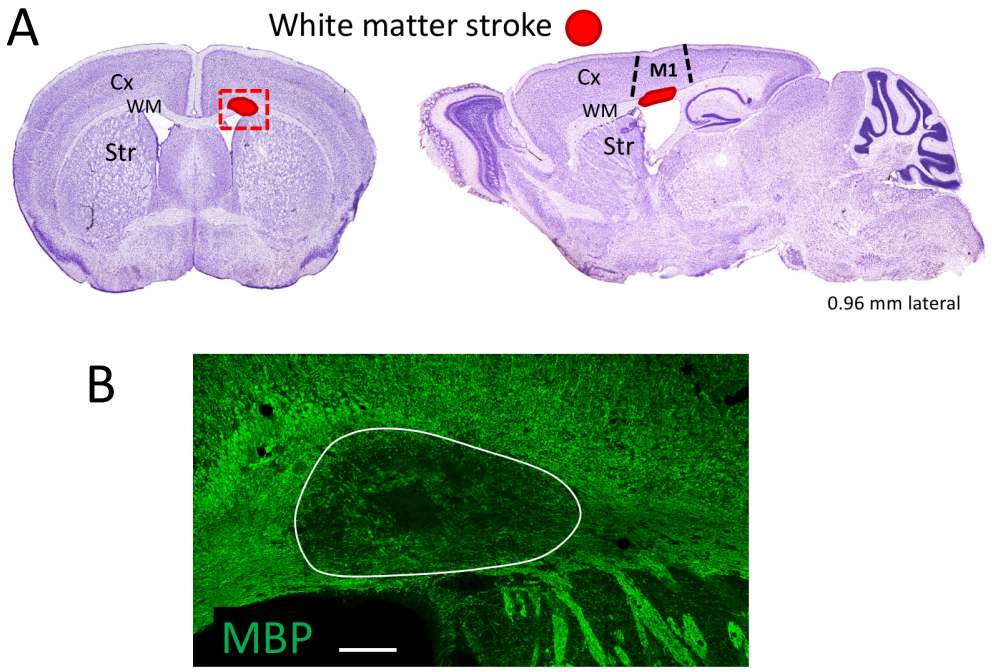

Figure 2-2. The mouse model of white matter stroke
(A) White matter stroke is induced by stereotactic injection of the vasoconstrictor N5-(1-Iminoethyl)-L-ornithine (L-NIO) into a localized area of the corpus callosum below the forelimb motor cortex, as indicated by the red area on the coronal and sagittal sections shown. **(B)** Staining tissue from stroke-induced animals at 5 days post-injury shows a well-demarcated area of demyelination, in the area indicated by the dashed red box from (A). The white line demarcates the area of ischemia as demonstrated by MBP hypointensity. Scale bar: 100 µm.

Figure 2-3

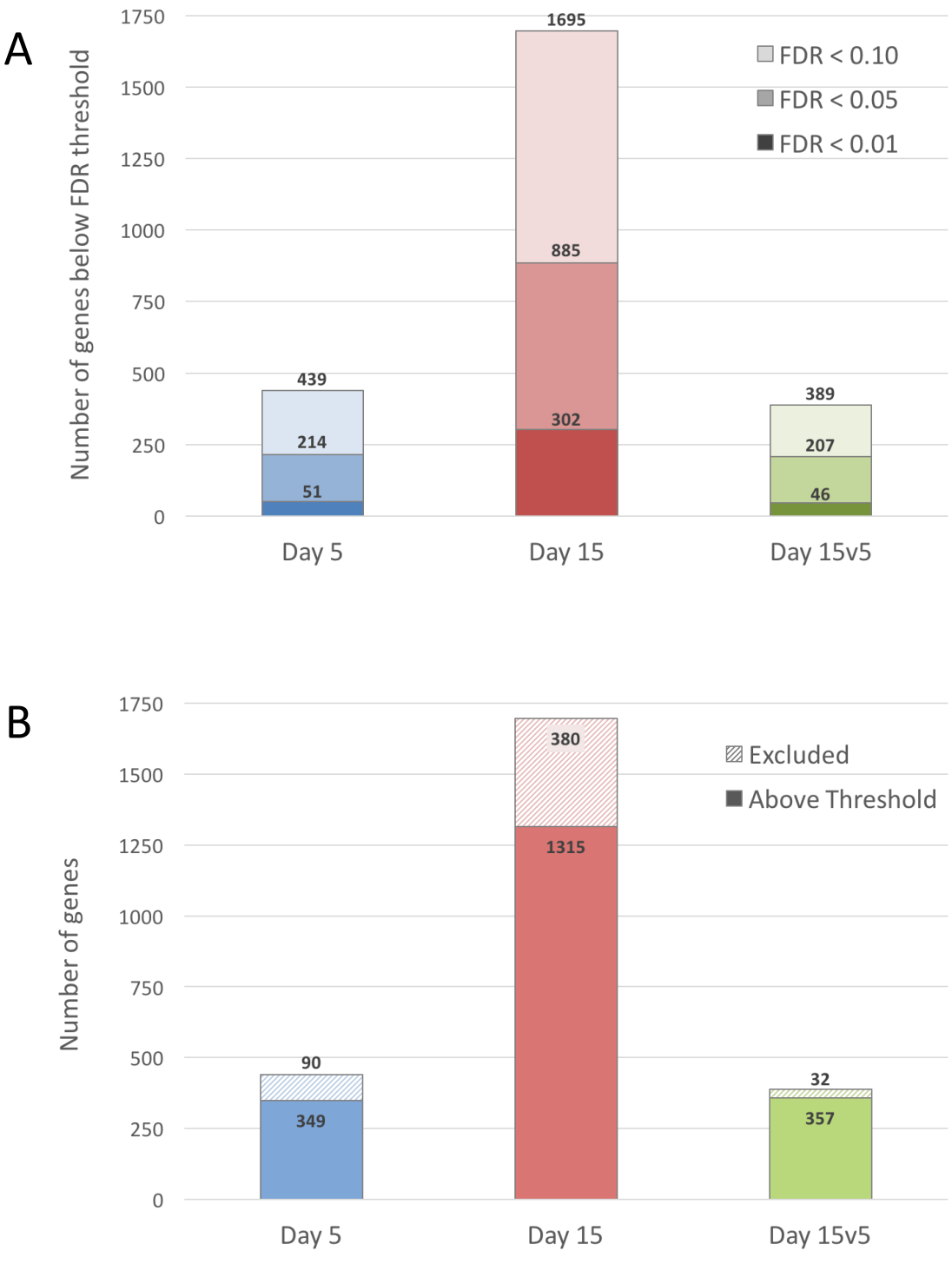
A
Number of genes below FDR threshold
1750
1500
1250
1000
750
500
250
0
439
214
51
1695
885
302
389
207
46
FDR < 0.10
FDR < 0.05
FDR < 0.01
Day 5
Day 15
Day 15v5
B
Number of genes
1750
1500
1250
1000
750
500
250
0
90
349
380
1315
32
357
Excluded
Above Threshold
Day 5
Day 15
Day 15v5

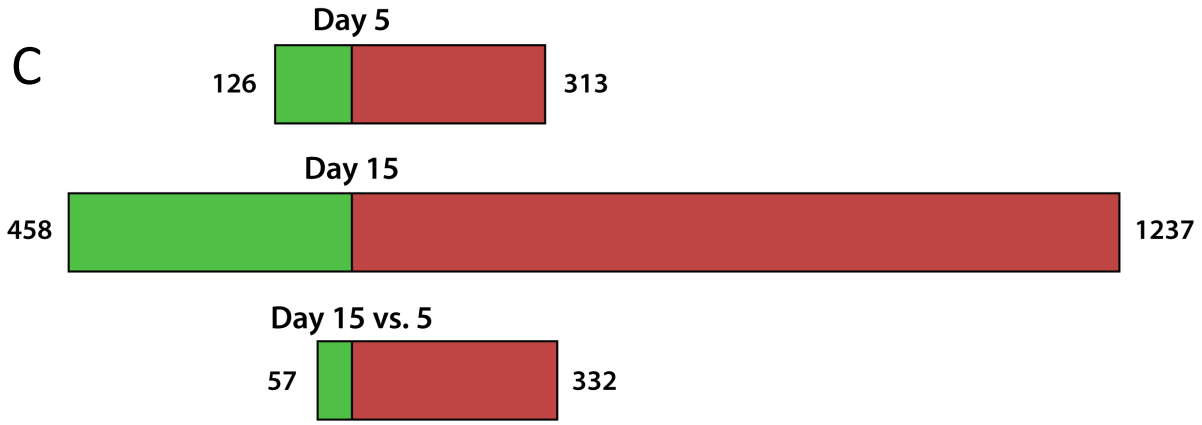

Figure 2-3. FDR and FPKM thresholding of the OPC transcriptome
Bioinformatics analysis led to introduction of two commonly used thresholding techniques to filter for statistically and biologically significant genes. **(A)** The false discovery rate (FDR), comparable to a *P*-value corrected for multiple comparisons, is selected to remove false positives. Different threshold values are shown, with total genes in each group indicated based on the given threshold. Note that "Day 5" refers to the comparison of Day 5 vs. control OPCs. **(B)** Fragments per kilobase of transcript per million reads mapped (FPKM) was calculated and comparisons for which both genes had average FPKM < 1 were excluded. **(C)** Gene expression characteristics with FDR < 0.1. Green bars indicate genes downregulated at the given time point (relative to control unless otherwise indicated), while red bars indicate genes upregulated at that time point.

Figure 2-4

A

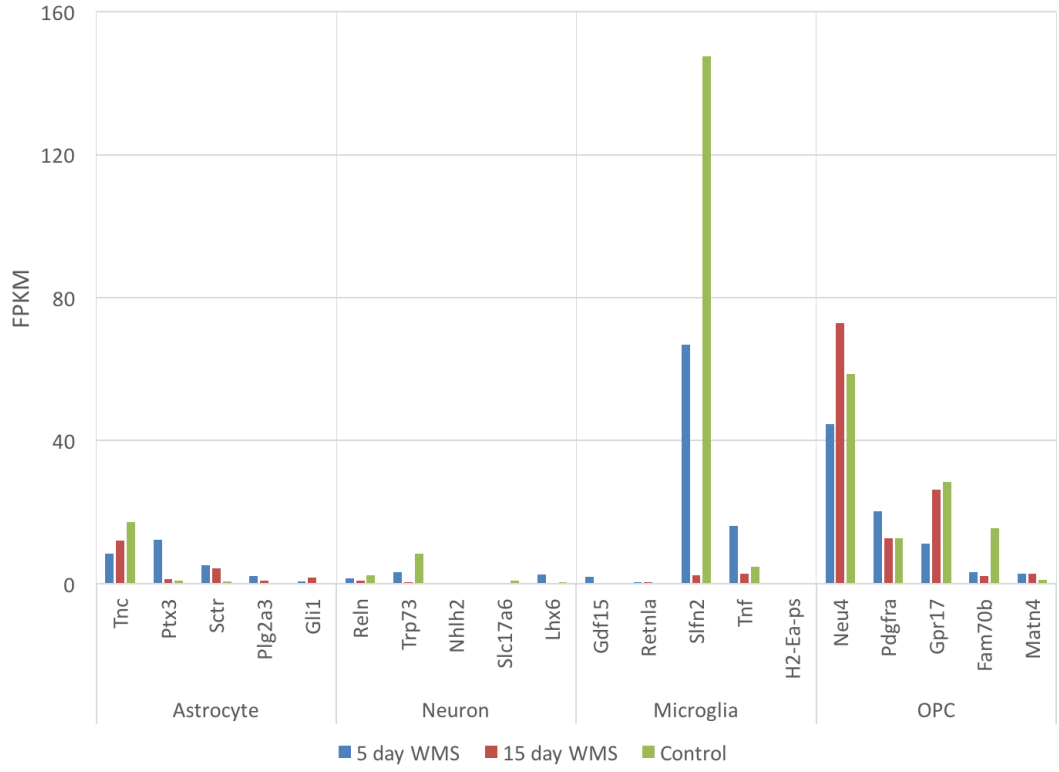
160
120
80
40
0
FPKM
Tnc
Ptx3
Sctr
Plg2a3
Gli1
Reln
Trp73
Nhlh2
Slc17a6
Lhx6
Gdf15
Retnla
Slfn2
Tnf
H2-Ea-ps
Neu4
Pdgfra
Gpr17
Fam70b
Matn4
Astrocyte
Neuron
Microglia
OPC
5 day WMS
15 day WMS
Control

B

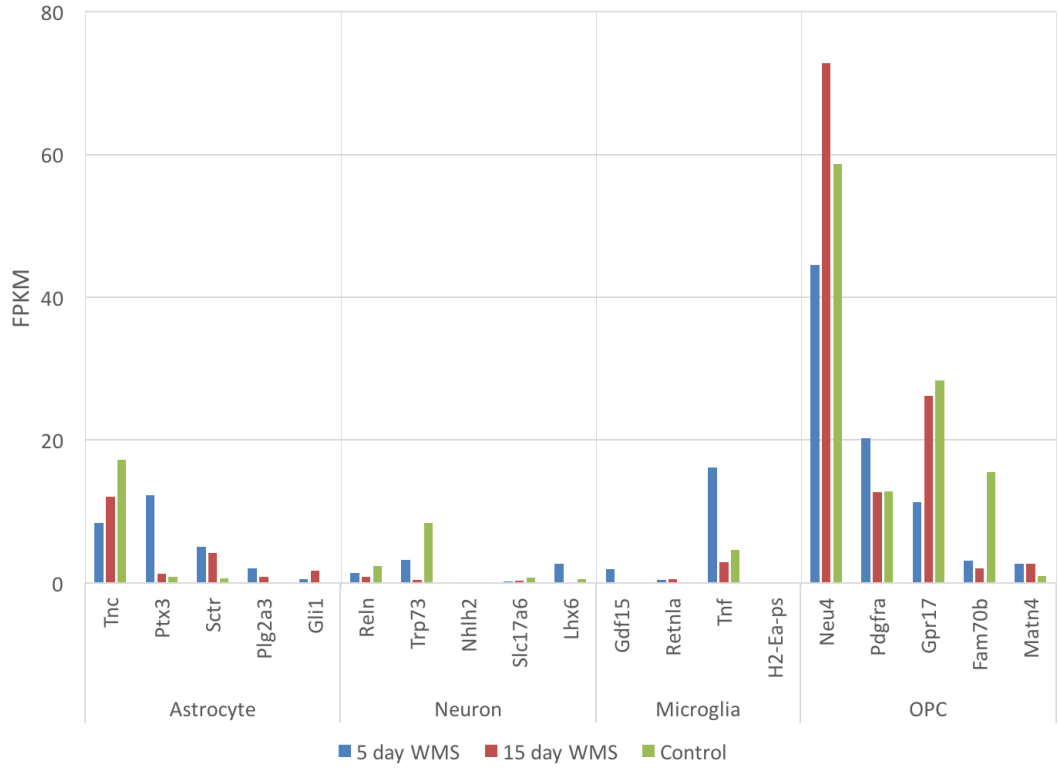
80
60
40
20
0
FPKM
Tnc
Ptx3
Sctr
Plg2a3
Gli1
Reln
Trp73
Nhlh2
Slc17a6
Lhx6
Gdf15
Retnla
Tnf
H2-Ea-ps
Neu4
Pdgfra
Gpr17
Fam70b
Matn4
Astrocyte
Neuron
Microglia
OPC
5 day WMS
15 day WMS
Control

Figure 2-4. Specificity of the OPC stroke transcriptome
To assess the OPC-specificity of the RNA-seq dataset, fragments per kilobase of transcript per million reads mapped (FPKM) data for each of the three treatment groups was compared to the most cell-type specific genes identified in the Barres lab RNA-seq online database (Zhang et al, 2014). **(A)** Unfiltered FPKM values for the top ten most cell-type specific genes of the indicated type (compared to OPCs). **(B)** The same data, but with the data for microglial gene *Slfn2* removed to increase resolution between the remaining cell types. Note the difference in scale for the *y*-axes between the two figures.

Figure 2-5

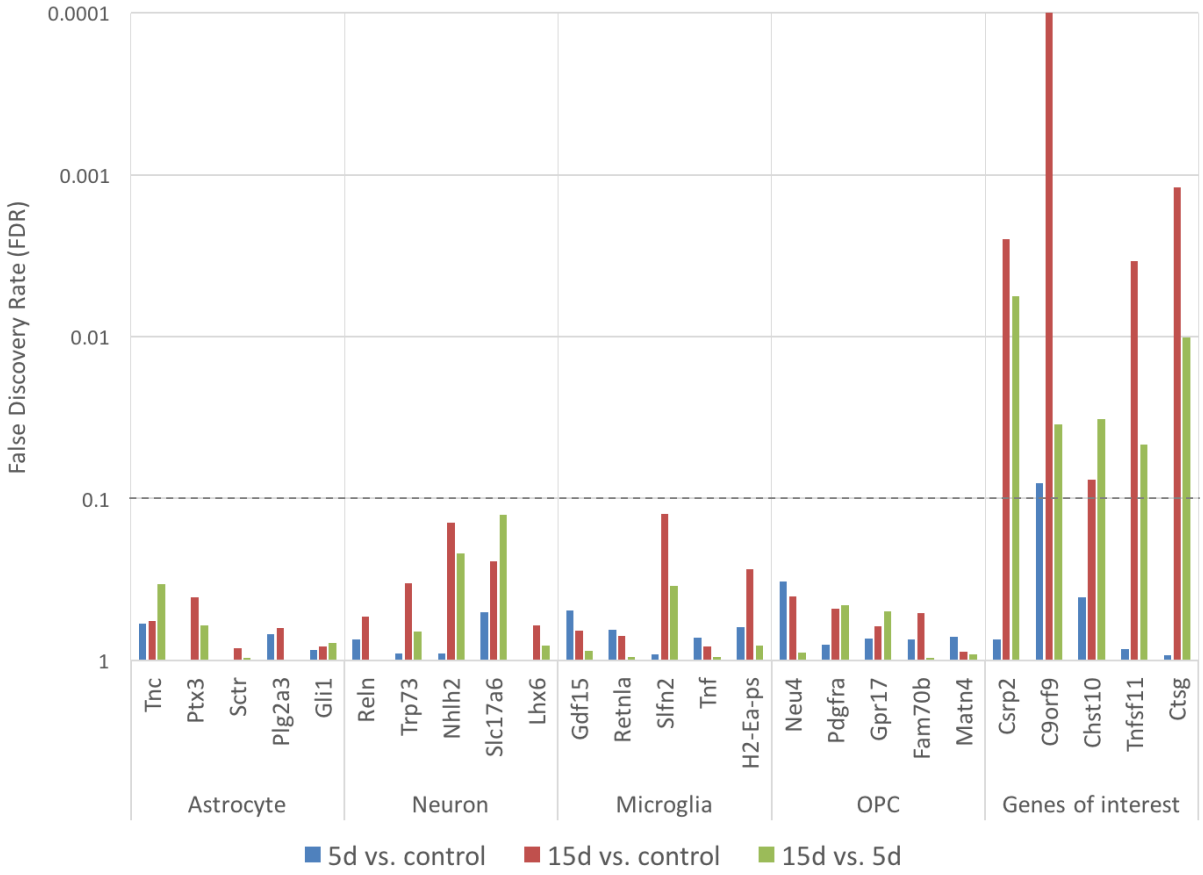

Figure 2-5. Non-oligodendrocyte lineage gene markers are excluded from analysis
To further validate the specificity of the OPC stroke transcriptome, false discovery rate (FDR) values were examined for each of the cell-type enriched genes displayed in **Fig. 2-3**. FDR values are shown for each pairwise comparison: (1) 5 days vs. control; (2) 15 days vs. control, and (3) 15 days vs. 5 days. The *y*-axis is logarithmic to enhance acuity and the threshold used in subsequent analysis (FDR < 0.1) is shown with the dashed line. To the right, for comparison, is a selection of genes of interest studied in subsequent experiments.

Figure 2-6

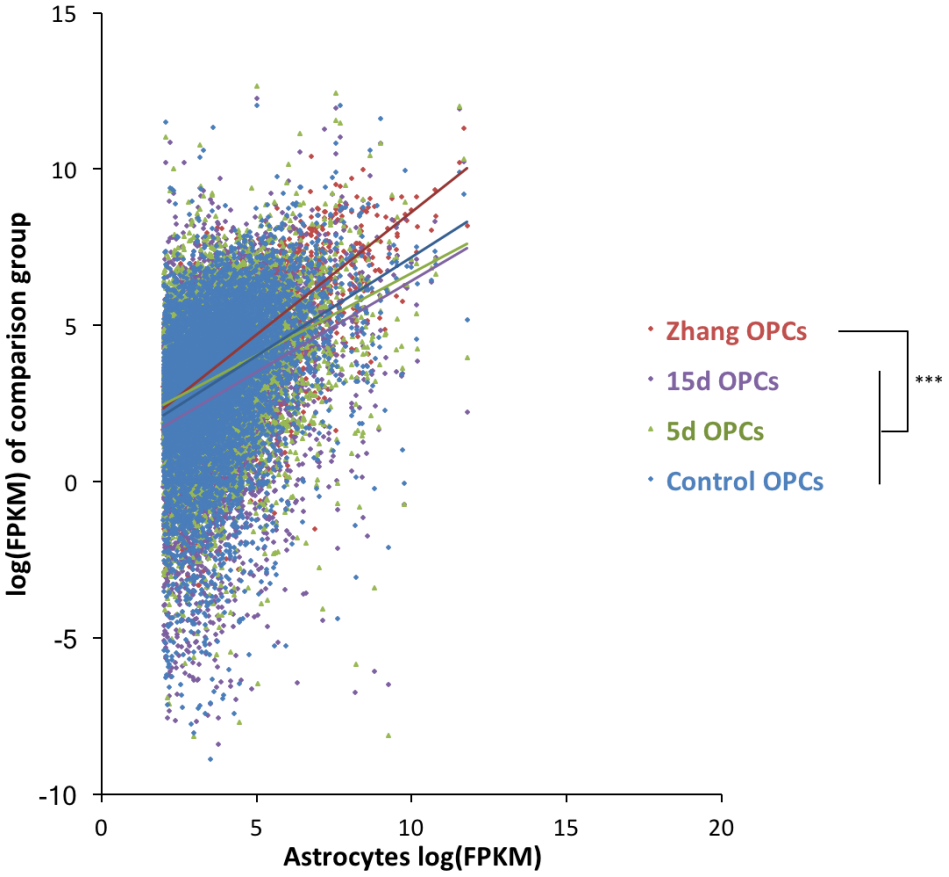

Figure 2-6. Dataset-wide comparison to astrocytes
Every gene in the OPC stroke transcriptome was compared to the set of genes in the Barres lab RNA-seq database for which astrocyte FPKM > 4 (Zhang et al. 2014). FPKM values were $\log_2$-transformed to minimize skew of highly expressed genes and genes with $\log_2$(FPKM) > 2 were selected from the Zhang dataset (n = 7885 genes). These FPKM values were plotted against Zhang OPCs as a baseline association, as well as the OPC stroke transcriptome FPKM values of each group: control, 5 day, and 15 day. For statistical analysis, linear regression tests comparing each distribution. * $P < 0.05$, ** $P < 0.01$, *** $P < 0.001$.

Figure 2-7

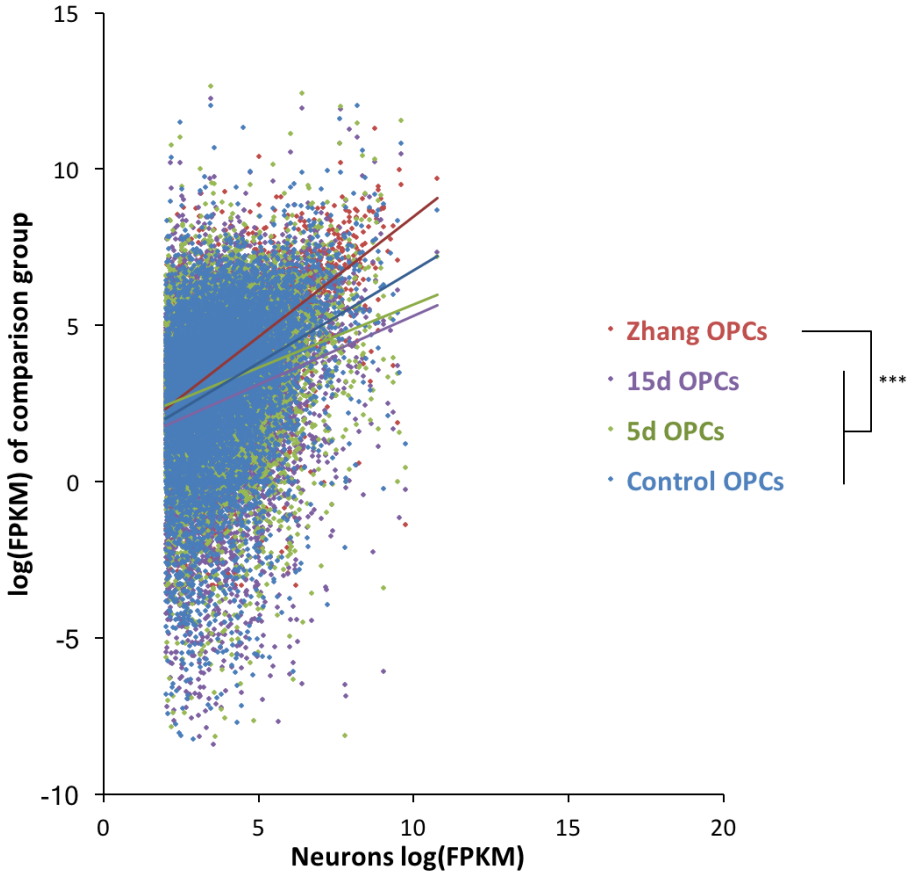

Figure 2-7. Dataset-wide comparison to neurons
Every gene in the OPC stroke transcriptome was compared to the set of genes in the Barres lab RNA-seq database for which neuron FPKM > 4 (Zhang et al. 2014). FPKM values were $\log_2$-transformed to minimize skew of highly expressed genes and genes with $\log_2$(FPKM) > 2 were selected from the Zhang dataset (n = 7926 genes). These FPKM values were plotted against Zhang OPCs as a baseline association, as well as the OPC stroke transcriptome FPKM values of each group: control, 5 day, and 15 day. For statistical analysis, linear regression tests comparing each distribution. * $P < 0.05$, ** $P < 0.01$, *** $P < 0.001$.

Figure 2-8

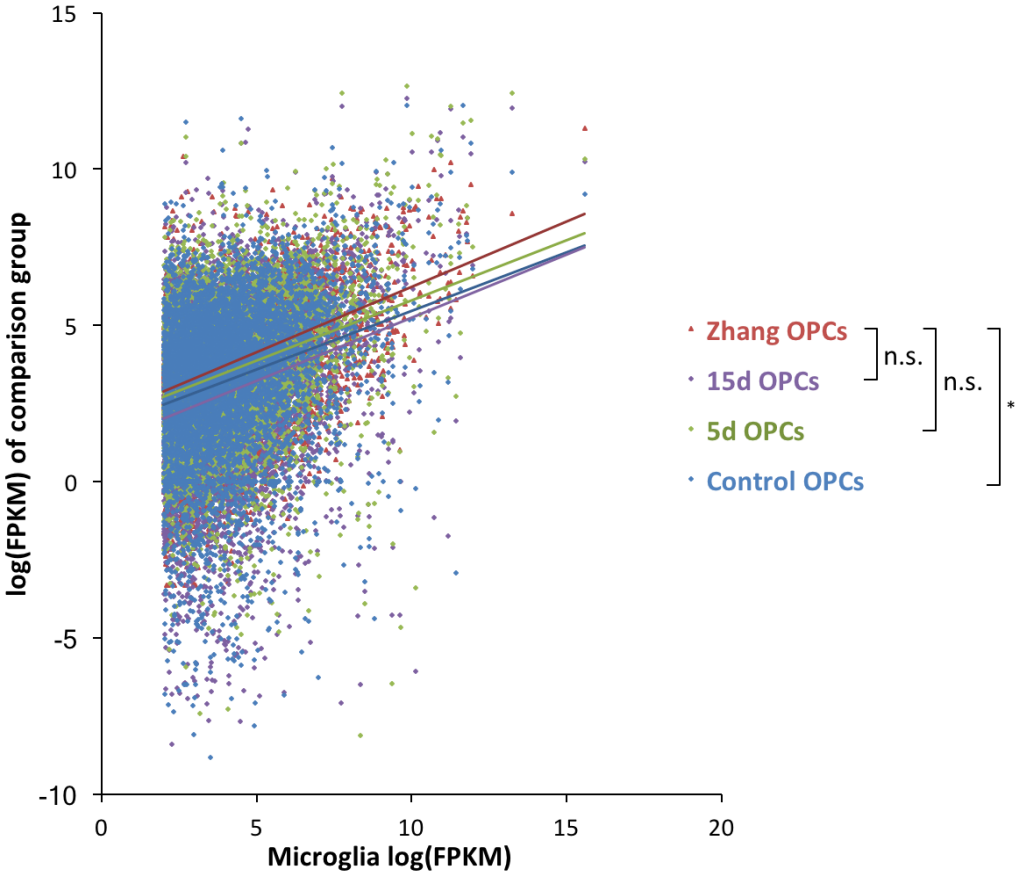

Figure 2-8. Dataset-wide comparison to microglia
Every gene in the OPC stroke transcriptome was compared to the set of genes in the Barres lab RNA-seq database for which microglia FPKM > 4 (Zhang et al. 2014). FPKM values were $\log_2$-transformed to minimize skew of highly expressed genes and genes with $\log_2$(FPKM) > 2 were selected from the Zhang dataset (n = 6162 genes). These FPKM values were plotted against Zhang OPCs as a baseline association, as well as the OPC stroke transcriptome FPKM values of each group: control, 5 day, and 15 day. For statistical analysis, linear regression tests comparing each distribution. * $P < 0.05$, ** $P < 0.01$, *** $P < 0.001$.

Figure 2-9

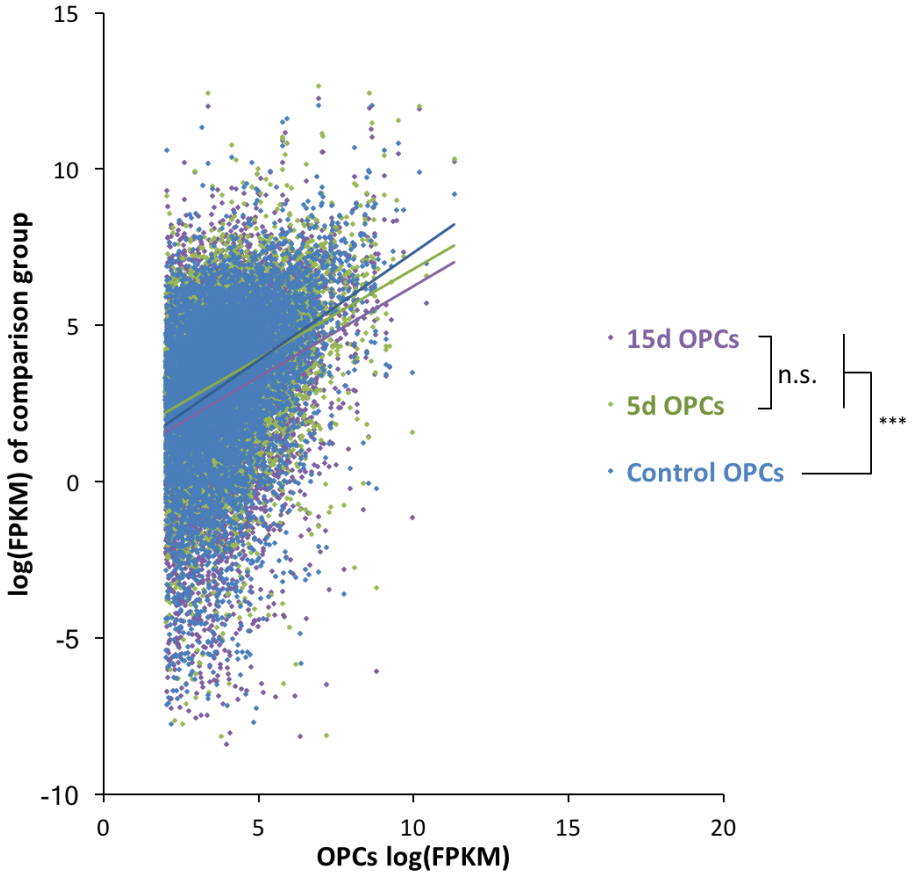

Figure 2-9. Dataset-wide comparison to OPCs
Every gene in the OPC stroke transcriptome was compared to the set of genes in the Barres lab RNA-seq database for which OPC FPKM > 4 (Zhang et al. 2014). FPKM values were $\log_2$-transformed to minimize skew of highly expressed genes and genes with $\log_2$(FPKM) > 2 were selected from the Zhang dataset (n = 8582 genes). These FPKM values were plotted against the OPC stroke transcriptome FPKM values of each group: control, 5 day, and 15 day. For statistical analysis, linear regression tests comparing each distribution. * $P < 0.05$, ** $P < 0.01$, *** $P < 0.001$.

Figure 2-10

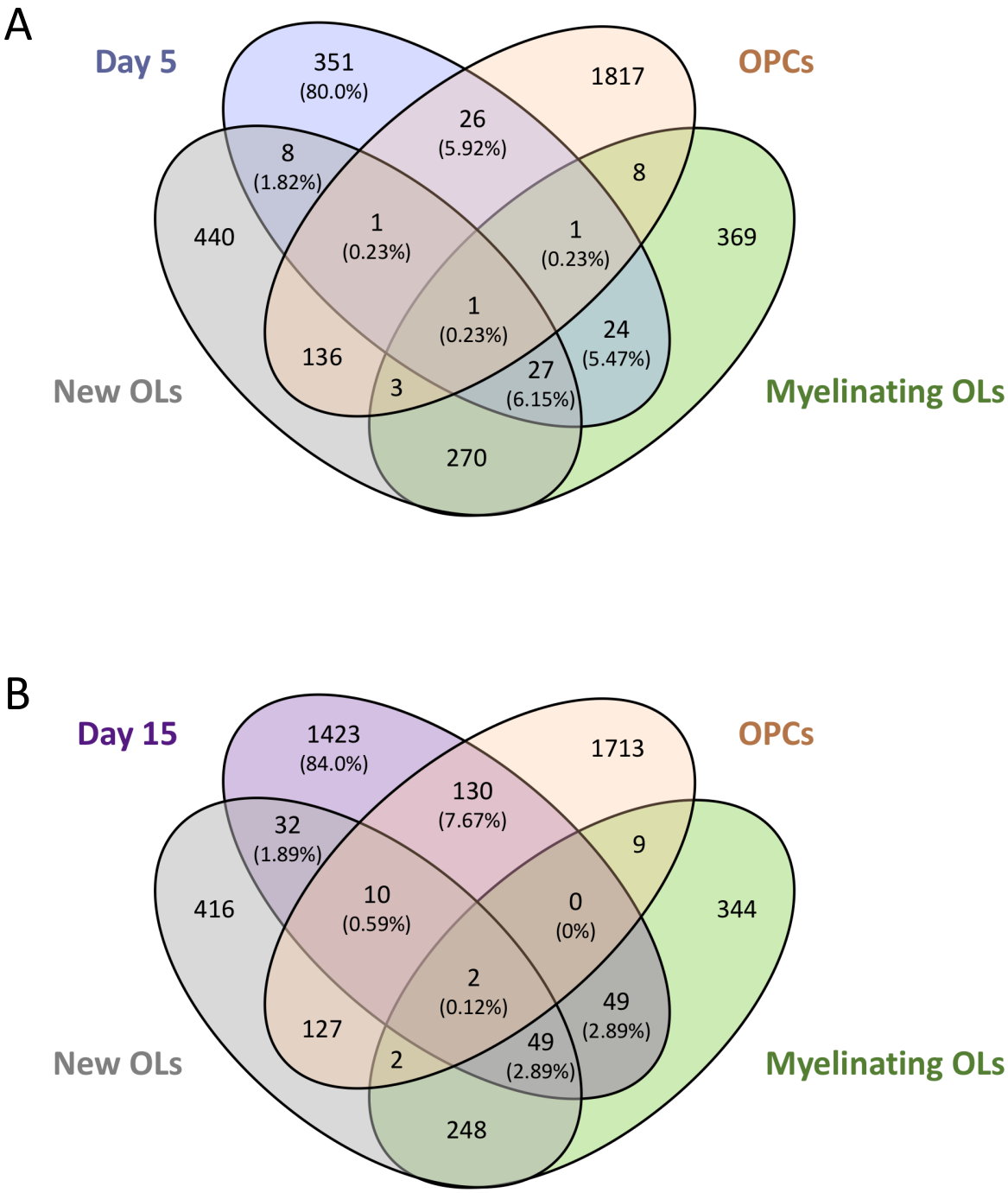
A
Day 5
OPCs
New OLs
Myelinating OLs
351
(80.0%)
1817
26
(5.92%)
8
(1.82%)
8
440
1
(0.23%)
1
(0.23%)
369
1
(0.23%)
24
(5.47%)
136
27
(6.15%)
3
270
B
Day 15
OPCs
New OLs
Myelinating OLs
1423
(84.0%)
1713
130
(7.67%)
32
(1.89%)
9
416
10
(0.59%)
0
(0%)
344
2
(0.12%)
49
(2.89%)
127
49
(2.89%)
2
248

Figure 2-10. Disease specificity of the OPC stroke transcriptome
Significantly overexpressed genes from **(A)** day 5 and **(B)** day 15 versus control OPCs, based on FDR < 0.1, were compared to the Barres dataset (Zhang et al. 2014). Specifically, genes for which FPKM in the indicated cell type was greater than 2-fold higher than the average of all other cell types was included. This led to similar numbers of genes compared between the stroke transcriptome and the Barres data. For each of the zones within the stroke-OPC condition, percentage of the total number of overexpressed genes is indicated.

Table 2-1

Genes of interest selected for further study

Gene	Description	Fold change (15v5)	Putative function	Citation
		Novel genes previously unstudied in OPCs		
Ctsg	Cathepsin G	3,455	Protease found in neutrophils, implicated in processing engulfed pathogens and tissue remodeling	(Shamamian et al., 2001)
Prg2	Proteoglycan 2 Major basic protein	1,075	Component of eosinophil granule core, high basic properties like MBP suggest potential enzyme inhibition	(Gleich et al., 1979; Temkin et al., 2004)
Chst10	Carbohydrate sulfotransferase 10	0.00219	Post-translational processing; HNK-1 synthesis, implicated in steroid hormone and myelin processing	(Bakker, 2014; McGarry et al., 1983)
C9orf9 (Spaca9)	Sperm acrosome associated 9	368	Suggested roles in development and function of cilia and flagella	(Bhattacharya et al., 2013; Stauber et al., 2017)
Zfp474	Zinc finger protein 474	335	Putative transcription factor, previously implicated in germ line cell differentiation	(Zhou et al., 2005)
Olfr652	Olfactory receptor 652	255	G-protein family gene; unknown function	n/a
Penk	Preproenkephalin	252	Precursor to the enkephalin opioids that act as neurotransmitters, as well as other products	(Nissen & Kragballe, 1997; Zagon et al., 1994)
Csrp2	Cysteine and glycine rich protein 2	145	Interacts with transcription factors, implicated in cardiomyocyte development and ordered cell growth	(Sagave et al., 2008)
		Genes implicated in CNS differentiation or myelination		
Mxd1	MAX dimerization protein 1	195	Transcription factor. Other members of this family have demonstrated roles in OPC differentiation	(Y. Yu et al., 2013)
Gpr126	G protein-coupled receptor 126	101	Orphan receptor thought to be required for differentiation of Schwann cells and PNS myelination	(Mogha et al., 2013)
Cxcl13	Chemokine (C-X-C motif) ligand 13	54.7	Chemokine. In MS models, identified in areas of active demyelination	(Weiss et al., 2010; Yuen et al., 2013)
Sall1	Sal-like 1 (Drosophila)	22.7	Transcriptional repressor shown to function in OPC differentiation, not studied in WMS	(Magri et al., 2014)

2.6 References

Anderson, M. A., Burda, J. E., Ren, Y., Ao, Y., O'Shea, T. M., Kawaguchi, R., … Sofroniew, M. V. (2016). Astrocyte scar formation aids central nervous system axon regeneration. *Nature*, *532*(7598), 195–200. https://doi.org/10.1038/nature17623

Arnett, H. A., Stephen P. J. Fancy, Alberta, J. A., Zhao, C., Plant, S. R., Kaing, S., … Stiles, C. D. (2004). bHLH Transcription Factor Olig1 Is Required to Repair Demyelinated Lesions in the CNS. *Science*, *306*, 2111–2115. https://doi.org/10.1126/science.1103709

Bakker, H. (2014). Carbohydrate sulfotransferase 10 (CHST10). In N. Taniguchi, K. Honke, M. Fukuda, H. Narimatsu, Y. Yamaguchi, & T. Angata (Eds.), *Handbook of Glycosyltransferases and Related Genes* (2nd ed., Vol. 1–2, pp. 1–1707). Japan: Springer. https://doi.org/10.1007/978-4-431-54240-7

Benjamini, Y., & Hochberg, Y. (1995). Controlling the false discovery rate: a practical and powerful approach to multiple testing. *Journal of the Royal Statistical Society*. https://doi.org/10.2307/2346101

Bennett, M. L., Bennett, F. C., Liddelow, S. A., Ajami, B., Zamanian, J. L., Fernhoff, N. B., … Barres, B. A. (2016). New tools for studying microglia in the mouse and human CNS. *Proceedings of the National Academy of Sciences*, 201525528. https://doi.org/10.1073/pnas.1525528113

Bhattacharya, R., Devi, M. S., Dhople, V. M., & Jesudasan, R. a. (2013). A mouse protein that localizes to acrosome and sperm tail is regulated by Y-chromosome. *BMC Cell Biology*, *14*, 50. https://doi.org/10.1186/1471-2121-14-50

Chai, H., Diaz-Castro, B., Shigetomi, E., Monte, E., Octeau, J. C., Yu, X., … Khakh, B. S. (2017). Neural Circuit-Specialized Astrocytes: Transcriptomic, Proteomic, Morphological,

and Functional Evidence. *Neuron*, *95*(3), 531–549.e9. https://doi.org/10.1016/j.neuron.2017.06.029

Franklin, R. J. M., & ffrench-Constant, C. (2017). Regenerating CNS myelin — from mechanisms to experimental medicines. *Nature Reviews Neuroscience*, *18*(12), 753–769. https://doi.org/10.1038/nrn.2017.136

Garber, M., Grabherr, M. G., Guttman, M., & Trapnell, C. (2011). Computational methods for transcriptome annotation and quantification using RNA-seq. *Nature Methods*, *8*(6), 469–477. https://doi.org/10.1038/nmeth.1613

Gleich, G. J., Frigas, E., Loegering, D. a, Wassom, D. L., & Steinmuller, D. (1979). Cytotoxic properties of the eosinophil major basic protein. *Journal of Immunology (Baltimore, Md. : 1950)*, *123*(6), 2925–7. Retrieved from http://www.ncbi.nlm.nih.gov/pubmed/501097

He, D., Wang, J., Lu, Y., Deng, Y., Zhao, C., Xu, L., … Lu, Q. R. (2016). lncRNA Functional Networks in Oligodendrocytes Reveal Stage-Specific Myelination Control by an lncOL1/Suz12 Complex in the CNS. *Neuron*, 1–17. https://doi.org/10.1016/j.neuron.2016.11.044

Jiang, K., Sun, X., Chen, Y., Shen, Y., & Jarvis, J. N. (2015). RNA sequencing from human neutrophils reveals distinct transcriptional differences associated with chronic inflammatory states. *BMC Medical Genomics*, *8*(1), 55. https://doi.org/10.1186/s12920-015-0128-7

Li, J., Witten, D. M., Johnstone, I. M., & Tibshirani, R. (2012). Normalization, testing, and false discovery rate estimation for RNA-sequencing data. *Biostatistics*, *13*(3), 523–538. https://doi.org/10.1093/biostatistics/kxr031

Li, S., Nie, E. H., Yin, Y., Benowitz, L. I., Tung, S., Vinters, H. V, … Carmichael, S. T. (2015). GDF10 is a signal for axonal sprouting and functional recovery after stroke. *Nature*

Neuroscience, *18*(12), 1737–1745. https://doi.org/10.1038/nn.4146

Li, S., Overman, J. J., Katsman, D., Kozlov, S. V, Donnelly, C. J., Twiss, J. L., … Carmichael, S. T. (2010). An age-related sprouting transcriptome provides molecular control of axonal sprouting after stroke. *Nature Neuroscience*, *13*(12), 1496–504. https://doi.org/10.1038/nn.2674

Magri, L., Gacias, M., Wu, M., Swiss, V. A., Janssen, W. G., & Casaccia, P. (2014). c-Myc-dependent transcriptional regulation of cell cycle and nucleosomal histones during oligodendrocyte differentiation. *Neuroscience*, *276*, 72–86. https://doi.org/10.1016/j.neuroscience.2014.01.051

Marques, S., Zeisel, A., Codeluppi, S., Bruggen, D. Van, Falcão, A. M., Xiao, L., … Castelo-branco, G. (2016). Oligodendrocyte heterogeneity in the mouse juvenile and adult central nervous system. *Science*, *352*(6291), 1326–9.

Matejuk, A., & Hopke, C. (2003). CNS gene expression pattern associated with spontaneous experimental autoimmune encephalomyelitis. *Journal of Neuroscience Research*, *678*(April), 667–678. Retrieved from http://onlinelibrary.wiley.com/doi/10.1002/jnr.10689/full

Mavrommatis, E., Fish, E. N., & Platanias, L. C. (2013). The Schlafen Family of Proteins and Their Regulation by Interferons. *Journal of Interferon & Cytokine Research*, *33*(4), 206–210. https://doi.org/10.1089/jir.2012.0133

McGarry, R. C., Helfand, S. L., Quarles, R. H., & Roder, J. C. (1983). Recognition of myelin-associated glycoprotein by the monoclonal antibody HNK-1. *Nature*, *306*, 376–378.

Mogha, A., Benesh, A. E., Patra, C., Engel, F. B., Schöneberg, T., Liebscher, I., & Monk, K. R. (2013). Gpr126 functions in Schwann cells to control differentiation and myelination via G-

protein activation. *The Journal of Neuroscience : The Official Journal of the Society for Neuroscience*, *33*(46), 17976–85. https://doi.org/10.1523/JNEUROSCI.1809-13.2013

Nave, K.-A. (2010). Myelination and support of axonal integrity by glia. *Nature*, *468*(7321), 244–252. https://doi.org/10.1038/nature09614

Nishiyama, A., Komitova, M., Suzuki, R., & Zhu, X. (2009). Polydendrocytes (NG2 cells): multifunctional cells with lineage plasticity. *Nature Reviews Neuroscience*, *10*(1), 9–22. https://doi.org/10.1038/nrn2495

Nissen, J. B., & Kragballe, K. (1997). Enkephalins modulate differentiation of normal human keratinocytes in vitro. *Experimental Dermatology*, *6*(5), 222–229. https://doi.org/10.1111/j.1600-0625.1997.tb00166.x

Novarino, G., Fenstermaker, A. G., Zaki, M. S., Hofree, M., Silhavy, J. L., Heiberg, A. D., … Gleeson, J. G. (2014). Exome Sequencing Links Corticospinal Neurodegenerative Disorders. *Science*, *343*(January), 506–11.

Overman, J. J., Clarkson, A. N., Wanner, I. B., Overman, W. T., Eckstein, I., Maguire, J. L., … Carmichael, S. T. (2012). A role for ephrin-A5 in axonal sprouting, recovery, and activity-dependent plasticity after stroke. *Proceedings of the National Academy of Sciences of the United States of America*, *109*(33), E2230-9. https://doi.org/10.1073/pnas.1204386109

Ozsolak, F., & Milos, P. M. (2011). RNA sequencing: advances, challenges and opportunities. *Nature Reviews Genetics*, *12*(2), 87–98. https://doi.org/10.1038/nrg2934

Paxinos, G., & Watson, K. B. J. (2001). *The Mouse Brain in Stereotaxic Coordinates 2nd ed.* San Diego: Academic Press.

Sagave, J. F., Moser, M., Ehler, E., Weiskirchen, S., Stoll, D., Günther, K., … Weiskirchen, R. (2008). Targeted disruption of the mouse Csrp2 gene encoding the cysteine- and glycine-

rich LIM domain protein CRP2 result in subtle alteration of cardiac ultrastructure. *BMC Developmental Biology*, *8*, 80. https://doi.org/10.1186/1471-213X-8-80

Shamamian, P., Schwartz, J. D., Pocock, B. J. Z., Monea, S., Whiting, D., Marcus, S. G., & Mignatti, P. (2001). Activation of progelatinase A (MMP-2) by neutrophil elastase, cathepsin G, and proteinase-3: A role for inflammatory cells in tumor invasion and angiogenesis. *Journal of Cellular Physiology*, *189*(2), 197–206. https://doi.org/10.1002/jcp.10014

Sozmen, E. G. (2013). *Remyelination failure following white matter stroke: new targets for repair identified by oligodendrocyte progenitor cell transcriptome database*. University of California, Los Angeles.

Sozmen, E. G., Rosenzweig, S., Llorente, I. L., DiTullio, D. J., Machnicki, M., Vinters, H. V., … Carmichael, S. T. (2016). Nogo receptor blockade overcomes remyelination failure after white matter stroke and stimulates functional recovery in aged mice. *Proceedings of the National Academy of Sciences*, *113*(52), E8453–E8462. https://doi.org/10.1073/pnas.1615322113

Stauber, M., Weidemann, M., Dittrich-Breiholz, O., Lobschat, K., Alten, L., Mai, M., … Gossler, A. (2017). Identification of FOXJ1 effectors during ciliogenesis in the foetal respiratory epithelium and embryonic left-right organiser of the mouse. *Developmental Biology*, *423*(2), 170–188. https://doi.org/10.1016/j.ydbio.2016.11.019

Temkin, V., Aingorn, H., Puxeddu, I., Goldshmidt, O., Zcharia, E., Gleich, G. J., … Levi-Schaffer, F. (2004). Eosinophil major basic protein: First identified natural heparanase-inhibiting protein. *Journal of Allergy and Clinical Immunology*, *113*(4), 703–709. https://doi.org/10.1016/j.jaci.2003.11.038

Toung, J. M., Morley, M., Li, M., & Cheung, V. G. (2011). RNA-sequence analysis of human B-cells. *Genome Research*, *21*, 991–998. https://doi.org/10.1101/gr.116335.110.21

Trapnell, C., Williams, B. A., Pertea, G., Mortazavi, A., Kwan, G., van Baren, M. J., … Pachter, L. (2010). Transcript assembly and quantification by RNA-Seq reveals unannotated transcripts and isoform switching during cell differentiation. *Nature Biotechnology*, *28*(5), 511–515. https://doi.org/10.1038/nbt.1621

Wang, Z., Gerstein, M., & Snyder, M. (2009). RNA-Seq: a revolutionary tool for transcriptomics. *Nature Reviews Genetics*, *10*(1), 57–63. https://doi.org/10.1038/nrg2484

Weiss, N., Deboux, C., Chaverot, N., Miller, F., Baron-Van Evercooren, A., Couraud, P.-O., & Cazaubon, S. (2010). IL8 and CXCL13 are potent chemokines for the recruitment of human neural precursor cells across brain endothelial cells. *Journal of Neuroimmunology*, *223*(1–2), 131–4. https://doi.org/10.1016/j.jneuroim.2010.03.009

Yu, T. W., Chahrour, M. H., Coulter, M. E., Jiralerspong, S., Okamura-Ikeda, K., Ataman, B., … Walsh, C. a. (2013). Using whole-exome sequencing to identify inherited causes of autism. *Neuron*, *77*(2), 259–73. https://doi.org/10.1016/j.neuron.2012.11.002

Yu, Y., Chen, Y., Kim, B., Wang, H., Zhao, C., He, X., … Lu, Q. R. (2013). Olig2 targets chromatin remodelers to enhancers to initiate oligodendrocyte differentiation. *Cell*, *152*(1–2), 248–61. https://doi.org/10.1016/j.cell.2012.12.006

Yuen, T. J., Johnson, K. R., Miron, V. E., Zhao, C., Quandt, J., Harrisingh, M. C., … Ffrench-Constant, C. (2013). Identification of endothelin 2 as an inflammatory factor that promotes central nervous system remyelination. *Brain : A Journal of Neurology*, *136*(Pt 4), 1035–47. https://doi.org/10.1093/brain/awt024

Zagon, I. S., Isayama, T., & McLaughlin, P. J. (1994). Preproenkephalin mRNA expression in

the developing and adult rat brain. *Brain Res Mol Brain Res*, *21*(1–2), 85–98. Retrieved from http://www.ncbi.nlm.nih.gov/pubmed/8164525

Zamanian, J. L., Xu, L., Foo, L. C., Nouri, N., Zhou, L., Giffard, R. G., & Barres, B. A. (2012). Genomic Analysis of Reactive Astrogliosis. *Journal of Neuroscience*, *32*(18), 6391–6410. https://doi.org/10.1523/JNEUROSCI.6221-11.2012

Zhang, Y., Chen, K., Sloan, S. A., Bennett, M. L., Scholze, A. R., Keeffe, S. O., … Wu, X. J. Q. (2014). An RNA-Sequencing Transcriptome and Splicing Database of Glia, Neurons, and Vascular Cells of the Cerebral Cortex. *The Journal of Neuroscience : The Official Journal of the Society for Neuroscience*, *34*(36), 1–19. https://doi.org/10.1523/JNEUROSCI.1860-14.2014

Zhao, X., He, X., Han, X., Yu, Y., Ye, F., Chen, Y., … Lu, Q. R. (2010). MicroRNA-Mediated Control of Oligodendrocyte Differentiation. *Neuron*, *65*(5), 612–626. https://doi.org/10.1016/j.neuron.2010.02.018

Zhou, C., Li, L.-Y., & Lu, G.-X. (2005). Molecular cloning and character analysis of the mouse zinc finger protein Zfp474 exclusively expressed in testis and ovary. *Acta Genetica Sinica*, *32*(2), 155–162.

Chapter 3

Development of an *in vitro* screen to assess impact of candidate genes on OPC differentiation

3.1 Introduction

Based on bioinformatics analysis of the transcriptome dataset described in Chapter 2, a list of candidate genes has been generated (**Table 2-1**). This list is balanced between those with known roles in oligodendrogenesis and myelination, and totally novel genes previously unstudied in the nervous system, or to our knowledge, at all since their initial annotation within the genome. This provides a strong foundation to drive new discoveries in oligodendrocyte biology, but it also presents a technical challenge: the list of genes is too long to study each mechanistically *in vivo* within a reasonable time frame. Furthermore, as discussed in Chapter 2, additional verification steps are important to validate the gene list as relevant to oligodendrocyte biology. Thus, an additional screening tool was necessary to prioritize this gene list, identifying the select group of highly promising genes which can be studied in depth in our animal model of WMS.

Motivated by this need, a pair of experiments were developed, combining *in vivo* expression studies with *in vitro* genetic manipulation. In the first stage, immunohistochemical stains on brain tissue of both control and stroke-induced animals were performed using antibodies for each protein product, a process that has been routinely used to validate RNA-sequencing results in the field (Anderson et al., 2016; Solga et al., 2014). Examining gene expression in the same model and at the same time points as were used to generate the RNA-seq

data aimed to validate expression of proteins in oligodendrocyte lineage cells in tissue, in either normal physiology or post-stroke. Ideally, this would provide confirmation of transcriptomic data insofar as genes were identified within OPCs and not contaminating cells, without any need for quantification, which would be left to subsequent experiments.

In addition to validating results and visualizing expression in control vs. stroke tissue, a complement of *in vitro* experiments will provide the ability to quantify each gene's impact on differentiation. Such approaches have been a powerful tool to examine oligodendrocyte differentiation, as they grow robustly in culture and are easily manipulated to maintain OPC state or differentiate into oligodendrocytes and even myelinate when desired (Emery & Dugas, 2013; Espinosa-Jeffrey et al., 2009). Two main culture systems are used to provide control over timing of experiments.

Two complementary culture systems

CG-4 cells were generated from rat OPC cultures by spontaneous transformation and have been well-characterized (Louis et al., 1992; Stariha & Kim, 2001). Furthermore, as a cell line, they can be produced in large numbers to facilitate high-throughput testing, and have been used in this way in previous studies (Suzuki et al., 2012; Ueno et al., 2012; Wang et al., 2009). Finally, they recapitulate key oligodendrocyte properties, showing capacity to differentiate and myelinate both *in vitro* and upon transplantation into the brain of rodent models (Espinosa de los Monteros et al., 2001; Olby & Blakemore, 1996).

In addition to the CG-4 line, primary OPC cultures are used to provide further characterization of behavior of these cells. The immunopanning technique developed and refined by the Barres lab provides a method to culture primary OPCs for immediate study less than 8

hours from animal sacrifice, minimizing time *ex vivo* compared to other culture preparation methods such as differential shaking, which involves preparation over ten days or more prior to initiating experiments (Chen et al., 2007; Emery & Dugas, 2013). Primary OPC cultures can be manipulated genetically using commercially available transfection reagents, making them tractable tools to study gene-specific effects on differentiation pathways in an isolated system (Bischof et al., 2015).

On the basis of these two well-established culture techniques, we initiated a series of tests to prioritize each gene of interest based on its propensity to either enhance or repress OPC differentiation in pure cultures. A series of experiments are presented below, along with challenges and subsequent adjustments, that provided the basis to initiate *in vivo* studies on a selection of three promising genes as outlined in Chapters 4 and 5. This represents the first step in an experimental flow focused on identifying novel mechanisms of oligodendrogenesis in WMS, the overarching goal of this dissertation (**Figure 3-1**).

3.2 Results

Validation of target gene expression in stroke tissue

The same mouse model of WMS used to generate the RNA-seq transcriptome was used to assess expression of candidate genes in oligodendrocyte lineage cells through immunohistochemistry. Briefly, WMS was induced by injection of the vasoconstrictor L-NIO (see Methods). Animals were sacrificed at either 5 days or 15 days post-surgery (control animals were sacrificed at the 5 day time point).

Tissue stains were carried out using a standard protocol (Sozmen et al., 2016; and Methods). To assess expression of each gene of interest within oligodendrocyte lineage cells,

antibodies were obtained when available and tested for optimal fluorescence as outlined in Methods. Summary images of the expression testing for a selection of key genes is shown in **Figure 3-2**.

As shown in the figure, genes showed variable evidence of expression in OPCs following white matter stroke. Overall quality was limited by novelty of the antibodies against candidate proteins, so high background or variable expression was a common issue. Notably, no quantification was carried out on these images, given both the quality of staining and the desire to use these studies only as a preliminary check for expression. In some cases, however, antibodies identified expression of a candidate gene in some cells, but not oligodendrocytes as marked by Olig2; or, they indicated expression in oligodendrocytes but with no discernable expression in OPCs after stroke. In such cases, those genes were not pursued further. However, when no staining was possible with a given gene construct, or when no antibody was available, studies continued to the next screening stage, and alternate validation options were pursued.

CG-4 and primary OPC screen validation

The CG4-16 clonal line of original CG-4 cells was a generous gift from the Ogata group (Ueno et al., 2012). Cultures were first validated by expression of key oligodendrocyte markers, including the transcription factor Olig2 and mature marker CC1 (**Figure 3-3**). Not only are these markers expressed, but treatment with differentiation media appears to enhance expression of the mature marker CC1 while also leading to cell growth an increased branching complexity, a hallmark of oligodendrocyte differentiation (Barratt et al., 2016).

The first approach to assessing CG4-16 differentiation, to validate its use as a screening tool, involved morphologic quantification. As a rapid test, epifluorescent imaging is readily

available. Staining against the early differentiation marker CNPase and quantifying fluorescence relative to actin expression, to normalize to cell size, was an ideal and straightforward study. Pilot tests utilized two treatment conditions in combination: first, triiodothyronine (T_3), is known to be a potent inducer of OPC differentiation (Dugas & Emery, 2013). Second, the extracellular matrix protein matrilin-2 was known by our group to play a role in differentiation, so validation of this result would verify this system as a screening tool in our hands (see Chapter 5). A time series experiment was undergone to quantify capacity of CG-4 cells to differentiation over time, the results of which are shown in **Figure 3-4**. These results indicate that, while there was some effect with combined treatment of matrilin-2 and T_3, the positive control of differentiation media vs. proliferation media did not show a significant difference, rendering this method unreliable for assessing meaningful differentiation.

At this point, several variations were tried with the media, and results were also compared with primary OPC cultures which had been successfully started. The first option tried was to use Sholl analysis to analyze increases in morphologic complexity, a known marker of OPC differentiation (Ferreira et al., 2014; Gensel et al., 2010). However, these results also indicated lack of power in using the CG4-16 cell line, using multiple media formulations, especially when compared to primary OPC cultures (**Figure 3-5**).

For a faster and more accurate readout of coordinated changes to gene expression, we explored the use of qPCR, a method increasingly used to assess OPC differentiation, especially as genetic markers for stages along the spectrum of oligodendrocyte development are well-described (Zhang et al., 2014). To this end, qPCR was tested as a third option for differentiation studies *in vitro*, again using both primary OPC cultures and CG4-16 cells. Primers were developed against both OPC-specific genes (*Cspg4* and *Pdgfra*) and differentiation-specific

genes (*Cnp*, *Mbp*, *Plp1*). The hypothesis is thus that upon differentiation, *Cspg4* and *Pdgfra* expression decreases, while *Cnp*, *Mbp*, and *Plp1* expression increases. Results of positive control tests are shown in **Figure 3-6**. In short, CG-4 cells do not show this hypothesized response, even when grown in the same serum-free media shown to support primary OPC cultures. Conversely, primary OPC cultures show highly significant and reproducible responses to induction of differentiation with the positive control T_3. This suggests that primary OPC cultures are a reliable tool to use to assess differentiation of OPCs in culture, while CG-4 cells are not.

Inducing expression of candidate genes

To overexpress candidate genes in primary OPC cultures, we generated a plasmid expression vector driving expression of the gene of interest containing a dual promoter system driving (1) expression of the gene of interest under an EF1 promoter, and (2) TagBFP2 under the CMV promoter (**Figure 3-7**). This enabled additional fluorescence studies if desired, and provided a flexible system for switching CANDIDATE GENEs out when necessary with minimal cloning. Gene sequences were obtained from Origene; specifically, mouse ORFs for each gene were available, while rat sequences were not. Since the goal was ultimately to bring promising genes *in vivo* in a mouse model, mouse ORFs were used. OPCs were transfected after two days in proliferation media to stabilize, using a polymer-based reagent (Xfect, Clontech), which we have found to have 55-60% transfection efficiency in primary OPCs (data not shown).

Csrp2 was the first gene tested with this system, and the first step was to validate that the construct led to significant overexpression of the gene. Three different qPCR primers were designed against *Csrp2*, one of which was designed to be specific to the mouse *Csrp2* mRNA sequence and the other two in areas of high homology between mouse and rat *Csrp2*. qPCR

assays of these test primers, 3 days after transfection with control plasmid versus *Csrp2-TagBFP2*, are shown in **Figure 3-8**. This verifies that the dual promoter plasmids significantly overexpress the genes of interest.

Effect of overexpression of genes of interest on OPC differentiation

With a validated tool available to induce expression of each gene of interest, a series of tests were performed to assess the effect of each gene of interest on OPC differentiation. In short, OPCs were transfected after two days in culture, and mRNA was extracted 4 days after transfection. The results are summarized in **Figure 3-9**. As is seen in the figure, there is a clear gradation of response to overexpression of CANDIDATE GENEs, with certain genes showing response and others with no significant difference to control. Furthermore, most genes show inversely correlative responses between proliferation markers and differentiation markers as seen in **Fig. 3-9B** and **Fig. 3-9C**, as would be hypothesized if cells were undergoing differentiation. Thus, these results provide strong evidence that a number of genes act to directly induce oligodendrocyte differentiation endogenously and provide a basis for the selection of genes to study *in vivo*, in the context of white matter stroke.

Knockdown of genes of interest

In addition to overexpressing each gene of interest, constructs were developed to attempt to knock down expression. This would allow for the detection of genes whose effect was to inhibit differentiation, rather than promote it as seen in the previous experiments. To do this, a set of microRNA constructs was developed for each gene using the BLOCK-iT system (Thermo Fisher). The plasmid schematic is shown in **Figure 3-10**. As in the overexpression studies, a

ubiquitous promoter drives expression of a microRNA construct, along with emGFP as a marker of transfection.

The first gene for which constructs were designed was *Csrp2*. This was done using the manufacturer primer designing software, with some adjustments. First, the two best predicted constructs were chosen, but these were noted to be specific to a region of low homology between mouse and rat *Csrp2* regions. Because constructs may be moved *in vivo*, additional targets were designed against regions of high homology, using the manufacturer's software but selecting for specific regions. This approach ideally maximizes knockdown *in vitro* as a validation step while also generating constructs that have utility *in vivo* (**Figure 3-11**). Assessment of *Csrp2* mRNA knockdown was tested for each microRNA (**Fig. 3-11B**). Results of these qPCR expreiments suggested that primers induce significant knockdown of the primers, of approximately 70-80% as judged by qPCR across three different primers against *Csrp2*.

Experiments were then conducted on primary OPC cultures to assess differentiation of OPCs after gene knockdown. Results are shown in **Figure 3-12**. Early time course studies indicate that in particular, expression of *Mbp* (a marker of early oligodendrocyte differentiation) is decreased in miRNA-treated cells as compared to controls over 2-3 days following addition of differentiation media. However, as seen in **Fig. 3-12B**, subsequent studies targeting this time point did not show similar results. Further studies are ongoing to attempt to ascertain the most effective setup to identify changes to differentiation following miRNA treatment.

3.3 Discussion

Development of an in vitro *screening system*

In this study, we explored a number of methodologies to assess propensity of candidate genes to induce or inhibit OPC differentiation using *in vitro* systems to reduce time and cost prior to initiating *in vivo* mechanistic studies. An oligodendrocyte-derived cell line, CG4-16, was explored as one avenue, but results indicated it lacked a robust response to differentiation signals and thus was not an ideal tool. Rather, primary OPCs have been successfully used throughout the field to assess response in a closed system to different factors (Back et al., 2005; He et al., 2016; Madsen et al., 2016; Sloane et al., 2010). Use of this system to overexpress candidate genes proved successful, and we saw a substantial differentiation effect for a majority of the genes tested (**Fig. 3-9**). On the other hand, knockdown experiments using miRNA constructs produced mixed results (**Fig. 3-12**). The result is that we have a strong list of candidates that play a role in facilitated oligodendrocyte differentiation, but lack a piece of the biological puzzle to (1) judge their necessity for differentiation and (2) identify genes that are involved in inhibition, rather than promotion, of differentiation.

Despite the challenges encountered particularly in the knockdown experiments, a number of promising questions arose that warrant testing in a complex biological system. For this reason, *in vivo* studies were initiated with a number of promising candidates identified through these experiments. The process of selecting those genes will be discussed in Chapter 4.

Validating gene expression in stroke tissue

The first set of experiments described here was the validation of expression of candidate genes in WMS tissue and specifically in oligodendrocytes. As noted in **Table 2-1**, a number of

these genes were completely novel to the field and had not been previously studied beyond investigation as part of a large-scale genetic study. Thus, many of the genes, and in particular the novel genes, did not have commercially available antibodies. Thus, in some cases validation was not possible. Even in those antibodies that did show expression, many had issues of quality, particularly in post-stroke tissue where background tends to be higher than in control. For example, although some co-localization with $Olig2^{+}$ cells was identified, for example when staining for Csrp2, expression was low and visual comparison between control and stroke tissue was difficult due to differences in background under the same imaging parameters. This approach thus provided limited utility even for an initial validation step.

One option to overcome this would be to utilize *in situ* hybridization, a process we have used before for similar purposes (Overman et al., 2012). These experiments were initially planned for candidate genes for which no antibodies were available, but should be expanded to include all 10 candidates to provide a unified approach to validation. In the meantime, our reason for moving forward prior to their completion was that the *in vitro* screens were tenable as a tool to screen through the 10 genes identified by our initial analysis. Furthermore, positive results in our studies, even if ultimately the gene was not found in oligodendrocytes natively (i.e. if the gene was a false positive) would still provide valuable insights into the biology of WMS. Thus, we continued with *in vitro* experiments, with the future goal of assessing oligodendrocyte expression of candidates in tissue using *in situ* hybridization.

Challenges of the CG-4 culture system

Although several groups have used the CG-4 cell line successfully for similar studies, we did not find success even in positive control experiments (Suzuki et al., 2012; Ueno et al., 2012).

This could be for several reasons. First, the line is clonally derived from the original and so has not been fully characterized; nor was the process used to clone fully described (Ueno et al., 2012). Thus, it is possible that the stock of CG4-16 cells used in these experiments acquired additional mutations that limited their utility in differentiation experiments at the resolution required for our studies involving genes with potentially subtle effects on differentiation. Second, genes selected for study here are specific to the OPC white matter stroke response (see Chapter 2). This specific biology may not be recapitulated in the CG4-16 cell line. In any case, our findings highlight that caution should be taken when using cell lines for experiments, and validation using known positive and negative controls is crucial. Fortunately, primary OPC cultures provided an efficient system for use in our studies.

Use of qPCR to assess differentiation

A number of techniques were explored both in CG4-16 cells as well as primary OPC cultures prior to selecting qPCR as the method to assess OPC differentiation. Based on early results, fluorescence quantification of CG4-16 cells had potential to be a rapid metric by which to assess differentiation, as it could be automated with a simple script. Unfortunately, even though visual inspection appeared to show evidence of cell differentiation, the effect was not consistent, and we saw substantial variability in the ratio of differentiation markers to actin (**Fig. 3-4**). This was also the case with Sholl analysis; while there is a basis to use this from studies in the literature, it did not prove consistent in our hands in the CG-4 cell line.

Use of Sholl analysis in primary OPC cultures was attractive as a supplementary readout to gene expression, since mRNA levels are imperfectly correlated with protein expression (Maier et al., 2009). Though the intial studies using Sholl analysis were promising, upon studies in

transfected cells, it was discovered that a substantial decrease in branching was seen in OPCs, likely due to the addition of the polymer reagent. Because the qPCR assay included multiple genes from different phases of development, it was determined that additional assays were redundant and it was preferable to move *in vivo* to gain a deeper understanding of the function of a set of promising genes.

Knockdown experiments presented substantial challenges

We were not able to reliably assay OPC behavior after knockdown of candidate genes, despite clear evidence that constructs did indeed produce significant knockdown of these genes. However, initial assays did suggest some effect in inhibiting differentiation based on sustained, diminished expression of *Mbp* after treatment with different microRNA constructs. This highlights one potential factor confounding attempts to run assays. The genes tested in this study are often truly novel, with unknown or limited understanding of their functions. In addition, kinetics of protein expression are poorly described. This means it is challenging to ascertain half-life of the native protein in the cell, and thus how long cells must be incubated post-transfection to identify meaningful decreases in protein levels versus mRNAs. One option to assess this would be to run Western blots and to determine protein levels at various time points (Zhao et al., 2010).

Another challenge with running such experiments *in vitro* is that primary OPC cultures are difficult to maintain past 7-10 days. Maintaining less than ~70% confluency is ideal as high density of cells is itself a pro-differentiation signal (Dugas & Emery, 2013). However, cells grow robustly in culture, so maintaining them long enough to ensure sufficient knockdown of proteins of interest may prove challenging.

A potential solution to this problem, which avoids the need to transfect cells and induce the stress of polymer addition, is to move to a model of soluble siRNA treatment (He et al., 2016). This bypasses the need for extensive cloning with each new gene construct until candidate genes are identified for study *in vivo*. At the same time, it allows for easier maintenance of cells and calculations of density without adjusting for a degree of cell death upon treatment with the transfection reagent. Western blots could still be run to assess efficacy of siRNAs, but this method, having been validated in OPCs in a number of recent papers, offers an attractive alternate path forward to bypass the challenges described above (Dai et al., 2015; Zuchero et al., 2015).

Future directions

Results outlined in this chapters, particularly of overexpression experiments, provide compelling evidence that a number of genes of interest to play significant roles in OPC differentiation in a closed system. In order to explore in more detail what this may entail in the context of white matter stroke, a selection of genes will be studied *in vivo* using the same animal model from which the OPC stroke transcriptome was initially derived. In the meantime *in vitro* studies will still continue, as refinement of a knockdown protocol is necessary. Additionally, the various techniques described here represent valuable resources for future assays, as will be described in Chapter 5. Thus, the primary OPC culture system has become a valuable and sustainable resource for studying OPCs in the context of white matter stroke, as well as other stroke subtypes or neural repair processes in which they may be involved.

3.4 Methods

Mice

All animals used in tissue expression studies were wild-type C57BL/6 males obtained from the Jackson Laboratory, aged 2-3 months at time of surgery. All experiments were performed in accordance with National Institutes of Health animal protection guidelines and were approved by the University of California, Los Angeles Animal Research Committee (protocol #00-159).

White matter stroke

The white matter stroke procedure was carried out as described, with some modifications (Sozmen et al., 2016). Anesthesia is induced with 5% isoflurane supplied with 100% O_2 and then maintained at 2% for the duration of the operation. After exposing the skull, craniectomy is produced with a high speed dental drill 0.96mm lateral and 0.75mm posterior to Bregma over the left hemisphere. The vasoconstrictor N5-(1-Iminoethyl)-L-ornithine (L-NIO) is preloaded into a pulled glass micropipette (tip diameter of 15-22μm) fitted onto a Picospritzer pressure injection system. L-NIO is then injected through the cortex at an angle of 45° with a dorso-medial to ventro-lateral injection path, into the white matter underlying the forelimb motor cortex. This procedure promotes intense vasoconstriction at the site of injection, leading to focal ischemia. Three stereotaxic injections (each of 200 nL of L-NIO solution) are made at coordinates of (AP, ML, DV) = (+0.75, –0.96, –2.20), (+1.00, –0.96, –2.15), (+1.25, –0.96, –2.10). The pipette is left in situ for 5 min post-injection to allow proper diffusion. After the procedure, the wound is closed and the animal is returned to its home cage for recovery.

Control animals receive craniectomy and insertion of the micropipette as above, but no injection is performed, to avoid inducing stroke-like tissue damage by mass effect (Rosenzweig & Carmichael, 2013; Sozmen et al., 2016).

Immunohistochemistry

Animals are perfused transcardially with ice-cold 0.1 M NaPBS followed by 4% paraformaldehyde prepared in the same solution. Following an overnight postfix in 4% PFA at 4°C, brains are cryoprotected in 30% sucrose at 4°C for 24 hours and then sectioned at 35 µm using a cryostat (Leica CM 0530) and stored in a 50% glycerol anti-freeze solution at –20°C until staining.

Immunohistochemistry is prepared according to a standard protocol (Rosenzweig & Carmichael, 2013; Sozmen et al., 2016). Prior to block, antigen retrieval is performed in pH 6 50mM sodium citrate buffer at 95°C for 10 minutes, followed by 20 minutes in citrate buffer at room temperature. After PBS washes, sections are blocked in a 5% normal donkey serum (NDS), 0.3% Triton-X solution for 1 hour at room temperature. Sections are then incubated in primary antibody overnight, in 2% NDS, 0.1% Triton-X. The next day, sections are washed 3x in PBS and then incubated in secondary antibody for 1 hour in the same solution as primary antibody, then dehydrated with ethanol washes 50-100% and 2x 1 minute xylene washes prior to coverslip application over DPX. Primary antibodies against candidate genes are from Abcam and used at 1:100; Olig2 antibody is from Millipore (rabbit anti-Olig2, AB9610; and mouse anti-Olig2, MABN50; both 1:500). Secondary antibodies are all from Jackson ImmunoResearch (donkey-raised AlexaFluor AffiniPure $F(ab')_2$ fragment antibodies, 1:1000 for all).

CG4-16 cell culture

CG4-16 cells were a generous gift from the Dr. Ogata at the National Rehabilitation Center for Persons with Disabilities, Saitama, Japan. Cultures were grown as described (Ueno et al., 2012). Briefly, media was 50/50 DMEM/F12 from Invitrogen, supplemented with 5 mg/L insulin, 16.1 mg/L putrescine, 50 mg/L apo-transferrin, 4.6 mg/L D-galactose, and 8 µg/L sodium selenite (all from Sigma). Cells were plated in PDL-coated flasks and grown in 2% FBS (generously supplied by Dr. Espinosa-Jeffrey, UCLA). For differentiation, cells were moved to 0.5% FBS with 50 nM triiodothyronine (T_3 hormone; Sigma) as described (Wang et al., 2009). Cells were passaged at 80% confluence with gentle trypsinization and spin for 5 min at 300*g* prior to cell counting and plating again in PDL-coated flasks.

For immunocytochemistry, a general protocol was followed (Abcam, 2014). Antibodies used were Olig2 (rabbit, Millipore as above, 1:1000), CNPase (Sigma C5922, 1:1000), CC-1 (Abcam anti-APC [CC-1], ab16794, 1:1000). Secondary antibodies were as above.

Matrilin-2 (R&D, 3234-MN-050-CF) was coated onto 24-well plates, after coating with PDL, at 20 µg/ml, and incubated overnight at 4°C prior to plating of cells, based on previous studies (Malin et al., 2009).

Primary OPC culture

Primary OPCs were isolated from P6-8 rat pups as described (Dugas & Emery, 2013), except that only olfactory bulbs and cerebellum was removed prior to papain digestion rather than isolating only cortex, with the reasoning that white matter is the tissue of interest for these studies. In brief, one brain (male or female) is dissected and digestion for 90 min in papain and then triturated into a single cell suspension. Cells are passed through three panning dishes: first,

Ran-2 binds astrocytes, O1 binds maturing oligodendrocytes, and O4 binds OPCs. Trypsinization of this final plate followed by quenching in FBS leads to 1.5 – 2 million OPCs from one brain.

OPCs are cultured in DMEM-Sato media according to protocol (Dugas & Emery, 2013). This media is similar to CG4 media but is serum-free and contains additionally 2 mM glutamine, 5 µg/ml *N*-acetyl-L-cysteine, 10 ng/ml d-biotin, 1x Trace Elements B (Cellgro 99-175-CI), 100 µg/ml BSA, and 60 ng/ml progesterone. For proliferation, growth factors are added: 4.2 µg/ml forskolin, 10 ng/ml CNTF, 10 ng/ml PDGF-AA, and 1 ng/ml NT-3. For differentiation, the final two factors are replaced with 40 ng/ml T_3. Media was changed every 2-3 days as recommended; if cells were nearing confluence (>50%, after which point growth rate accelerates), PDGF-AA concentration was doubled.

Transfection

Primary OPCs were plated at 12-15,000 per cm^2 on PDL-coated 12-well plates. Cells were maintained for at least 36-48 hours in proliferation media, or longer if necessary to reach appropriate confluence. At 60-70% confluence, cells were treated with DNA in Xfect reagent as outlined in the manufacturer's protocol (Clontech 631317), with the stipulation that 1 µg DNA per 12-well plate was added; this is the low end of the recommended range and was found to maintain highest cell viability while still leading to ~60% transfection efficiency.

After transfection, media was changed to fresh warmed proliferation media after 4 hours. For differentiation experiments, cells were maintained in proliferation media for 2 days to allow for recovery, and then switched to differentiation media (day 0).

RNA isolation and qPCR

RNA was prepared from primary OPCs using the RNeasy Plus Micro Kit (Qiagen 74034) according to manufacturer protocols. Concentration was measured using a Nanodrop spectrophotometer. 150-300 ng of mRNA was reverse transcribed into cDNA, with the amount depending on needs of the particular experiment. RT was carried out using oligo-dT_{12-18} primers (Invitrogen 18418012), Superscript III reverse transcriptase (Invitrogen 18080044), and RNaseOUT (Invitorgen 10777019). Annealing for 5 minutes at 65°C was followed by 5 min on ice. After addition of Superscript and RNaseOUT, RT was carried out at 50°C for 45 min followed by enzyme inactivation at 70°C for 15 min.

Quantitative PCR was carried out using the LightCycler system and the SYBR Green I 2X Master (Roche 4707516001) with 200 nM primers and 5 ng DNA per 10 µl reaction. Annealing temperature was carried out at 60°C and 45 cycles were run, followed by melting temperature curve run. Melting temperatures were between 70-75°C. Analysis was carried out using the dCp method, with statistics run using ANOVA prior to converting to fold change values (i.e., on raw dCp data).

3.5 Methods

Figure 3-1

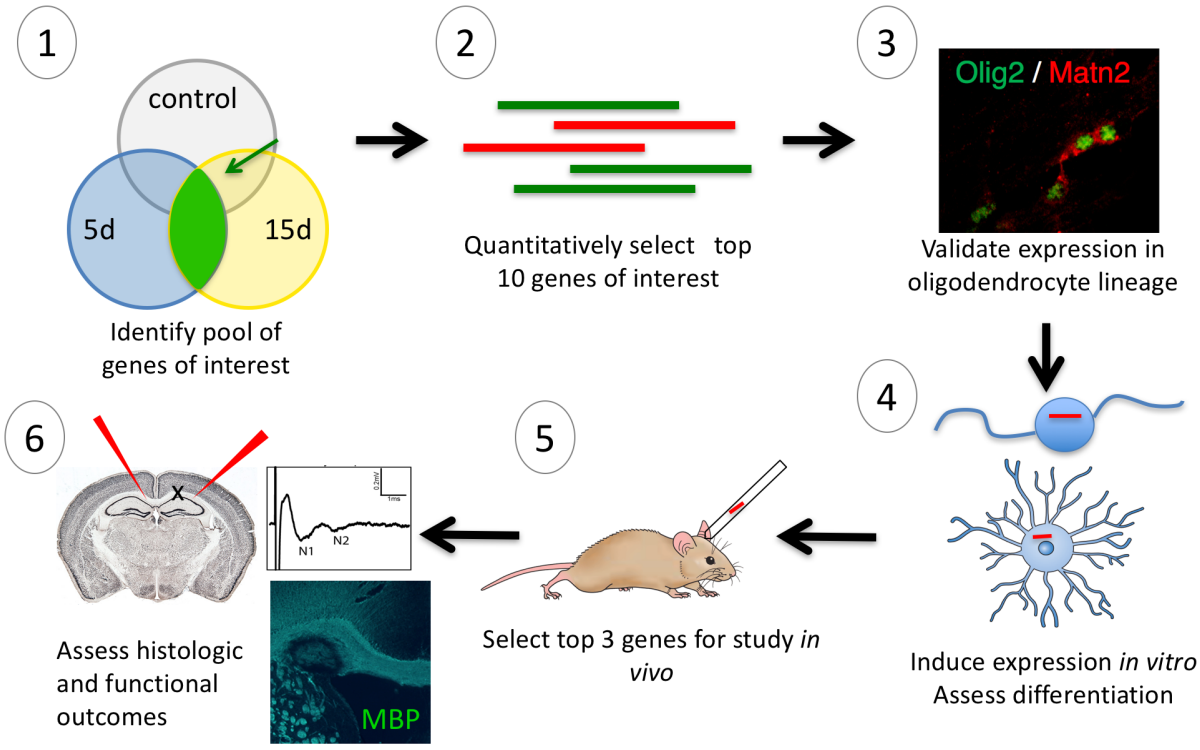

Figure 3-1. Overview of experimental design
This schematic represents the experimental plan and the role of studies outlined in this chapter. Steps 1-2 were outlined in Chapter 2. Both validation of expression of markers (Step 3) and expression studies *in vitro* (Step 4) are outlined in this chapter. Steps 5 and 6 are described in Chapter 4, and additional studies supplementing *in vivo* studies are the focus of Chapter 5.

Figure 3-2

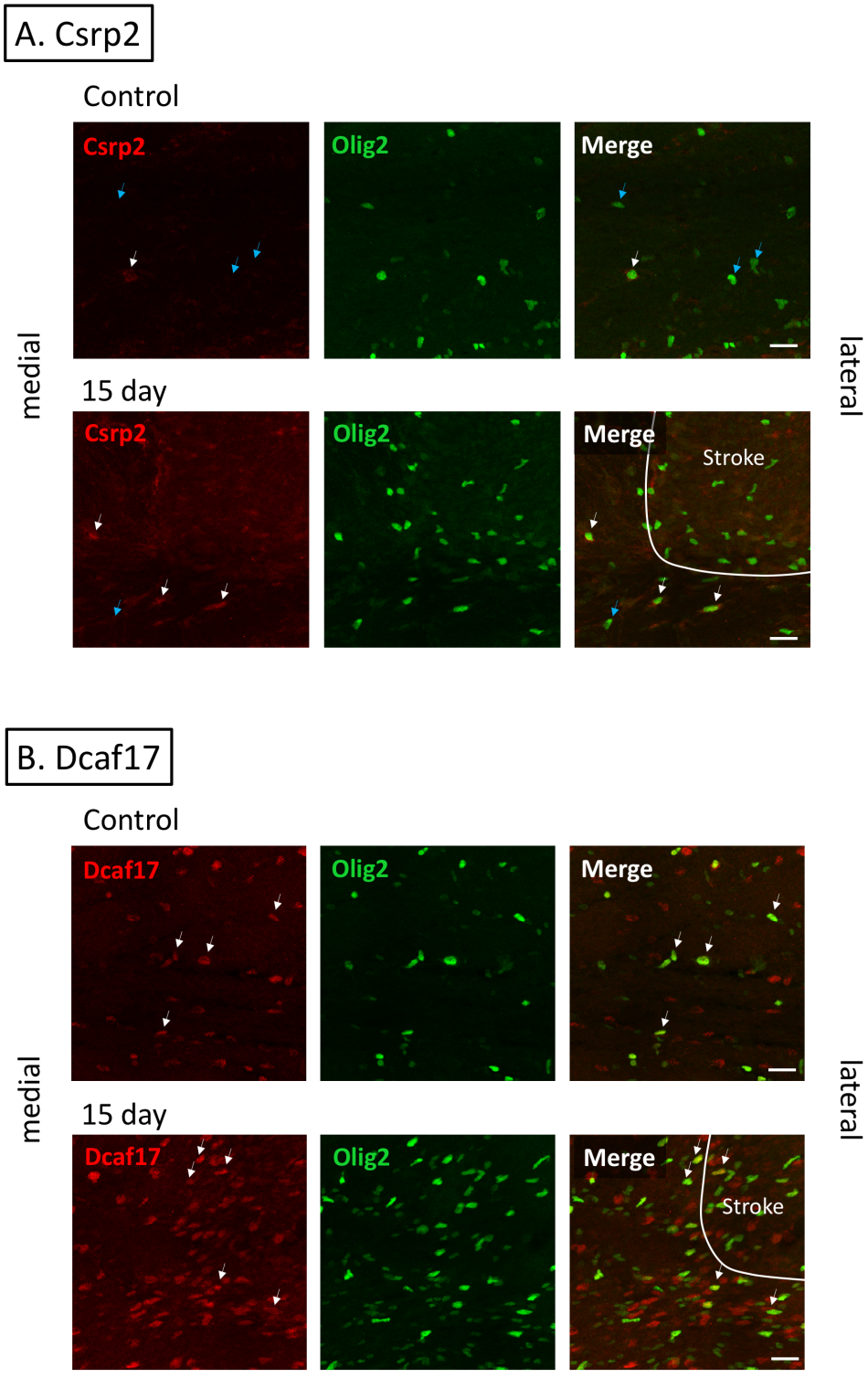
A. Csrp2
Control
Csrp2
Olig2
Merge
medial
lateral
15 day
Csrp2
Olig2
Merge
Stroke
B. Dcaf17
Control
Dcaf17
Olig2
Merge
medial
lateral
15 day
Dcaf17
Olig2
Merge
Stroke

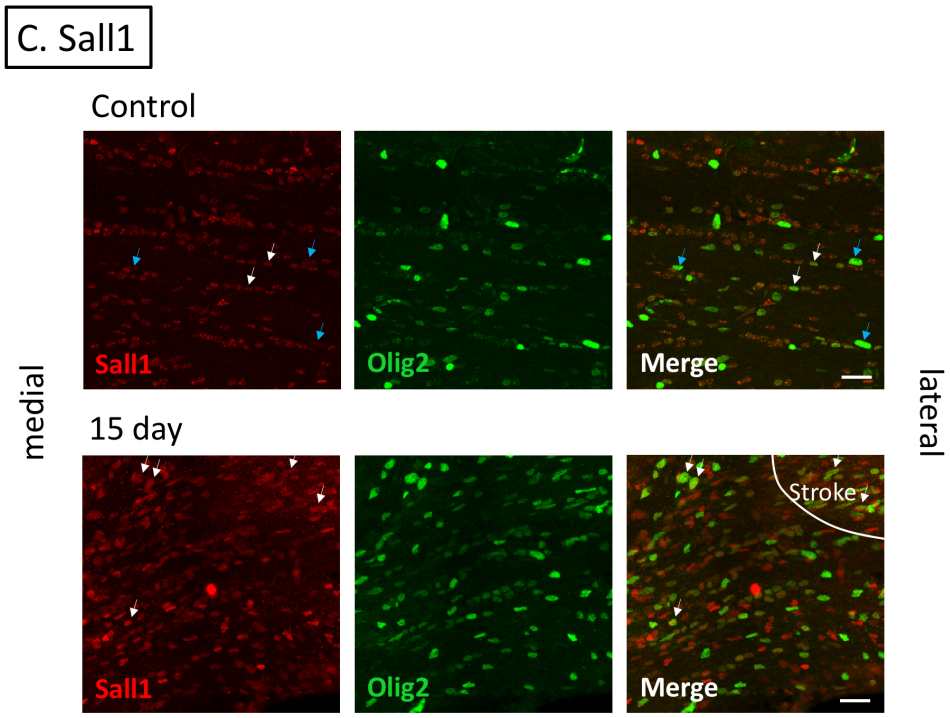

Figure 3-2. Validation of candidate gene expression *in vivo*
A selection of colocalization stains for **(A)** Csrp2, **(B)** Dcaf17, and **(C)** Sall1, genes of interest identified in Chapter 2 (Table 2-1). To maximize ability to detect expression differences as suggested by transcriptomic data, control tissue is compared to time point of maximum differential expression; in each case, this represents day 15 tissue as each gene was overexpressed at this later time point relative to control and day 5 WMS OPCs. Expression in OPCs is verified by colocalization to Olig2, a marker characteristic of OPCs but also present in newly differentiating OPCs, ensuring detection of gene product in a wider spread of oligodendrocyte lineage cells is possible. Stroke site is indicated in each slice, and arrowheads indicate examples of cells with (white) or without (blue) evidence of expression of the indicated gene of interest. Scale bars in all image sets: 20µm.

Figure 3-3

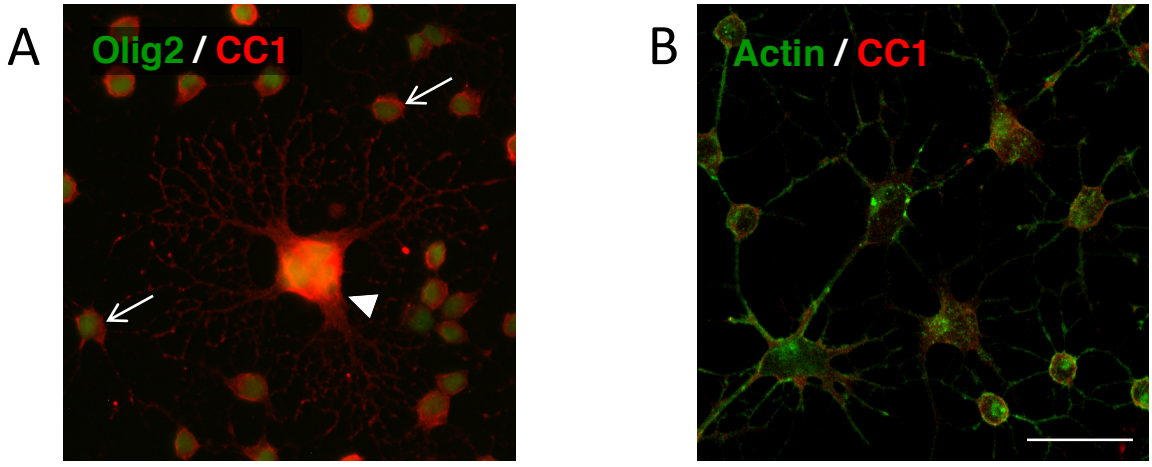

Figure 3-3. CG4-16 cells express oligodendrocyte markers and exhibit differentiation capacity
Initial studies indicate that CG4-16 cells express key markers of oligodendrocyte lineage cells and express morphological signs of differentiation. **(A)** Olig2 is visible in all CG4-16 cells at relatively stable levels (arrows), while the mature marker CC1 appears in higher expression levels in differentiating cells (arrowhead), which are also larger in size as expected. **(B)** Comparing CC1 expression to actin expression allows for a method to control for cell size when quantifying gene expression through fluorescence. Scale bar: 50 µm

Figure 3-4

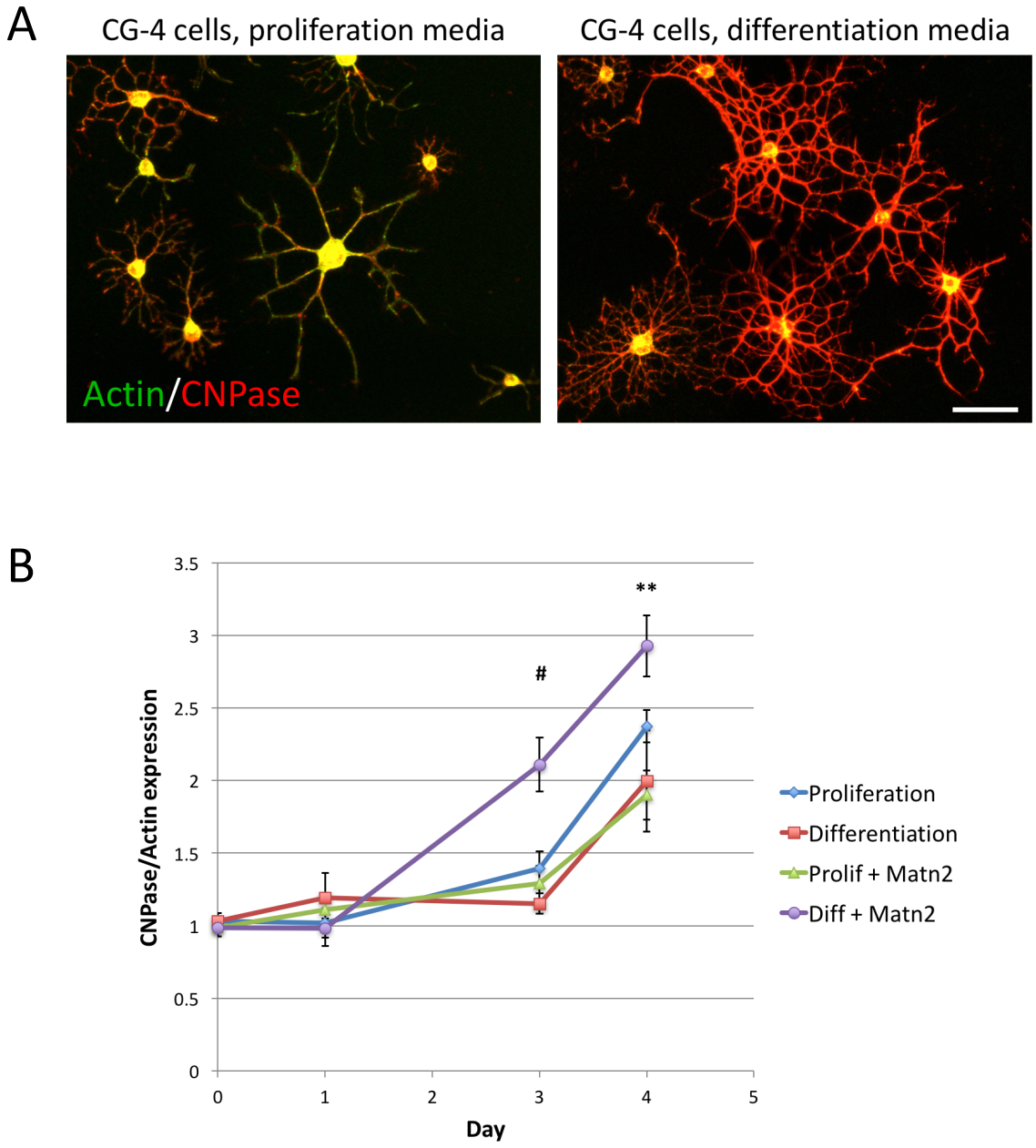

Figure 3-4. CG4-16 cells to not demonstrate specificity of differentiation capacity *in vitro* **(A)** Fluorescence of CNPase was measured and normalized to actin to control for cell size. The ratio of CNPase/actin was used as a readout of differentiation of CG4-16 cells. **(B)** Initial assays using this method did not demonstrate good resolution when assessing differentiation after treatment with positive controls. Note that proliferation-only and differentiation-only treatments are not significantly different throughout the treatment period. # $P < 0.05$, "Diff + Matn2" group compared to others; ** $P < 0.01$, all groups compared to day 0 values. Scale bar: 50 µm

Figure 3-5

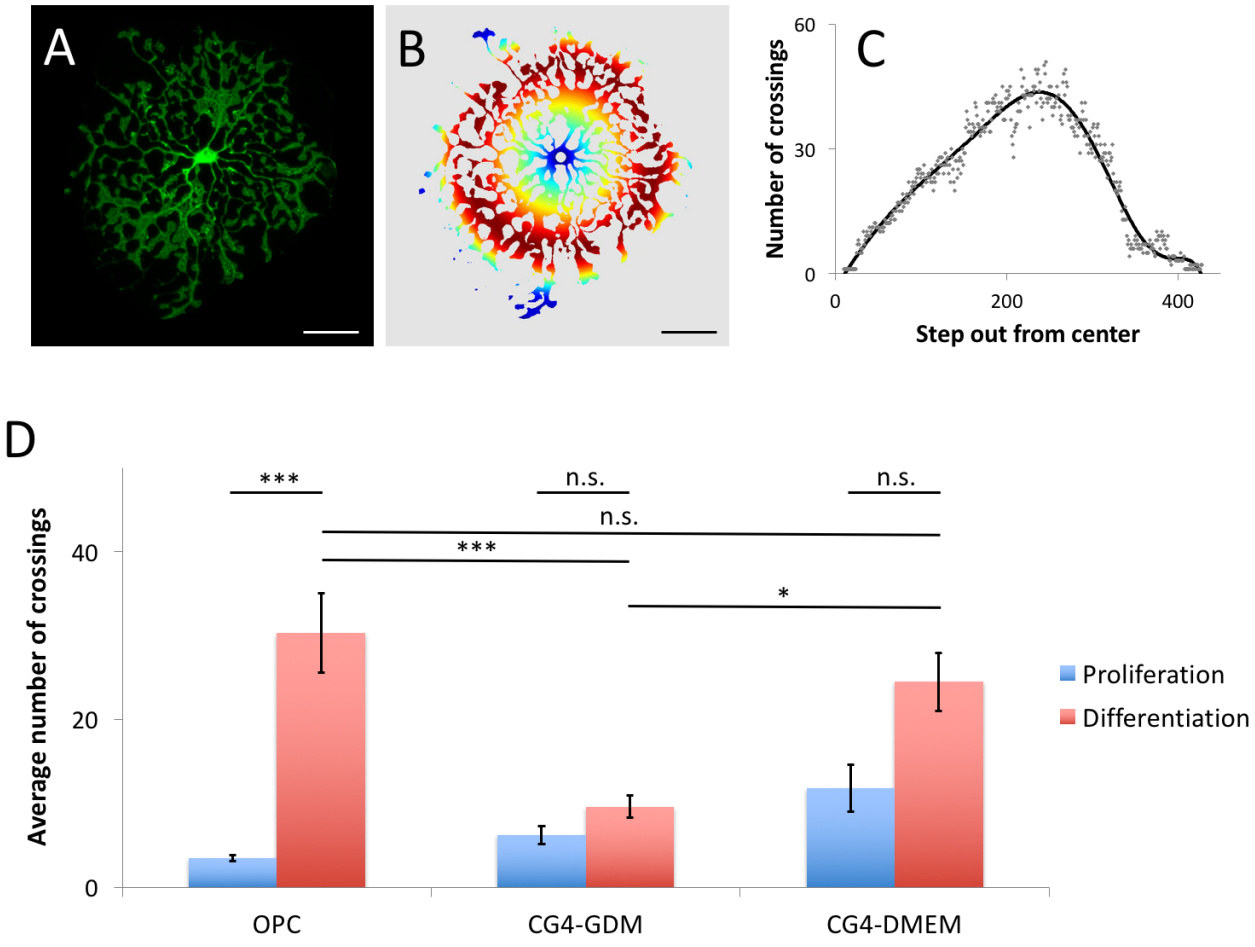

Figure 3-5. Sholl analysis to quantify complexity of cellular branching and morphology
(A) A representative primary OPC grown in DMEM-Sato differentiation media, imaged using Acti-stain 488 phalloidin. **(B)** Sholl analysis processing. Images were processed in Fiji by thresholding with the Triangle method and manually defining maximum radius before quantification using published software (Ferreira *et al.* 2014). Each color in this image represents a concentric ring across which all process crossings were counted. **(C)** All crossings through the rings shown in (B) are graphed and a polynomial line of best fit is shown. From these data, the average number of crossings per cell is computed. **(D)** Comparison of average number of crossings across each test condition. Data were analyzed in GraphPad Prism using one-way ANOVA with Tukey's correction for multiple comparisons. Scale bar in (A) and (B), 50 µm. Error bars in (D), SEM. * $P < 0.05$, *** $P < 0.001$.

Figure 3-6

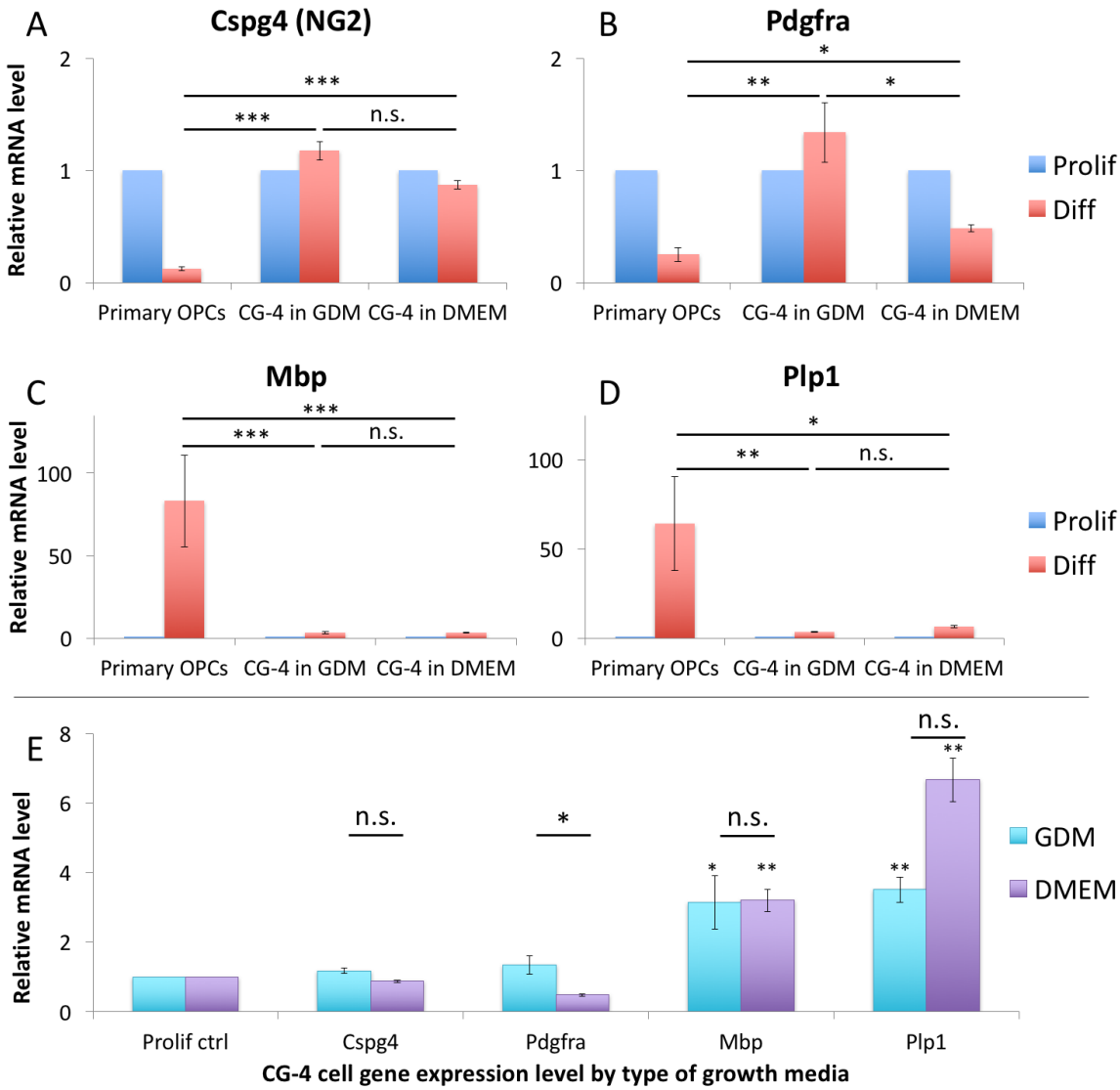

Figure 3-6. Quantitative PCR of primary OPCs and CG-4 cells.
(A-D) Gene-by-gene comparison of primary OPCs, CG-4 cells grown in standard GDM, and CG-4 cells grown in the same DMEM-Sato media as primary OPCs. **(A-B)** show genes characteristic of OPC state, while **(C-D)** show genes characteristic of differentiated oligodendrocytes. Gene expression is normalized to expression of each cell type when grown in proliferation media for 5 days. **(E)** Summary of gene expression in CG-4 cells. For each gene of interest, gene expression levels of CG-4 cells grown in differentiation media are shown, normalized to cells grown in proliferation media (Prolif ctrl). Statistics were performed in GraphPad prism on ddCp data using one-way ANOVA with Tukey's correction for multiple comparisons between groups, and one-sample *t*-test to test for significant up- or down-regulation compared to proliferation control (E, asterisks above columns). * $P < 0.05$, ** $P < 0.01$, *** $P < 0.001$. Error bars represent SEM. GDM, glial defined medium; DMEM, DMEM-Sato growth medium.

Figure 3-7

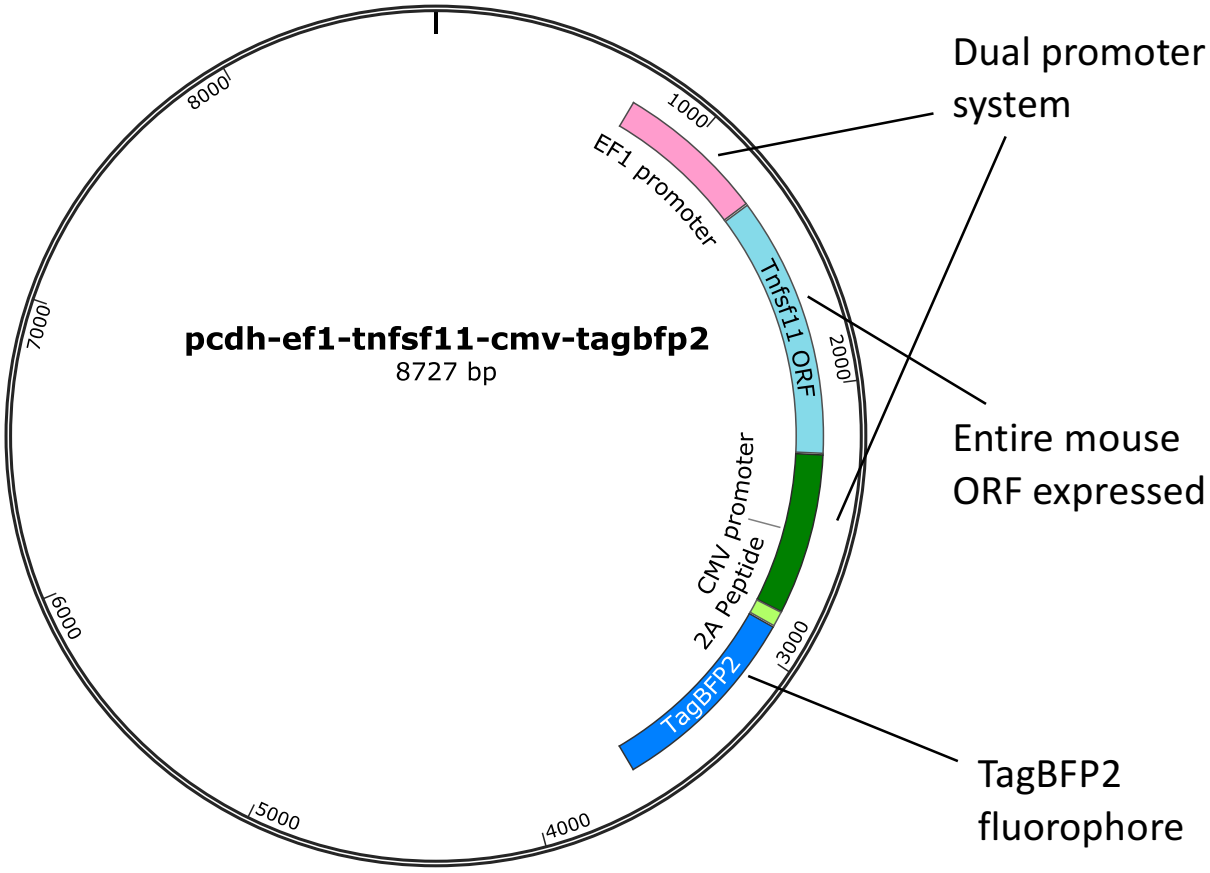

Figure 3-7. Dual promoter expression system for gene induction in OPC cultures
A dual promoter plasmid was generated to express the gene of interest driven by the ubiquitous promoter EF1. A second ubiquitous promoter, CMV, drives expression of the fluorophore, TagBFP2, which identifies transfected cells to assess transfection efficiency. Here, the gene of interest represented is *Tnfsf11*, but any gene can be inserted in its place. Control plasmid has no insert in that location, while keeping intact TagBFP2 expression.

Figure 3-8

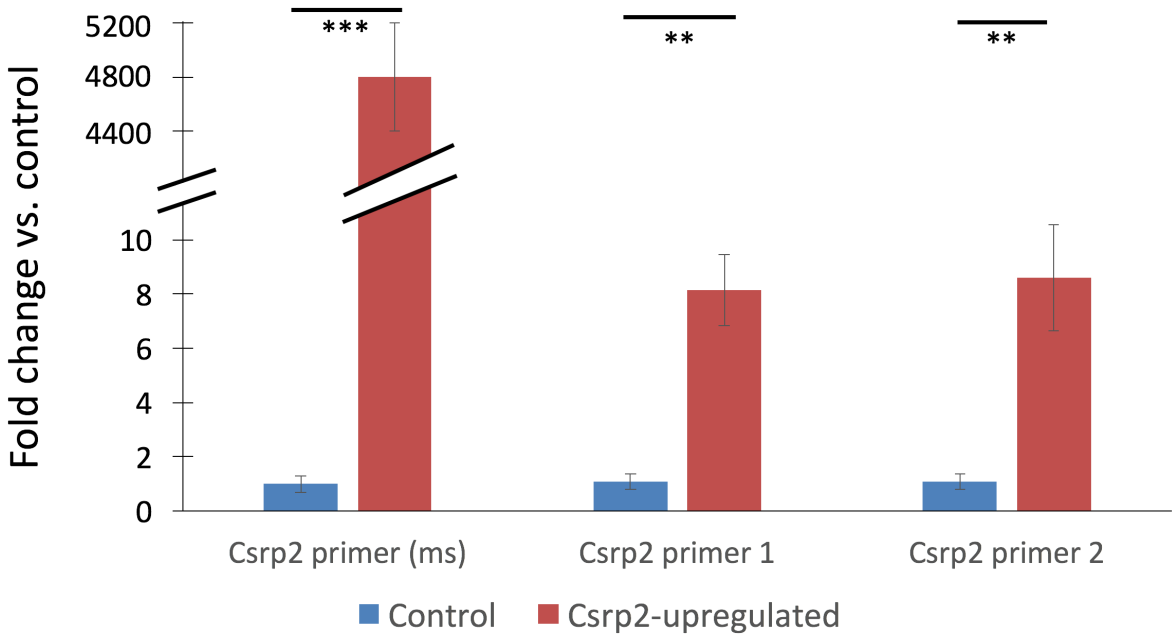

Figure 3-8. Overexpression plasmid successfully drives expression of candidate genes
Validation of overexpression plasmid was conducted using qPCR with three primers specific to the gene of interest (*Csrp2*). The first is specific to the mouse *Csrp2* sequence, while the second two are in regions of high homology between rat and mouse *Csrp2* sequences. Cells transfected with control plasmid are normalized to 1 and *Csrp2*-transfected samples are expressed relative to that. Error bars: SEM. * $P < 0.05$, ** $P < 0.01$, *** $P < 0.001$.

Figure 3-9

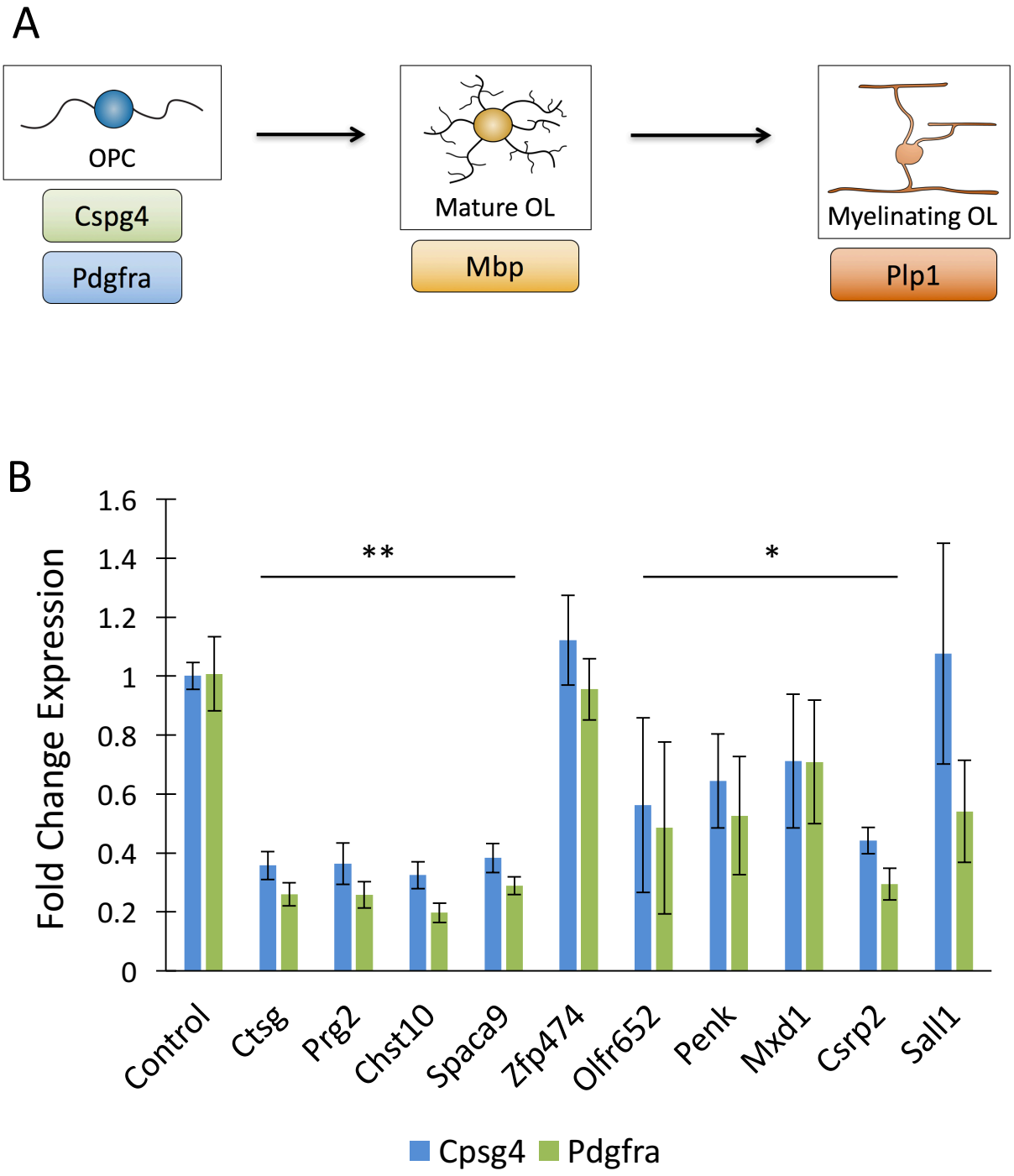
A
OPC
Cspg4
Pdgfra
Mature OL
Mbp
Myelinating OL
Plp1
B
Fold Change Expression
1.6
1.4
1.2
1
0.8
0.6
0.4
0.2
0
**
*
Control
Ctsg
Prg2
Chst10
Spaca9
Zfp474
Olfr652
Penk
Mxd1
Csrp2
Sall1
Cpsg4
Pdgfra

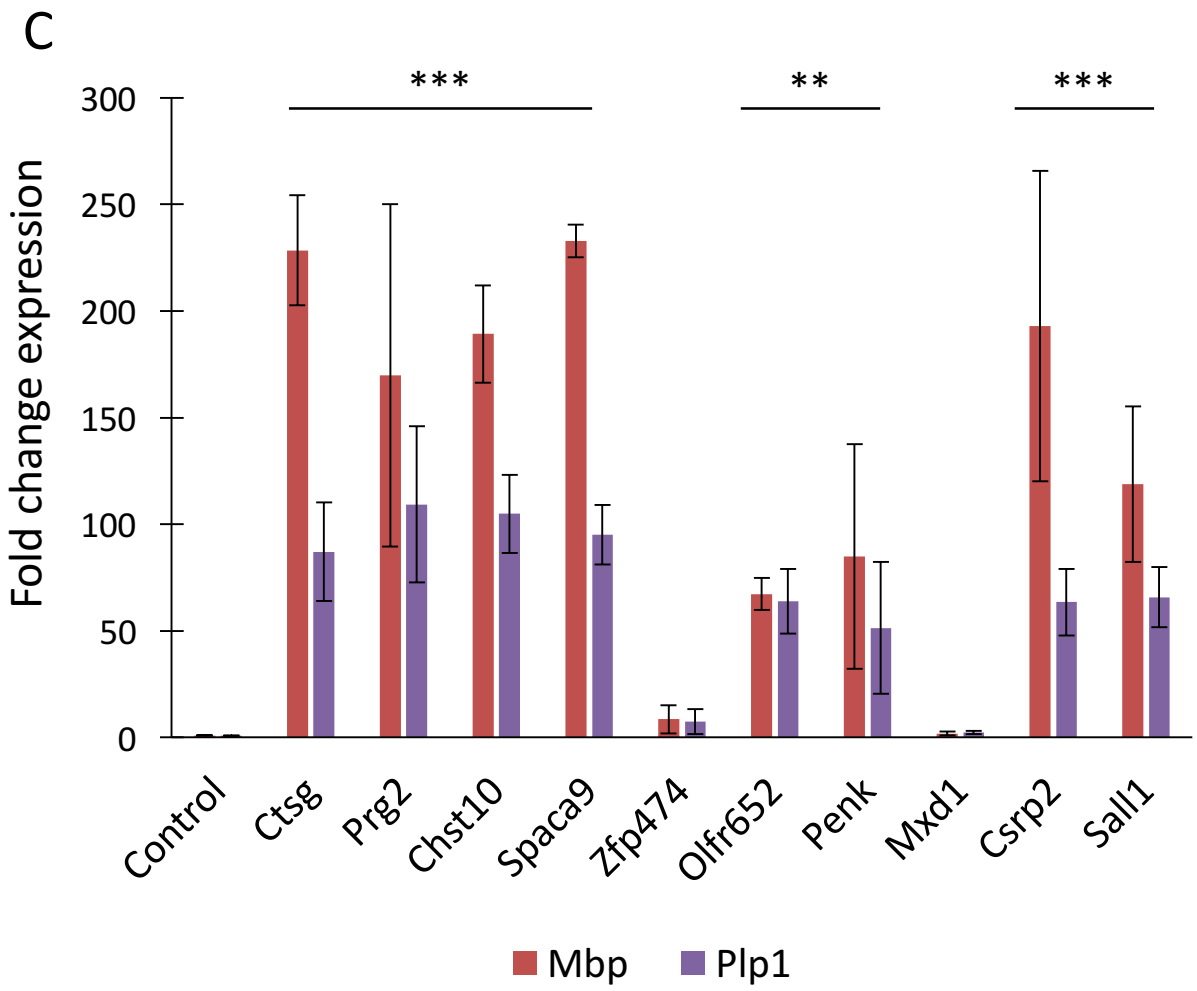

Figure 3-9. Assessment of OPC differentiation after overexpressing candidate genes
Transfection of OPCs with genes of interest or control plasmid shown in Fig. 3-7 was followed by mRNA isolation and qPCR after 4 days in culture. **(A)** Schematic of primer targets used to assess OPC differentiation; two are specific for OPCs and two for differentiating oligodendrocytes. **(B)** qpCR results for OPC-specific targets shows a number of genes lead to knockdown of these progenitor-characteristic genes. **(C)** Results for differentiation markers shows good correlation with results seen in (B). Statistics were performed in Graphpad Prism using one-way ANOVA with Tukey's correction for multiple comparisons. Error bars show SEM. * $P < 0.05$, ** $P < 0.01$, *** $P < 0.001$.

Figure 3-10

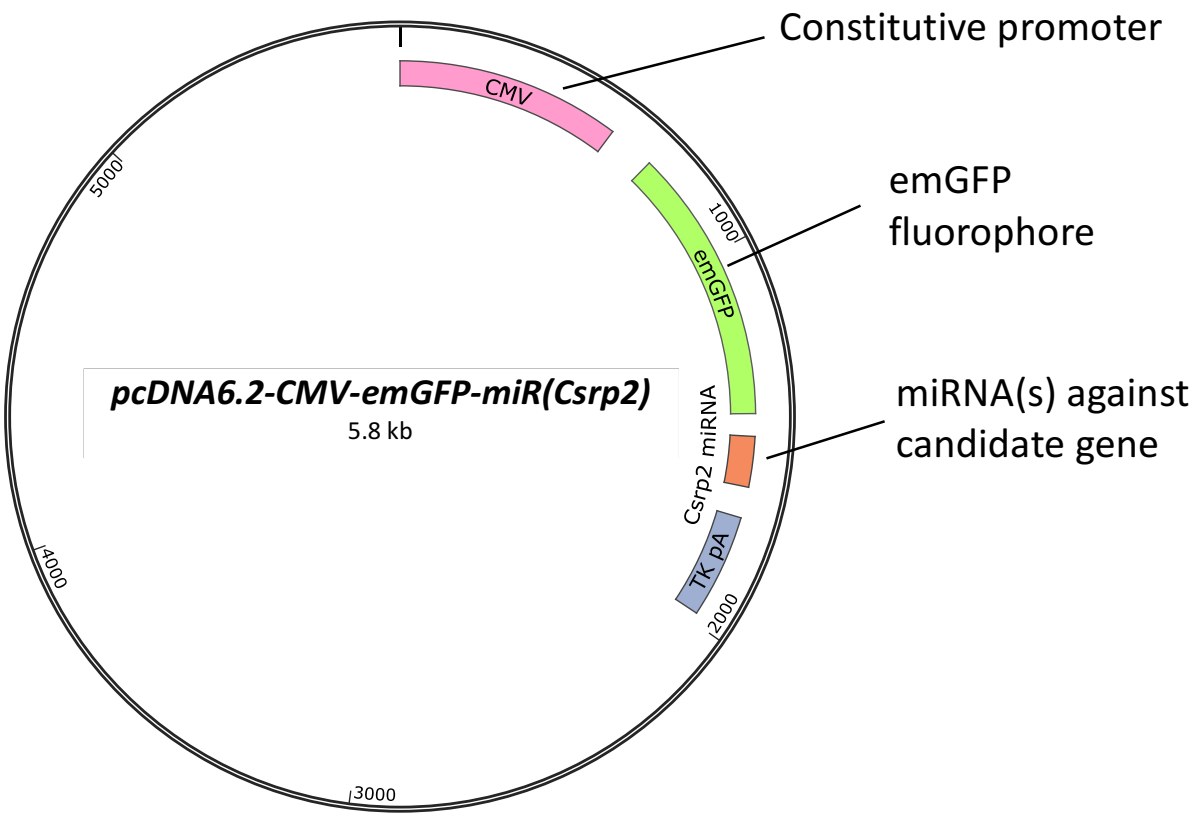

Figure 3-10. BLOCK-iT system for microRNA expression *in vitro*
The provided expression plasmid from the BLOCK-iT kit was prepared according to manufacturer protocol with the addition of miRNAs designed against *Csrp2* as outlined in Fig. 3-11. Control plasmid includes the provided scramble miRNA in place of gene-specific miRNAs.

Figure 3-11

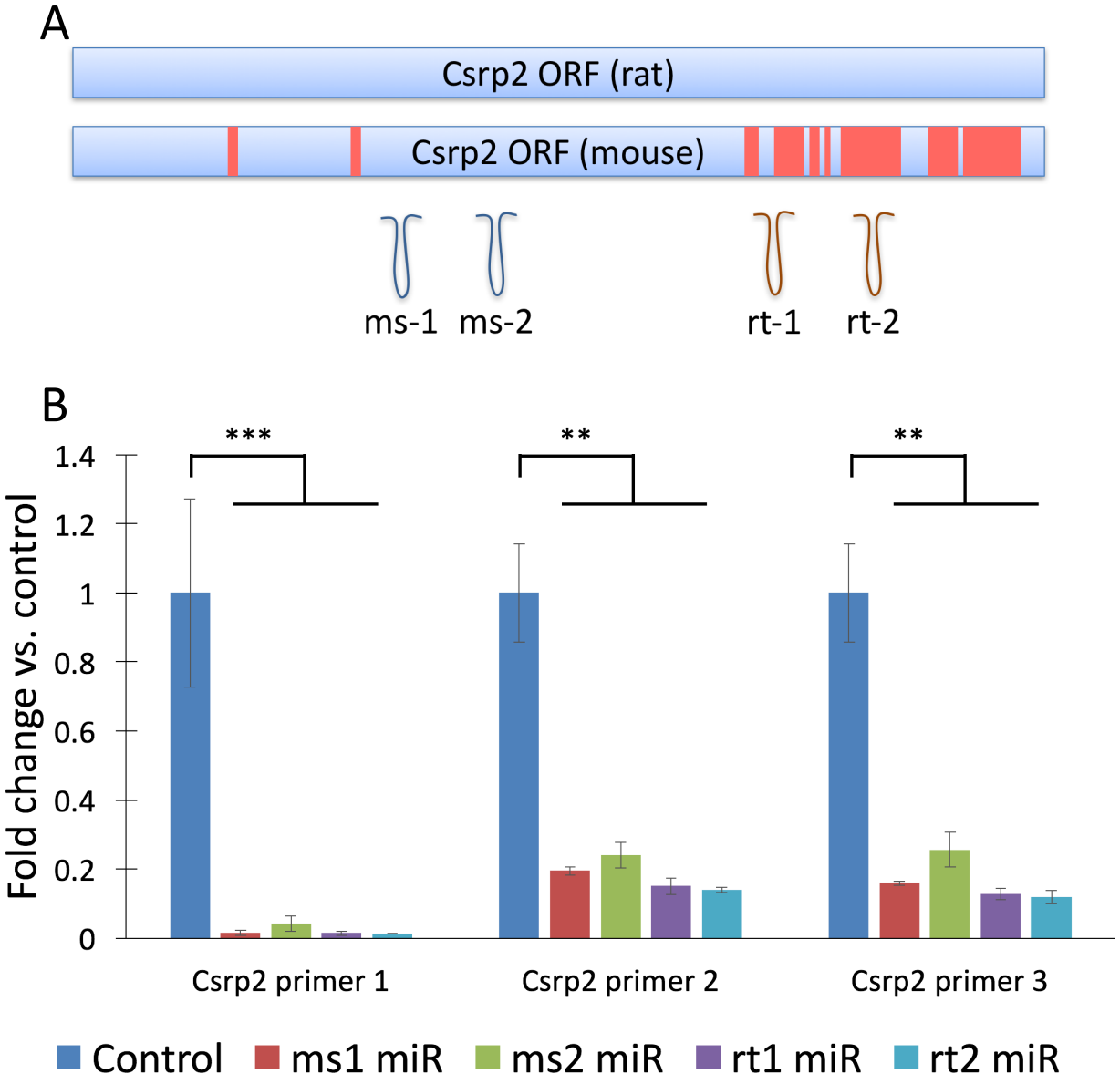

Figure 3-11. Validation of microRNA constructs using *Csrp2*
(A) Schematic detailing design of *Csrp2* miRNA primers. The open reading frames (ORFs) of rat and mouse *Csrp2* sequences are shown. Red areas indicate low homology between mouse and rat constructs. Primer targets are shown by the hairpin cartoons, indicating that two are specific to the rat ORF (rt-1 and rt-2) while two are targeted to an area of high homology (ms-1 and ms-2). **(B)** Validation of miRNA knockdown in primary OPC cultures. After transfection with each the noted construct, knockdown was assessed after 4 days in culture using three different qPCR primers against *Csrp2* mRNA. One-way ANOVA with Tukey's correction for multiple comparisons. Error bars: SEM. ** $P < 0.01$, *** $P < 0.001$.

Figure 3-12

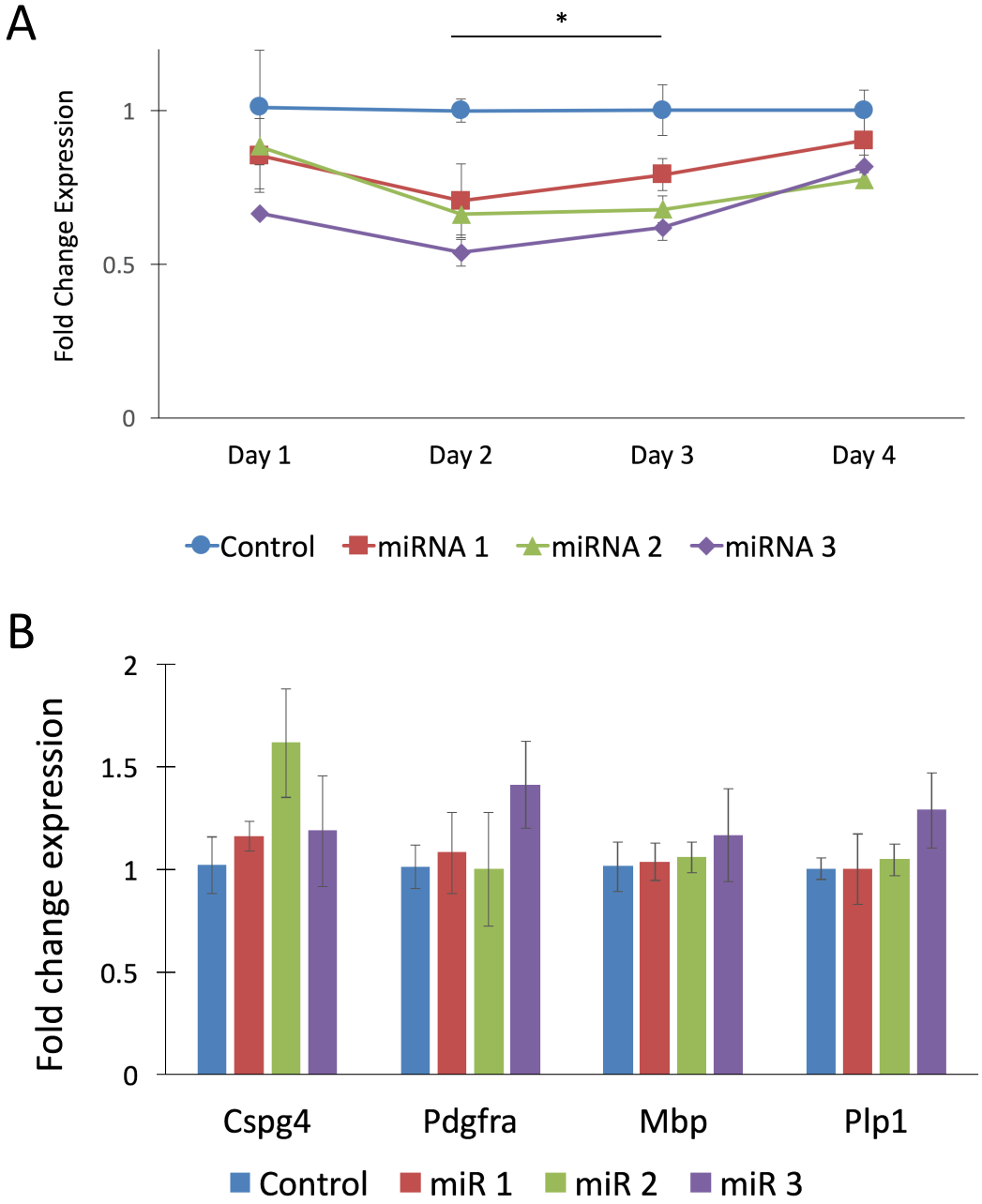

Figure 3-12. Results of miRNA knockdown studies on OPC differentiation
(A) A time-course study of miRNA knockdown of *Csrp2* in OPCs grown in differentiation media for the indicated amount of time showed knockdown of *Mbp* significant across different *Csrp2* miRNA constructs at 2 and 3 days following addition of differentiation media. **(B)** Subsequent studies, however, could not replicate this result, perhaps due to difficulty in titrating the correct degree of knockdown and power to detect inhibition of differentiation. One-way ANOVA with Tukey's correction for multiple comparisons. Error bars: SEM. * $P < 0.05$.

3.6 References

Abcam. (2014). Immunocytochemistry and immunofluorescence protocol.

Anderson, M. A., Burda, J. E., Ren, Y., Ao, Y., O'Shea, T. M., Kawaguchi, R., … Sofroniew, M. V. (2016). Astrocyte scar formation aids central nervous system axon regeneration. *Nature*, *532*(7598), 195–200. https://doi.org/10.1038/nature17623

Back, S. A., Tuohy, T. M. F., Chen, H., Wallingford, N., Craig, A., Struve, J., … Sherman, L. S. (2005). Hyaluronan accumulates in demyelinated lesions and inhibits oligodendrocyte progenitor maturation. *Nature Medicine*, *11*(9), 966–72. https://doi.org/10.1038/nm1279

Barratt, H. E., Budnick, H. C., Parra, R., Lolley, R. J., Perry, C. N., & Nesic, O. (2016). Tamoxifen promotes differentiation of oligodendrocyte progenitors in vitro. *Neuroscience*, *319*, 146–154. https://doi.org/10.1016/j.neuroscience.2016.01.026

Bischof, M., Weider, M., Kuspert, M., Nave, K.-A., & Wegner, M. (2015). Brg1-Dependent Chromatin Remodelling Is Not Essentially Required during Oligodendroglial Differentiation. *Journal of Neuroscience*, *35*(1), 21–35. https://doi.org/10.1523/JNEUROSCI.1468-14.2015

Chen, Y., Balasubramaniyan, V., Peng, J., Hurlock, E. C., Tallquist, M., Li, J., & Lu, Q. R. (2007). Isolation and culture of rat and mouse oligodendrocyte precursor cells. *Nature Protocols*, *2*(5), 1044–1051. https://doi.org/10.1038/nprot.2007.149

Dai, J., Bercury, K. K., Ahrendsen, J. T., & Macklin, W. B. (2015). Olig1 Function Is Required for Oligodendrocyte Differentiation in the Mouse Brain. *Journal of Neuroscience*, *35*(10), 4386–4402. https://doi.org/10.1523/JNEUROSCI.4962-14.2015

Dugas, J. C., & Emery, B. (2013). Purification of oligodendrocyte precursor cells from rat cortices by immunopanning. *Cold Spring Harbor Protocols*, *2013*(8), 745–58.

https://doi.org/10.1101/pdb.prot070862

Emery, B., & Dugas, J. C. (2013). Purification of oligodendrocyte lineage cells from mouse cortices by immunopanning. *Cold Spring Harbor Protocols*, *2013*, 854–868. https://doi.org/10.1101/pdb.prot073973

Espinosa-Jeffrey, A., Wakeman, D. R., Kim, S. U., Snyder, E. Y., & de Vellis, J. (2009). Culture system for rodent and human oligodendrocyte specification, lineage progression, and maturation. *Current Protocols in Stem Cell Biology*, *Chapter 2*(September), Unit 2D.4. https://doi.org/10.1002/9780470151808.sc02d04s10

Espinosa de los Monteros, A., Baba, H., Zhao, P. M., Pan, T., Chang, R., Vellis, J. De, & Ikenaka, K. (2001). Remyelination of the Adult Demyelinated Mouse Brain by Grafted Oligodendrocyte Progenitors and the Effect of B-104 Cografts. *Neurochemical Research*, *26*(6), 673–682.

Ferreira, T. A., Blackman, A. V., Oryer, J., Jayabal, S., Chung, A. J., Watt, A. J., … van Meyel, D. J. (2014). Neuronal morphometry directly from bitmap images. *Nature Methods*, *11*(10), 982–984. https://doi.org/10.1038/nmeth.3102

Gensel, J. C., Schonberg, D. L., Alexander, J. K., McTigue, D. M., & Popovich, P. G. (2010). Semi-automated Sholl analysis for quantifying changes in growth and differentiation of neurons and glia. *Journal of Neuroscience Methods*, *190*(1), 71–9. https://doi.org/10.1016/j.jneumeth.2010.04.026

He, D., Wang, J., Lu, Y., Deng, Y., Zhao, C., Xu, L., … Lu, Q. R. (2016). lncRNA Functional Networks in Oligodendrocytes Reveal Stage-Specific Myelination Control by an lncOL1/Suz12 Complex in the CNS. *Neuron*, 1–17. https://doi.org/10.1016/j.neuron.2016.11.044

Louis, J. C., Magal, E., Muir, D., Manthorpe, M., & Varon, S. (1992). CG-4, a new bipotential glial cell line from rat brain, is capable of differentiating in vitro into either mature oligodendrocytes or type-2 astrocytes. *Journal of Neuroscience Research*, *31*(1), 193–204. https://doi.org/10.1002/jnr.490310125

Madsen, P. M., Motti, D., Karmally, S., Szymkowski, D. E., Lambertsen, K. L., Bethea, J. R., & Brambilla, R. (2016). Oligodendroglial TNFR2 Mediates Membrane TNF-Dependent Repair in Experimental Autoimmune Encephalomyelitis by Promoting Oligodendrocyte Differentiation and Remyelination. *Journal of Neuroscience*, *36*(18), 5128–5143. https://doi.org/10.1523/JNEUROSCI.0211-16.2016

Maier, T., Güell, M., & Serrano, L. (2009). Correlation of mRNA and protein in complex biological samples. *FEBS Letters*, *583*(24), 3966–3973. https://doi.org/10.1016/j.febslet.2009.10.036

Malin, D., Sonnenberg-Riethmacher, E., Guseva, D., Wagener, R., Aszodi, A., Irintchev, A., & Riethmacher, D. (2009). The extracellular-matrix protein matrilin 2 participates in peripheral nerve regeneration. *Journal of Cell Science*, *122*(9), 1471–1471. https://doi.org/10.1242/jcs.052936

Olby, N. J., & Blakemore, W. F. (1996). Reconstruction of the glial environment of a photochemically induced lesion in the rat spinal cord by transplantation of mixed glial cells. *Journal of Neurocytology*, *25*(8), 481–98. https://doi.org/10.1007/BF02284817

Overman, J. J., Clarkson, A. N., Wanner, I. B., Overman, W. T., Eckstein, I., Maguire, J. L., … Carmichael, S. T. (2012). A role for ephrin-A5 in axonal sprouting, recovery, and activity-dependent plasticity after stroke. *Proceedings of the National Academy of Sciences of the United States of America*, *109*(33), E2230-9. https://doi.org/10.1073/pnas.1204386109

Paxinos, G., & Watson, K. B. J. (2001). *The Mouse Brain in Stereotaxic Coordinates 2nd ed.* San Diego: Academic Press.

Rosenzweig, S., & Carmichael, S. T. (2013). Age-dependent exacerbation of white matter stroke outcomes: a role for oxidative damage and inflammatory mediators. *Stroke; a Journal of Cerebral Circulation*, *44*(9), 2579–86. https://doi.org/10.1161/STROKEAHA.113.001796

Sloane, J. A., Batt, C., Ma, Y., Harris, Z. M., Trapp, B., & Vartanian, T. (2010). Hyaluronan blocks oligodendrocyte progenitor maturation and remyelination through TLR2. *Proceedings of the National Academy of Sciences of the United States of America*, *107*(25), 11555–60. https://doi.org/10.1073/pnas.1006496107

Solga, A. C., Pong, W. W., Walker, J., Wylie, T., Magrini, V., Apicelli, A. J., … Gutmann, D. H. (2014). RNA-sequencing reveals oligodendrocyte and neuronal transcripts in microglia relevant to central nervous system disease. *Glia*, n/a-n/a. https://doi.org/10.1002/glia.22754

Sozmen, E. G., Rosenzweig, S., Llorente, I. L., DiTullio, D. J., Machnicki, M., Vinters, H. V., … Carmichael, S. T. (2016). Nogo receptor blockade overcomes remyelination failure after white matter stroke and stimulates functional recovery in aged mice. *Proceedings of the National Academy of Sciences*, *113*(52), E8453–E8462. https://doi.org/10.1073/pnas.1615322113

Stariha, R. L., & Kim, S. U. (2001). Mitogen-activated protein kinase signalling in oligodendrocytes: a comparison of primary cultures and CG-4. *International Journal of Developmental Neuroscience : The Official Journal of the International Society for Developmental Neuroscience*, *19*(4), 427–37. Retrieved from http://www.ncbi.nlm.nih.gov/pubmed/11378302

Suzuki, N., Fukushi, M., Kosaki, K., Doyle, A. D., de Vega, S., Yoshizaki, K., … Yamada, Y.

(2012). Teneurin-4 is a novel regulator of oligodendrocyte differentiation and myelination of small-diameter axons in the CNS. *The Journal of Neuroscience : The Official Journal of the Society for Neuroscience*, *32*(34), 11586–99. https://doi.org/10.1523/JNEUROSCI.2045-11.2012

Ueno, T., Ito, J., Hoshikawa, S., Ohori, Y., Fujiwara, S., Yamamoto, S., … Ogata, T. (2012). The identification of transcriptional targets of Ascl1 in oligodendrocyte development. *Glia*, *60*(10), 1495–505. https://doi.org/10.1002/glia.22369

Wang, P.-S., Wang, J., Xiao, Z.-C., & Pallen, C. J. (2009). Protein-tyrosine phosphatase alpha acts as an upstream regulator of Fyn signaling to promote oligodendrocyte differentiation and myelination. *The Journal of Biological Chemistry*, *284*(48), 33692–702. https://doi.org/10.1074/jbc.M109.061770

Zhang, Y., Chen, K., Sloan, S. A., Bennett, M. L., Scholze, A. R., Keeffe, S. O., … Wu, X. J. Q. (2014). An RNA-Sequencing Transcriptome and Splicing Database of Glia, Neurons, and Vascular Cells of the Cerebral Cortex. *The Journal of Neuroscience : The Official Journal of the Society for Neuroscience*, *34*(36), 1–19. https://doi.org/10.1523/JNEUROSCI.1860-14.2014

Zhao, X., He, X., Han, X., Yu, Y., Ye, F., Chen, Y., … Lu, Q. R. (2010). MicroRNA-Mediated Control of Oligodendrocyte Differentiation. *Neuron*, *65*(5), 612–626. https://doi.org/10.1016/j.neuron.2010.02.018

Zuchero, J. B., Fu, M., Sloan, S. A., Ibrahim, A., Olson, A., Zaremba, A., … Barres, B. A. (2015). CNS Myelin Wrapping Is Driven by Actin Disassembly. *Developmental Cell*, *34*(2), 152–167. https://doi.org/10.1016/j.devcel.2015.06.011

Chapter 4

Investigating the role of candidate genes in an animal model of white matter stroke

4.1 Introduction

In the previous set of experiments, we screened a candidate set of 10 genes for their role in OPC differentiation in a simplified system. The goal of this approach was to prioritize genes for further study *in vivo*, to examine gene function within the context of white matter stroke specifically. This chapter focuses on that set of studies. It begins with the selection of three candidate genes based on the cell culture data. These genes are moved into lentiviral constructs for cell-type specific expression in the white matter, and transduction efficiency and specificity are validated. Next, a series of immunohistochemical studies focuses on the three major phases of oligodendrocyte lineage response to injury: proliferation, differentiation, and myelination. These studies rest on a solid foundation of tissue studies in oligodendrocyte biology, and well-established approaches are available to interrogate each step of oligodendrocyte proliferation (Dai et al., 2015; Sozmen et al., 2016).

Upon characterization of the response to white matter stroke on a cellular level, functional studies are explored to correlate changes seen on the tissue level with measurable alterations to CNS function. This is an area in which there is less consensus within the field, as deficits in CNS injury typically relate to the disease in which they are studied (Crawford, Mangiardi, Xia, et al., 2009; Ransohoff, 2012; Rosenzweig & Carmichael, 2013). In particular, in the field of ischemia, large cortical strokes produce significant functional deficits in mouse

models, which can be quantitatively assessed through behavioral assays (Barratt et al., 2014; Tennant & Jones, 2009). However, recent studies of behavioral deficits in the focal model of white matter stroke developed to closely model human disease, functional effects of stroke were transient unless mice were aged significantly prior to induction of ischemia (Rosenzweig & Carmichael, 2013). The use of aged animals to model a disease whose principal risk factor is age has been a long-standing idea garnering theoretical support for its biological motivations (Buga et al., 2013). Unfortunately, the financial barriers to procuring such animals in sufficient quantity to power studies has as of yet made this approach untenable, as aged animals are ten times more expensive than young adults from common commercial vendors.

Thus, a further aim of studies in this chapter is to identify potential functional readouts of improved recovery after white matter stroke and overexpression of candidate genes. The multiple sclerosis field and others commonly use electrophysiological metrics, derived from field recordings of corpus callosum, to assess functional myelination and axon integrity in the injury site and adjacent areas (Crawford et al., 2010; Remaud et al., 2017; Saab et al., 2016). The use of compound action potentials (CAPs) would provide an efficient readout of functional remyelination while simultaneously providing the opportunity to closely correlate with observations seen in tissue studies to effects on other cell types like neurons. Thus, field recordings are explored as a potential supplement to tissue studies and to validate cell-level effects on a larger scale as an alternative to behavioral testing.

In total, the studies presented below represent the first step in bringing the theoretical analyses conducted previously back into a model of injury in an animal model and offers the important opportunity to uncover in more detail potentially novel pathways in oligodendrocyte differentiation and remyelination.

4.2 Results

Prioritization of candidate genes for study in the animal model

Quantitative PCR studies presented in Chapter 3 provided a foundational set of data related to the impact of candidate genes on OPC differentiation (**Fig. 3-9**). These candidate genes were initially chosen in an unbiased approach by applying a set of quantitative metrics on the gene list and sorting by fold change expression between time points. To begin examining the results from *in vitro* studies, then, a similar approach was taken. **Table 4-1** shows each of the ten genes tested in primary OPC cultures with fold change values listed the four target genes used in the qPCR assay. For each target gene, candidate genes are ranked based on their propensity to promote differentiation. For *Cspg4* and *Pdgfra*, this means genes with the lowest fold change relative to control are ranked first due to knockdown of genes characteristic of OPCs. In contrast, *Mbp* and *Plp1* would be expected to increase in expression as OPCs differentiate, so high fold change values are ranked highly for these genes. Each candidate gene is given a rank per target, and these are averaged across the four targets to produce an overall rank based on equal weighting of the four targets. Of note, control is ranked last using this system, which would be consistent with the hypothesis that none of the candidate genes are actively inhibiting differentiation.

The top gene ranked using this system was *Chst10*, a gene encoding a post-translational modification protein not previously described in oligodendrocytes or the CNS (Bakker, 2014; McGarry et al., 1983). Of note, *Chst10* was the only gene studied for which expression was lower at day 15 relative to day 5. The next highest ranked genes, *Ctsg* and *Prg2*, encode proteins well-described in inflammatory pathways. *Ctsg* encodes cathepsin G, a protease found in neutrophils; while *Prg2* encodes major basic protein, a core component of eosinophil granules

(Gleich et al., 1979; Shamamian et al., 2001; Temkin et al., 2004). Because these proteins had known roles in inflammation, they were not pursued for the *in vivo* phase of the study at this time. The next two genes, *C9orf9* and *Csrp2*, encode proteins not previously described in inflammation or the CNS (Bhattacharya et al., 2013; Sagave et al., 2008; Stauber et al., 2017). Given their novelty and the strong pro-differentiation effects observed *in vitro*, these two genes were selected, in addition to *Chst10*, for study *in vivo*.

Development of lentiviral constructs

The first set of *in vivo* studies paralleled the approach taken *in vitro*; that is, each candidate gene was to be overexpressed in the WMS animal model. In order to overexpress genes of interest, a lentivirus approach was taken, building on previous experience in a variety of stroke models as well as in oligodendrocytes (Overman et al., 2012; Rosenzweig & Carmichael, 2013). Nonetheless, in order to ensure full control over the lentivirus construct and sequence, a fresh construct was designed and cloned. The primary task was twofold: first, a promoter sequence had to be selected that would confer cell-type specificity once injected into the white matter. Second, an appropriate reporter gene had to be added that would allow for visualization *in vivo.*

Previous studies used ubiquitous promoters since plasmids were transfected into pure cultures. Based on previous research into OPC-specific genes, commonly-used options include promoter sequences associated with Ng2, Pdgfrα, Olig1, and Olig2 (Dai et al., 2015; Sozmen et al., 2016; Zhao et al., 2010). For the purposes of this study, Pdgfrα was chosen to match the approach taken to generate the transcriptome, as well as to minimize the proportion of target cells already moving into newly-differentiated oligodendrocyte stages (see **Fig. 1-3**).

Lentiviruses have stringent size requirements, as the maximum length of the insert between LTR sequences is 10 kilobases (Lois et al., 2002). Thus, to accommodate potentially large candidate gene inserts, a short, efficient promoter sequence was desirable. A report looking at promoter sequences specifically in CNS cells identified a 500 bp + UTR sequence from as the most cell-type specific and efficient promoter sequence, and thus this was chosen (Geller et al., 2008).

The second modification made to the base lentiviral construct was to insert a reporter gene and determine an effective expression strategy. In the *in vitro* study protocol, a dual promoter plasmid was used; but in that case, two ubiquitous promoters ensured high expression of both candidate gene and TagBFP2. As the activity of the Pdgfrα promoter was likely lower, especially *in vivo*, a single promoter system was used, and a 2A site was inserted downstream of the gene of interest to express mCherry at roughly stoichiometric levels but without requiring a chimeric protein (Szymczak-Workman et al., 2012). A Kozak sequence was also introduced before the fluorophore in the control construct, and upstream of the candidate gene in test constructs. The lentiviral schematic for *Csrp2* is shown in **Figure 4-1**.

The resulting constructs were cloned and packed into lentiviruses adapted from established protocols (Dull et al., 1998; and Methods). Viruses were injected into white matter in a pilot experiment to determine time course of expression as well as specificity of expression. As seen in **Figure 4-2**, expression of the constructs is seen primarily in OPCs as evidenced by Olig2 colocalization, and it remains localized to the peri-infarct and stroke core region. Based on Olig2 and additional Pdgfrα staining, transduction specificity is estimated to be approximately 60% at minimum (**Fig. 4-2B**), though staining with many OPC markers is incomplete and thus actual efficiency may be higher.

Experimental design of overexpression studies

Having validated the expression construct and prepared viruses for control and test viruses, *in vivo* experiments were designed to assess three steps in oligodendrocyte response to WMS (**Figure 4-3**). Proliferation is quantified by counting $mCherry^+$ cells incorporating nucleoside analogs 5-ethynyl-2'-deoxyuridine (EdU) over the first 5 days post-WMS, and 5-bromo-2'-deoxyuridine (BrdU) over the subsequent 10 days (Gitlin et al., 2014). Differentiation is assessed by quantifying relative expression within $mCherry^+$ cells of markers expressed at various time points along the oligodendrocyte lineage: Pdgfrα, Olig2, and CC1 (De Biase et al., 2010). Finally, remyelination was assessed by staining for the markers of paranodes and nodes of Ranvier, Caspr and βIV-spectrin, respectively (Sozmen et al., 2016).

Effect of candidate genes on OPC proliferation

Pulse labeling of nucleoside analogs was designed to distinguish between OPC proliferation in the first 5 days post-WMS and long-term proliferation between 5-15 days post-WMS, as these were the time points assessed previously in the study. A sample stain of these experiments is shown in **Figure 4-4**, and aggregated results, N = 5-6 per group, are shown in **Figure 4-5**.

Aggregate results show that EdU incorporation averages >50%, while BrdU incorporation is approximately 20% across conditions, matching previous studies showing a peak of proliferation by 5 days post-WMS. However, there were no significant differences in EdU or BrdU incorporation into $mCherry^+$ cells between control virus and any of the three candidate gene conditions. This suggests that there is no evidence for a pro- or anti-proliferative effect for any of the genes of interest.

Candidate genes variably impact OPC differentiation

Studies of differentiation were performed by staining tissue with a set of three oligodendrocyte lineage cells: Pdgfrα, Olig2, and CC1. $mCherry^+$ cells were quantified for each of these markers, and the proportion of oligodendrocyte lineage cells was quantified for each time point and candidate gene treatment. Sample stains and results are shown in **Figure 4-6**.

Results indicate that, on one hand, C9orf9 does not appear to play significant role in OPC differentiation as measured by proportion of Pdgfrα- or CC1-positive cells, with the only result significantly different from the control virus condition is an increase in $Pdgfr\alpha^+$ cells at 5 days post-WMS. In contrast, there is a distinct, sustained impact of both Csrp2 and Chst10 expression on oligodendrocyte differentiation. In both non-stroke and stroke tissue, the proportion of $CC1^+$ cells is significantly increased in Csrp2 animals as well as Chst10 animals. Of note, this increase is present in the no-stroke condition as well as in the 5 day and 15 day post-stroke conditions.

Effect of candidate gene knockdown on OPC differentiation

In addition to overexpression studies for each of the three candidate genes, a microRNA expression lentivirus was developed using the same Pdgfrα promoter system to induce *Csrp2* knockdown; a schematic of the construct is shown in **Figure 4-7**. The three miRNAs most effective in knocking down *Csrp2* expression seen *in vitro* through qPCR quantification were chained together as described by the manufacturer's protocol (see Methods). These constructs were injected into animals and strokes were performed in the same experimental setup as with overexpression studies.

Results of *Csrp2* knockdown are shown in **Figure 4-8**. There were no significant differences in either $Pdgfr\alpha^+$ or $CC1^+$ oligodendrocyte lineage, virally transduced cells ($emGFP^+$)

between control and Csrp2 miRNA viruses. Thus, like the *in vitro* miRNA studies, knockdown studies *in vivo* did not demonstrate significant results to support overexpression studies.

Assessment of remyelination

Upon demyelination, axonal architecture is lost, including well-demarcated nodes of Ranvier (Hinman et al., 2013; Sozmen et al., 2016). Thus, quantification of node-paranode pairs is used as a metric of myelination in peri-infarct tissue, using the proteins Caspr and βIV-spectrin to stain paranodes and nodes of Ranvier, respectively.

A schematic and sample image used in analysis is shown in **Figure 4-9**. Quantification counts the number of intact paranode-node-paranode triads within a selection of 50-µm square fields in peri-infarct zones as previously described (Hinman et al., 2015). Quantification focused on 15 days post-WMS to allow maximal time for remyelination after OPC differentiation. Results of quantification between control virus and Csrp2 overexpression virus are shown in **Fig. 4-9C**. Although there is a significant decrease in intact node-paranode triplets in stroke as compared to control tissue, there was not a significant difference between control and Csrp2 overexpression virus-transduced animals.

Functional readouts of remyelination

To assess whether molecular changes seen in tissue studies of candidate gene treatment in WMS led to measurable physiologic improvements, various methods were considered. Previously, deficits have been shown in this focal WMS model, but are most robust in aged animals, making this a time- and resource-intensive endeavor (Rosenzweig & Carmichael, 2013). Thus, other approaches were considered.

Compound action potentials (CAP) recordings are commonly used to assess functional myelination of the corpus callosum in other models of myelination and demyelination, including multiple sclerosis (Crawford et al., 2010). Thus, if there was indeed enhanced recovery of mature oligodendrocytes upon candidate gene overexpression, we hypothesized that an improvement in action potential propagation through peri-infarct tissue would lead to improved signal using this electrophysiological method.

Figure 4-7 shows preliminary CAP recordings in control and stroke tissue. In control tissue, two peaks, N1 and N2, are visible. These correlate to different groups of variably myelinated axon bundles. The N1 peak, with a faster propagation time, is thought to represent more densely myelinated fibers; while N2 may represent non-myelinated fibers (Crawford et al., 2010; Crawford, Mangiardi, & Tiwari-Woodruff, 2009). In stroke animals, however, no N1 or N2 peaks were observed upon repeated attempts to measure such deficits.

Due to time and resource constraints, CAP studies were not run on gene candidates for this dissertation; however, because a clear deficit is present in stroke compared to control, they represent a promising avenue forward for functional studies when tissue studies suggest a pro-differentiation effect *in vivo*.

4.3 Discussion

Selection of genes for further study is based on complementary biology

As shown in **Table 4-1**, a number of genes showed significant impact on differentiation of OPCs *in vitro*. When genes were ranked according to degree of this response, the top ranked genes were *Chst10*, *Ctsg*, and *Prg2*. These genes are all previously unstudied in oligodendrocyte biology and stroke. *Chst10*, or Carbohydrate sulfotransferase 10, is involved in post-translational

processing (Bakker, 2014; McGarry et al., 1983). *Ctsg*, or cathepsin G, was the most differentially expressed gene between day 15 and day 5 post-WMS, at with a fold change of over 3,400. Cathepsins are proteases, previously described in immune cells such as neutrophils, but also have been investigated for roles in tissue remodeling (Shamamian et al., 2001). Finally, Prg2, known as proteoglycan 2 or major basic protein, is a major component of the eosinophil granule core. It was the second-highest differentially expressed gene in this group, with a fold change of 1,000 (day 15 vs. day 5). Of note, this protein shares a highly basic property with myelin basic protein, potentially conferring a role in enzyme inhibition (Gleich et al., 1979; Temkin et al., 2004).

Chst10 was particularly interesting as it was the only protein underexpressed at day 15 relative to day 5. This, combined with its role in post-translational modification, made it a compelling candidate for further study. However, for additional targets, choosing two proteins involved in immunity and inflammation, a well-studied pathology of stroke, led us to consider other promising options. C9orf9 is also novel in glial biology studies but has known roles in cell structure and motility (Bhattacharya et al., 2013; Stauber et al., 2017). Given recent discoveries related to the importance of actin and oligodendrocyte motility in remyelination, combined with its strong effect relative to control-transfected OPCs, we selected this gene for further study (Zuchero et al., 2015). Finally, Csrp2 encodes a transcription factor binding protein, making it the only gene significant in our screen involved in regulation of gene expression (Sagave et al., 2008). This, combined with its reported role in cell growth and cardiomyocyte development, provided a foundation to examine it further as well.

Thus, the three genes selected for study in this report have distinct localizations and putative functions within the cell, allowing us to interrogate oligodendrocyte biology on multiple

levels. Other genes identified in **Table 4-1** may be interesting targets for further analysis in future experiments, as this chapter reports the design of an experimental workflow that can be used to characterize other genes for their impacts in oligodendrocyte behavior in normal brain tissue as well as in pathology.

Tissue studies

The results presented here offer evidence in support of trends observed *in vitro*, particularly for Csrp2 and Chst10. Overexpression of these proteins in tissue not only leads to enhanced oligodendrocyte differentiation after WMS, but also has this effect in normal tissue as well, suggesting a mechanism that may act in oligodendrocytes more universally. Of note, proliferation of OPCs, as measured by changes in EdU^+ or $BrdU^+$ cell populations, was not significantly impacted by Chst10 or Csrp2 overexpression (**Fig. 4-5**). A modest effect was seen at 5 days post-WMS in C9orf9 animals, but considering this was not seen at 15 days post-WMS or in control animals, combined with the lack of a pro-differentiation effect, C9orf9 does not seem to otherwise play a compelling role in OPC response to WMS.

That the pro-differentiation effect of Csrp2 and Chst10 was seen also in non-stroke animals raises an important question: does this study actually contribute to our understanding of OPC responses to white matter stroke, or does this just describe a new, general pathway of OPC differentiation? Certainly, these proteins appear able to promote differentiation in normal tissue. However, this does not mean these pathways play a significant role in normal differentiation of OPCs, as we saw effects only after exogenous overexpression. Thus, a pathway important for stroke pathology may be manipulated to impact OPCs in other contexts, but their expression levels may be important primarily in pathology. Second, identification of these genes from the

WMS transcriptome indicates that these genes play a role in WMS. In contrast, we cannot comment on whether genes would impact recovery after other demyelinating diseases such as multiple sclerosis. Similarly, genes identified as promoting differentiation in other disease contexts may not impact WMS recovery. Thus, the fact that these were identified through a disease-specific screen highlights their potential utility in treatment of this disease, regardless of (or in addition to) their effect in normal physiology. This makes studies of particular disease processes particularly important, especially given the complexity of the white matter milieu.

In contrast to the significant pro-differentiation effect seen after candidate gene overexpression *in vivo*, microRNA knockdown of *Csrp2* did not impact OPC differentiation *in vivo* (**Fig. 4-8**). This is consistent with the lack of reproducible results *in vitro*. Two main conclusions seem plausible based on these results. On one hand, these miRNA constructs may not induce a large enough knockdown of Csrp2 protein to detect differences using the power of our studies. Similarly, it is possible that the half-life of Csrp2 is long enough that protein levels were not significantly reduced during the post-stroke period. However, it is also possible that Csrp2 is not required to achieve a base level of OPC differentiation; or, in other words, OPC differentiation has reached a "floor," or minimum level, in post-stroke tissue, so that anti-differentiation treatment has limited capacity to further reduce differentiation. Given a differentiation block was seen already post-WMS, this seems like a potentially viable explanation.

In any case, given the lack of significant results after candidate gene knockdown, two avenues forward will be pursued. First, as discussed in Chapter 3, siRNA treatment of OPC cultures may provide a higher, faster knockdown of gene expression *in vitro* and provide additional power for qPCR studies. This would provide a foundation on which to plan *in vivo*

studies; for example, by providing evidence of an inhibitory effect and some sense of the time course of this effect.

Second, and perhaps more promising initially, is the possibility of co-overexpressing Chst10 and Csrp2. Both of these genes have shown significant impact on OPC differentiation upon overexpression, so combining lentiviral overexpression *in vivo* would provide insight into whether these effects are complementary. In addition to helping to uncover potential pathways engaged by these candidate genes, this could also be an initial step into unifying seemingly disparate pro-differentiation effects into a larger picture of OPC biology.

Compound action potential recordings

CAP recordings offered a promising opportunity to assess functional recovery over traditional behavioral tests, which required aged animals and were time-intensive, taking many weeks to complete (Rosenzweig & Carmichael, 2013). Indeed, **Fig. 4-8** provides a proof of concept series of studies that indicate such studies deserve further exploration.

A number of challenges arose in the context of the present studies that made these experiments difficult to complete. One was limited availability of electrophysiology equipment set up for field recordings. The second, and more important challenge, was technical expertise. Given the wealth of other experiments involved in this study, there was limited time available to devote to these studies. Technical aptitude was thus lacking, and to accurately measure improvement over a baseline of no signal, it is important to be eminently confident in technical skills.

Completion of these experiments thus may require initiation of a collaboration with a group well-versed in CAP recording procedures, or training and practice over a period of 2-3 months to attain the high level of technical skill necessary to run these experiments efficiently.

Node quantification

An additional approach to quantifying remyelination was through the analysis of nodes of Ranvier, and corresponding paranodes, whose organization depends on successful myelination (Hinman et al., 2015). Quantification of node-paranode structures is one method of assessing not only remyelination of axons, but a functional organization of myelination in a way that enables proper action potential propagation of wrapped axons.

Preliminary quantification of nodes of Ranvier in post-WMS animals did not show significant results (**Fig 4-9**). However, additional analysis is necessary to verify that this does not provide insight into functional remyelination. In particular, while in this case sections were chosen randomly from the peri-infarct area for analysis, it is worth using advanced analysis software such as Imaris (Bitplane) to quantify nodal organization throughout the peri-infarct region. This would allow for region-specific analysis as well as quantify the region of successful remyelination such that changes to area of demyelination could be detected with higher power. Thus, further analysis of node-paranode structures post-WMS is necessary, not just in Csrp2 but also in Chst10 animals, to accurately determine the utility of this analysis technique.

Future directions

Preliminary results from tissue studies suggest a promising role for Csrp2 in promoting OPC differentiation. However, little is known about this protein or its function within the cell. In

addition, this highlights a challenge of the approach taken up to this point: if new candidates are identified, how can this be used to improve disease outlook? Though identification of new treatments is beyond the scope of these animal model experiments, returning to bioinformatics to guide an exploration of small molecules that impact these novel pathways offers a promising first step. These two extension studies will be the focus of the final chapter.

4.4 Methods

Lentivirus preparation

Third-generation lentiviruses were packed according to lab protocols and based on published techniques (Dull et al., 1998). Briefly, packing plasmids pMDLg/pRRE (Addgene 12251), pRSV-Rev (Addgene 12253) and pMD2.G (Addgene 12259) were transfected into 293T/17 cells (ATCC CRL-11268) using calcium phosphate transfection protocols with BES buffer prepared according to standard recipe (CSH protocols, 2x BBS). At 18 hours after transfection, cells were treated fresh media containing 10 mM sodium butyrate and incubated another 24 hours. Viruses were purified from supernatant with a 2.5 hour, 20,000 rpm spin in a Beckson ultracentrifuge, followed by a 2.5 hour 32,000 rpm through 20% sucrose. Viruses were titrated by serial dilution transduction of 293 cells as well as p24 assays (UCLA Center for AIDS Research core).

Lentivirus injection

Injection of lentivirus was done 3 days prior to stroke or control procedure, via a similar method. In brief, animals were prepared as outlined in Chapter 3, and then 2x 400 nL injections were made with the same angle of injection but at coordinates (AP, ML, DV) = (+0.88, –0.91, –2.18), (+1.12, –1.01, –2.13). Skin was closed over the skull and reopened 3 days later where the craniectomy was still intact for immediate injection of L-NIO.

EdU and BrdU treatment

EdU and BrdU were given in the drinking water as follows. EdU (Carbosynth NE08701) was dosed in water at a final concentration of 200 μg/ml along with antibiotic (cherry flavored

TMS for taste) at the recommended dose. If animals are not drinking the water, 2% sucrose can be added. EdU water was changed every 48 hours.

BrdU (Sigma B5002) was added to drinking water at a final concentration of 1 mg/ml along with TMS as above. Water was changed every 3-4 days. Otherwise, preparation was identical to above.

Development of BrdU was achieved with a standard IHC protocol with one alteration: addition of a 2N HCl incubation at 37.5°C for 30 min following antigen retrieval, and then 30 min room temperature incubation with 100 mM sodium tetraporate, pH 8.6. Abcam rat anti-BrdU (ab6326, 1:500) was used for visualization.

EdU was developed with a protocol modified from the Click-IT EdU imaging kit (Thermo Fisher). Briefly, prior to antigen retrieval, sections are incubated for 30 minutes in a 100 mM TBS, pH 7.6 containing 100 mM sodium ascorbate, 4 mM $CuSO_4$, and 2 μM sulfo-Cy5 azide (Lumiprobe D3330). Sections are then protected from light for the remainder of the IHC protocol, which is continued normally.

Additional immunohistochemistry reagents

Additional antibodies used were mouse anti-Caspr (UC Davis NeuroMab) at 1:500, and rabbit anti-βIV spectrin (a gift from Dr. Matthew Rasband; 1:200), and chicken anti-GFP for miRNA studies (Abcam ab13970; 1:1000).

Compound action potentials

Compound action potential recordings were performed with the generous assistance of Kathy Myers in the laboratory of Dr. Felix Schweizer (UCLA) and of Kelli Lauderdale in the

laboratory of Dr. Seema Tiwari-Woodruff (UC Riverside) according to published protocols (Crawford et al., 2010). Briefly, 2-3 month animals receiving WMS or control procedure are sacrificed and brains sectioned at 350μm using a Leica VT1000S vibrating knife microtome. Sections are maintained in buffers as outlined, and recording and stimulating electrodes are inserted 1 mm apart. Electrodes are adjusted to minimize noise and until signal is detected at which point a series of CAP recordings are taken at that location (5-7). The pipette is then removed, and reinserted to obtain another set of recordings as before. Recordings are taken and processed using LabView software (National Instruments).

4.5 Figures

Table 4-1

Genes of interest prioritized by differentiation capacity *in vitro*

Candidate	Fold change expression vs. control				Overall rank
	OPC markers		*Mature OL markers*		
	Cpsg4	**Pdgfra**	**Mbp**	**Plp1**	
Chst10	0.325	0.197	189.2	104.9	1
Ctsg	0.357	0.260	228.4	87.1	2
Prg2	0.364	0.258	169.8	109.3	2
C9orf9	0.383	0.289	232.9	95.1	4
Csrp2	0.442	0.294	193.0	63.5	5
Olfr652	0.562	0.485	67.3	63.8	6
Penk	0.644	0.527	84.8	51.4	7
Sall1	1.076	0.541	118.8	65.8	7
Mxd1	0.712	0.709	1.8	2.3	9
Zfp474	1.122	0.955	8.6	7.5	10
Control	1.001	1.008	1.0	1.0	11

[1] Colors indicate fold change expression relative to control, with green = decreased expression, red = increased expression.

Figure 4-1

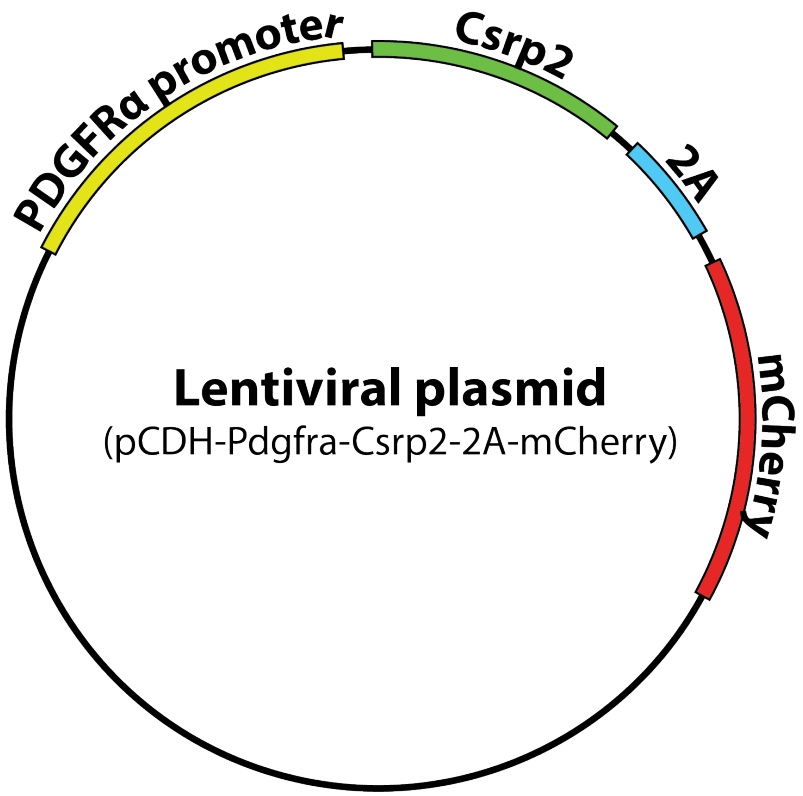

Figure 4-1. Lentiviral construct designed for *in vivo* transduction of OPCs
A lentiviral construct was designed for expression of candidate genes *in vivo*. Key elements are shown, including the OPC-specific Pdgfrα promoter sequence; the candidate gene ORF, the fluorophore mCherry, and a 2A site for co-expression of both proteins under a single promoter. Of note, Kozak sequences appear before the candidate gene ORF or mCherry when no GOI is present. All constructs are sequenced prior to packaging to ensure the entire transcript remains in frame.

Figure 4-2

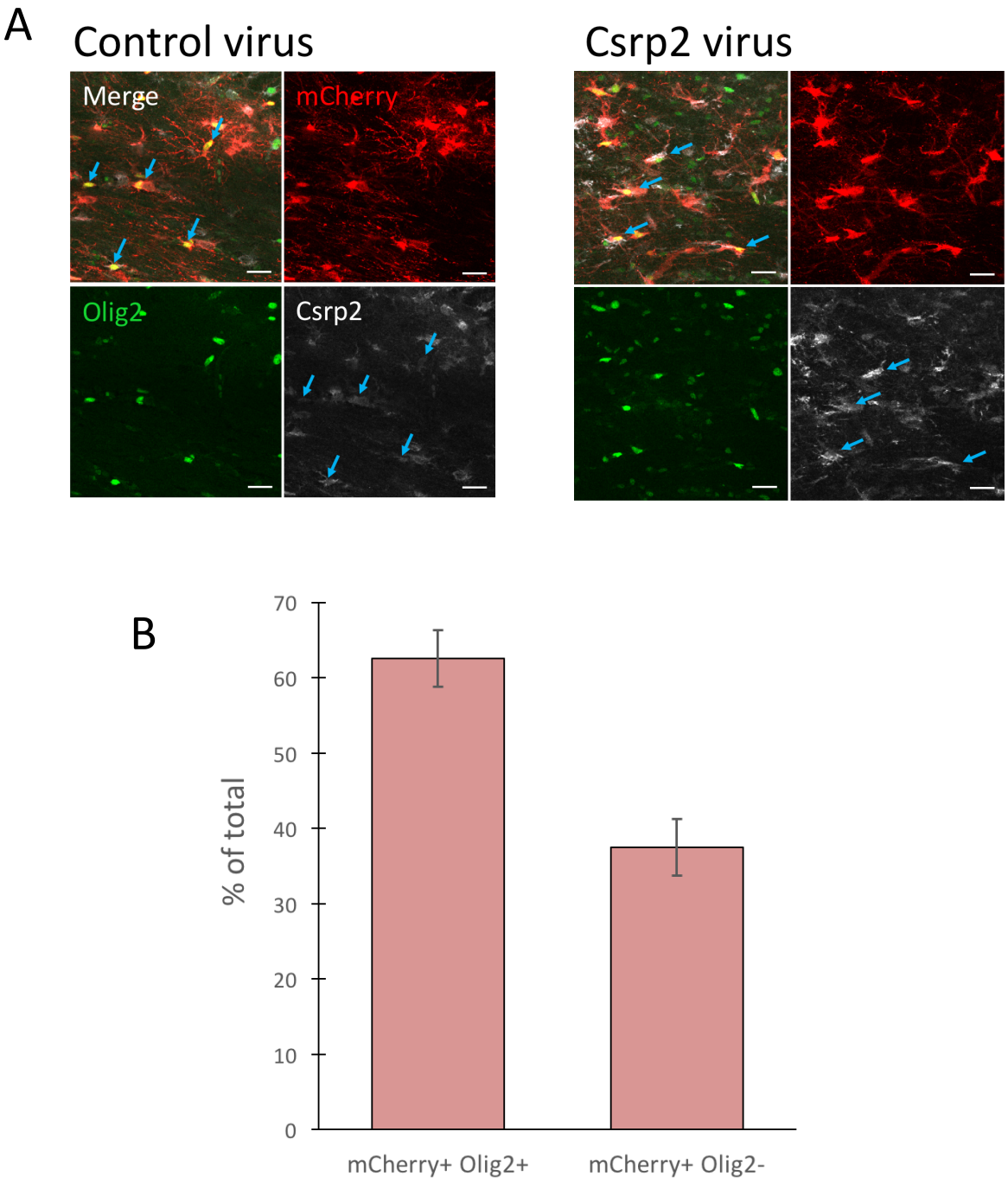
A
Control virus
Csrp2 virus
Merge
mCherry
Olig2
Csrp2
B
% of total
70
60
50
40
30
20
10
0
mCherry+ Olig2+
mCherry+ Olig2-

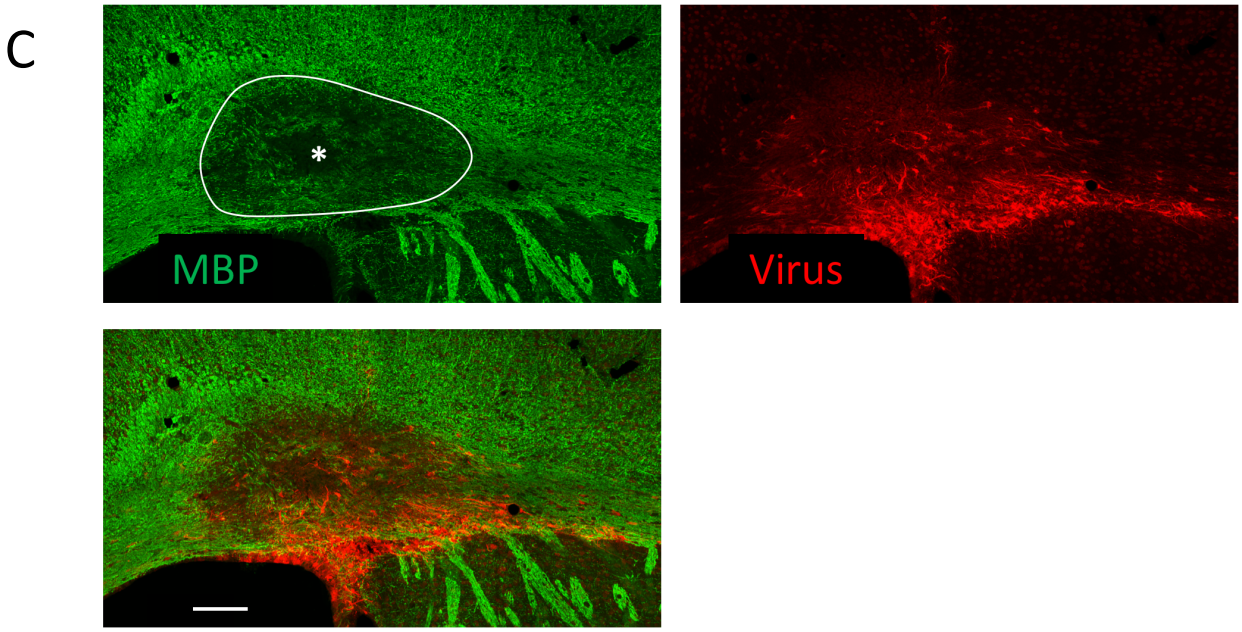

Figure 4-2. Lentivirus is specific to OPCs and targeted to the white matter stroke site
(A) *In vivo* immunofluorescence images of wild-type mice 5 days post-injection of control or *Csrp2*-overexpressing lentivirus constructs shown in **Fig. 4-1**. Specificity to oligodendrocyte lineage is assessed via Olig2 colocalization. Antibody against Csrp2 is also included to highlight overexpression in test animals. **(B)** Quantification of mCherry/Olig2 colocalization as a measure of transduction efficiency. $n = 5$ animals; mean ± SD. **(C)** Virus is targeted to the site of WMS when injected 3 days before injury as shown here. Note cells are resident in both peri-infarct and core (*) regions. Scale bar in (A) 20 μm, (C) 100 μm.

Figure 4-3

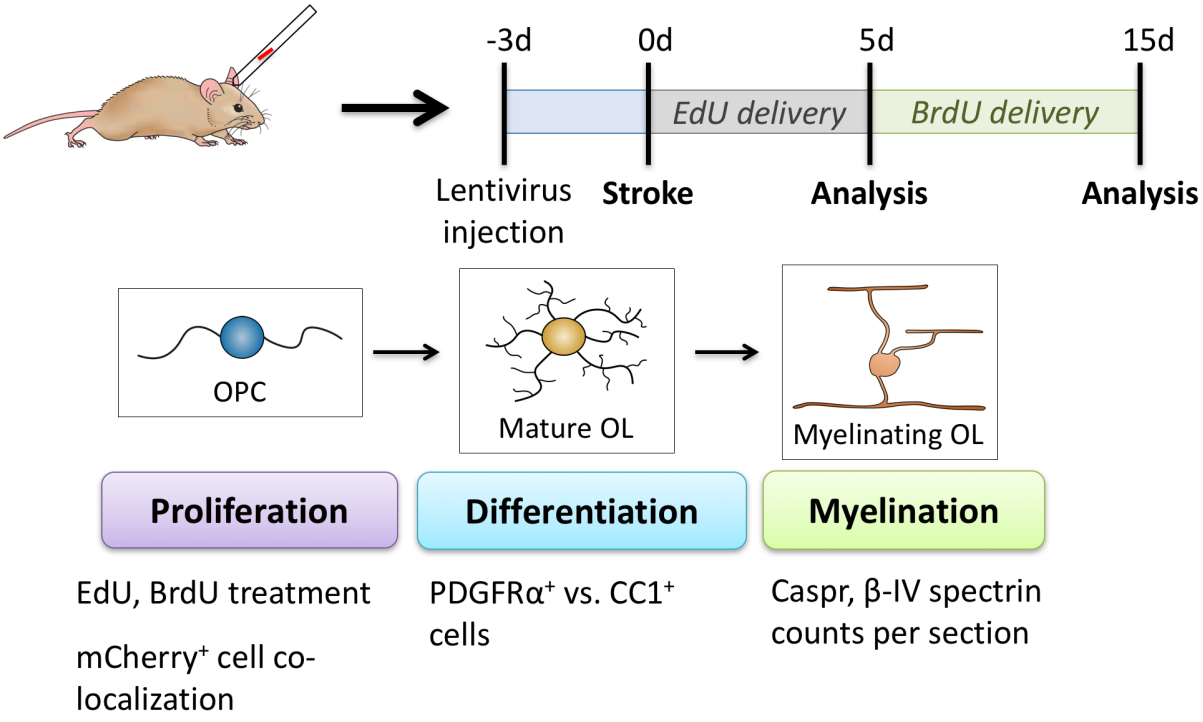

Figure 4-3. Experimental design of *in vivo* experiments
Experimental schematic demonstrates plan for *in vivo* experiments of candidate genes. Lentiviruses are injected 3 days prior to induction of WMS based on expression time course studies. EdU is delivered during the 5 day post-WMS period, and BrdU for the remainder when relevant. The tissue stains planned for assessing OPC response to injury are outlined in three phases: proliferation, differentiation, and myelination, as outlined.

Figure 4-4

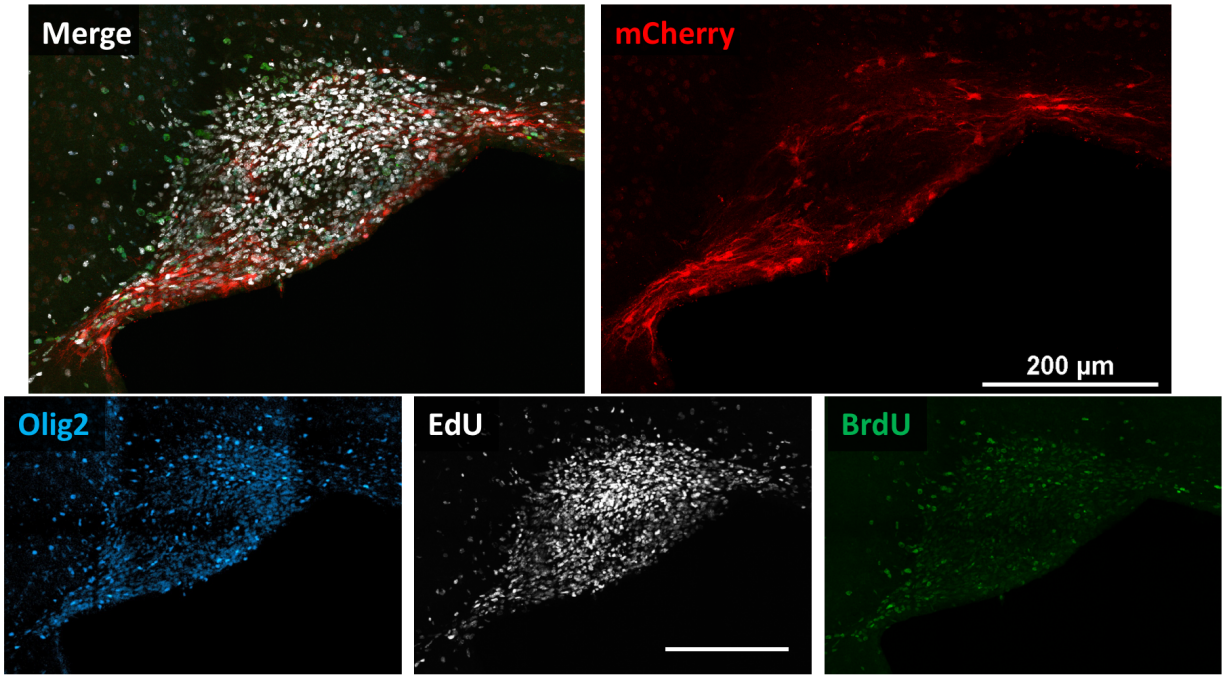

Figure 4-4. Example of proliferation stains
EdU and BrdU incorporation into proliferating cells is shown in Chst10-overexpression virus-injected sacrificed 15 days post-WMS. EdU was delivered in drinking water beginning ~18 hours prior to induction of stroke, while BrdU was delivered in water from 6d to 15d post-stroke. EdU^+/$mCherry^+$ and $BrdU^+$/$mCherry^+$ cells are quantified to assess overall proliferation rate of OPCs. Scale bars: 200 µm.

Figure 4-5

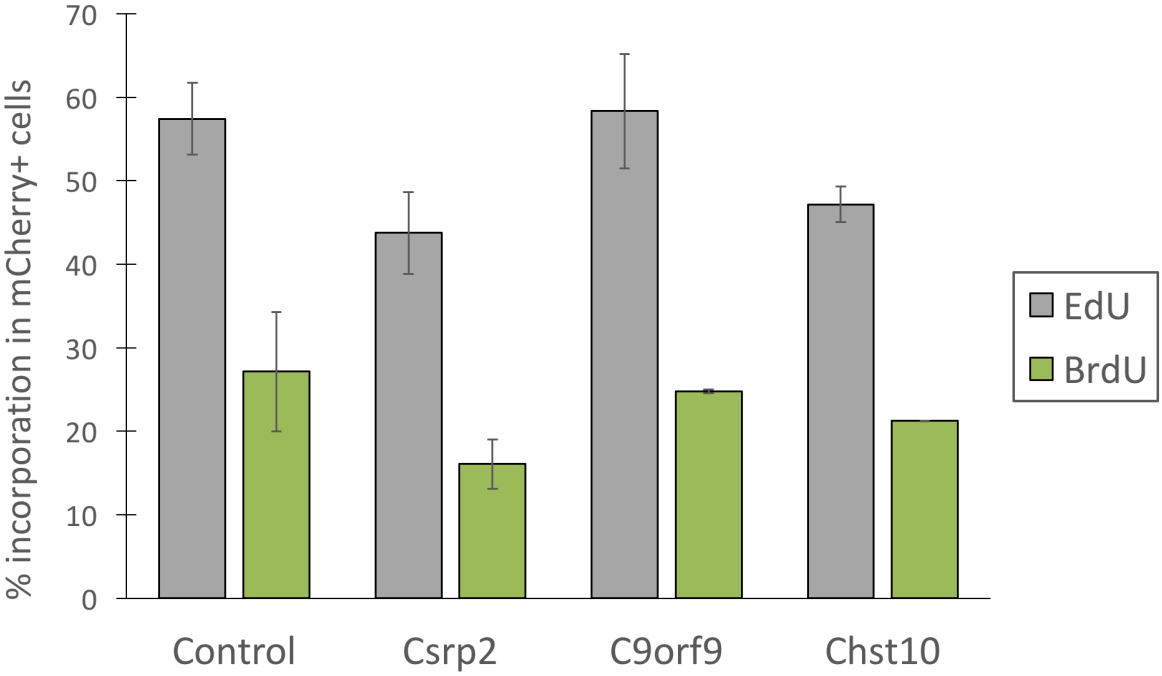

Figure 4-5. Quantification of proliferation after candidate gene overexpression
EdU (gray) and BrdU (green) incorporation into mCherry^{+} transduced cells is quantified for the candidate gene overexpression studies. There are no significant differences in EdU or BrdU incorporation into control virus vs. candidate gene-tranduced cells. n = 5-6 per group. Statistics were performed in Graphpad Prism using one-way ANOVA with Tukey's correction for multiple comparisons. Error bars show SEM. * $P < 0.05$.

Figure 4-6

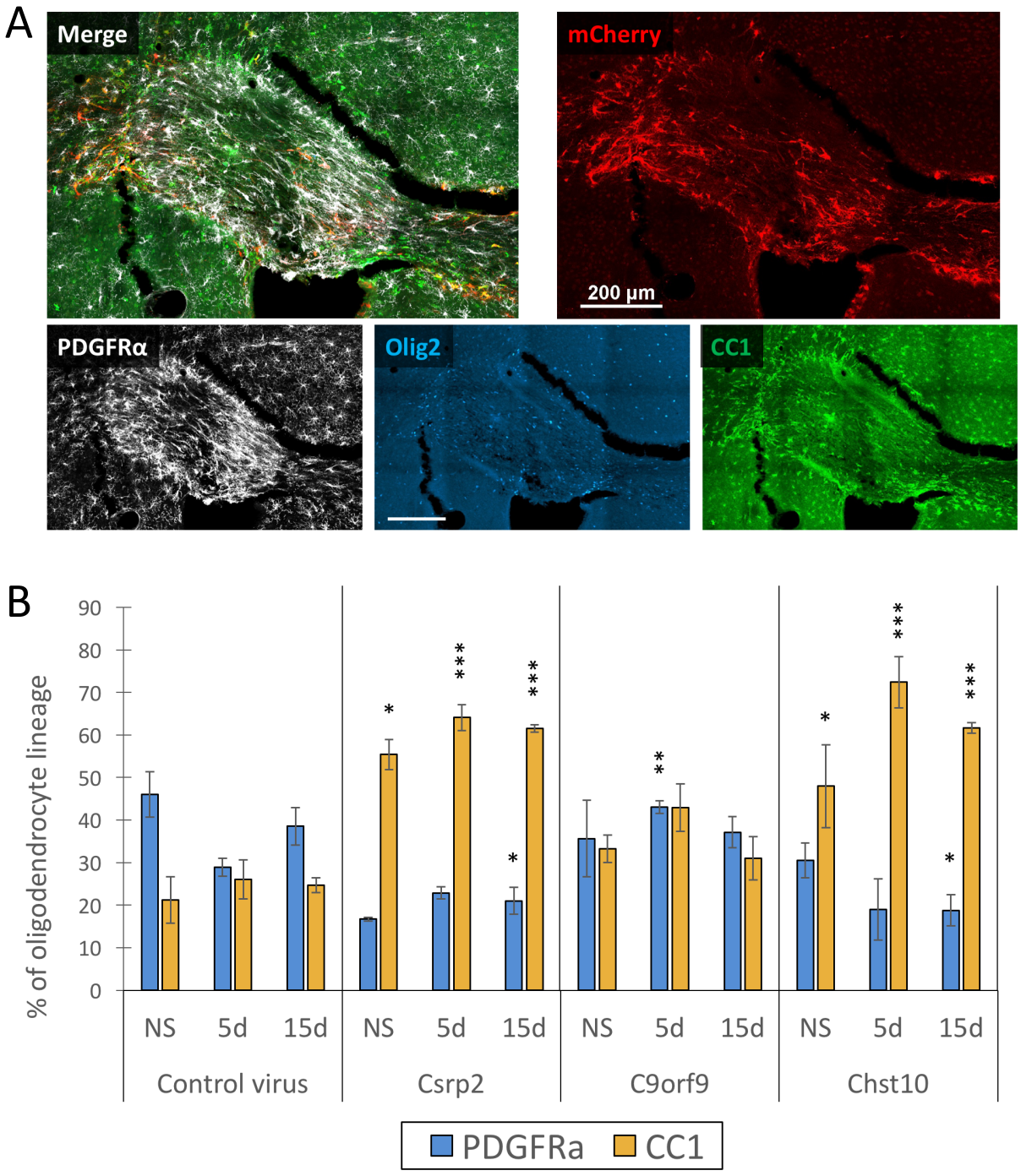
A
Merge
mCherry
200 µm
PDGFRα
Olig2
CC1
B
% of oligodendrocyte lineage
90
80
70
60
50
40
30
20
10
0
NS
5d
15d
Control virus
Csrp2
C9orf9
Chst10
PDGFRa
CC1

Figure 4-6. Quantification of differentiation after candidate gene overexpression
(A) mCherry colocalization with Pdgfrα, Olig2, and CC1 was quantified to assess OPC differentiation. This example image shows Chst10-overexpression tissue from an animal sacrificed 5 days post-WMS. Scale bars: 200 μm. **(B)** Quantification of differentiation as assessed by proportion of $mCherry^+$ cells within the oligodendrocyte lineage that were $Pdgfr\alpha^+$ vs. $CC1^+$ indicates a significant impact of Csrp2 expression on OPC differentiation. Statistics were performed in Graphpad Prism using one-way ANOVA with Tukey's correction for multiple comparisons. n = 5-6 per group. Error bars show SEM. * $P < 0.05$, ** $P < 0.01$.

Figure 4-7

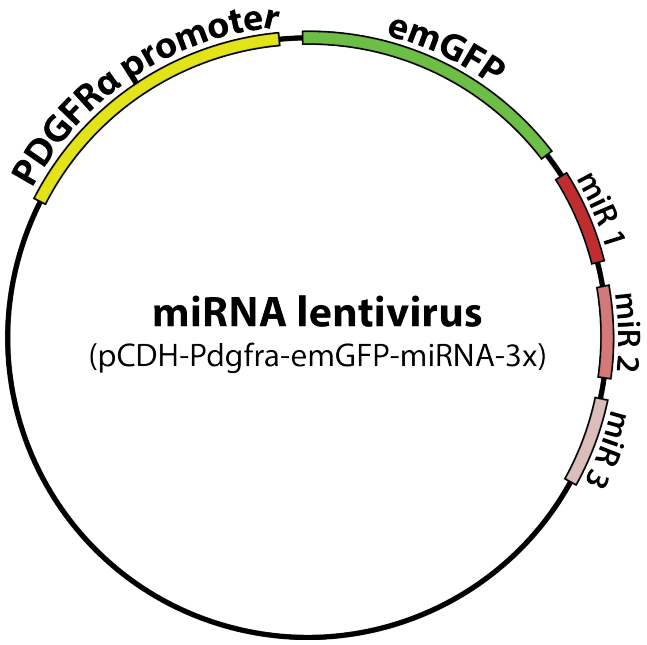

Figure 4-7. Lentiviral construct used for miRNA knockdown of *Csrp2*
Schematic showing the plasmid used to induce *Csrp2* knockdown *in vivo* is shown. The same Pdgfrα promoter used for overexpression studies drives expression of the emGFP fluorophore, followed by a chain of the three most effective miRNA sequences seen *in vitro*.

Figure 4-8

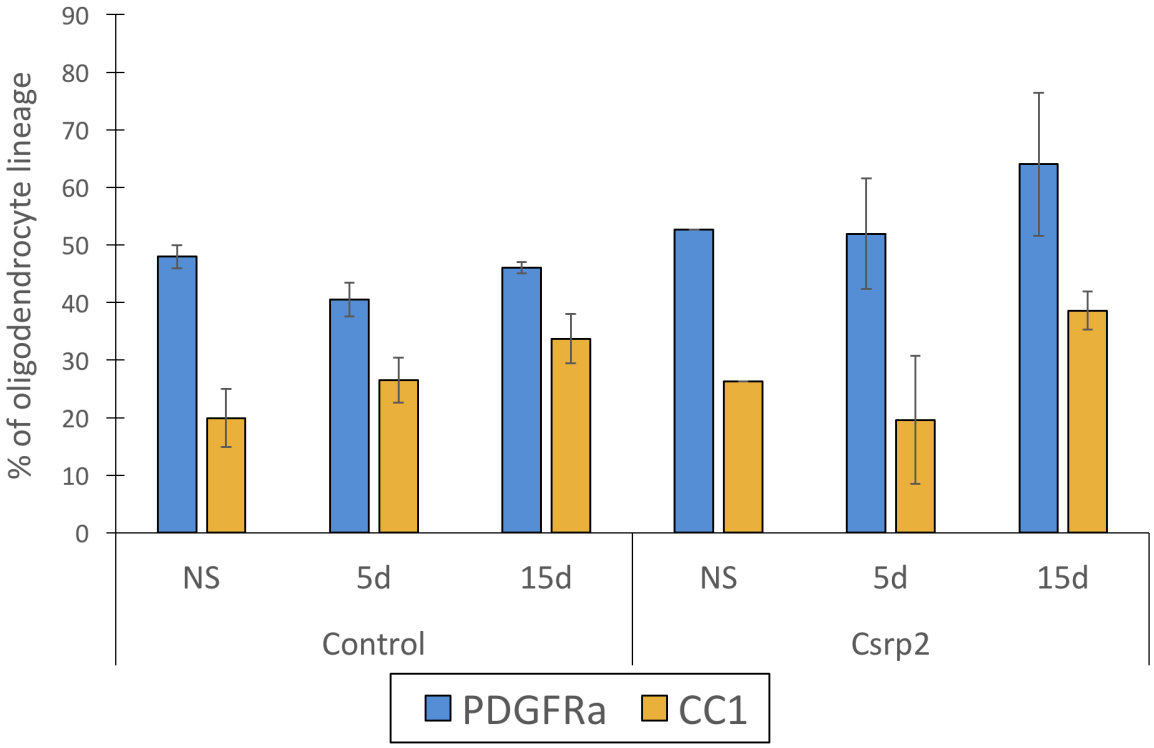

Figure 4-8. miRNA knockdown of *Csrp2* does not significantly impact OPC differentiation Similar quantification of differentiation was carried out on animals after viral knockdown of *Csrp2* as was used in overexpression studies. No significant differences were seen in proportion of emGFP$^+$ cells that were CC1$^+$ as compared to Pdgfrα$^+$ between control virus and *Csrp2* knockdown virus. Statistics were performed in Graphpad Prism using one-way ANOVA with Tukey's correction for multiple comparisons. $n = 3$ per group except *Csrp2* control where due to technical error, $n = 1$. (This was not included in statistics.) Error bars show SEM. * $P < 0.05$.

Figure 4-9

A

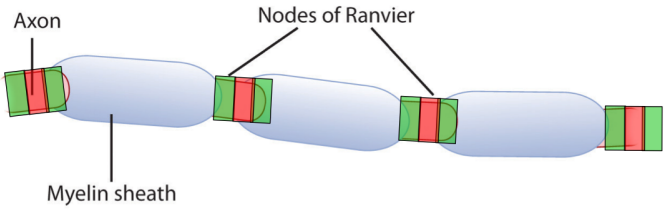

B

No stroke

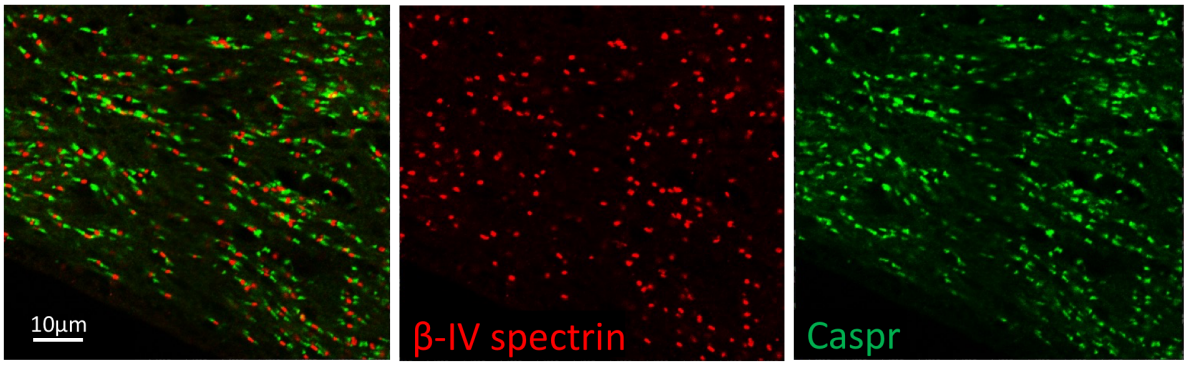

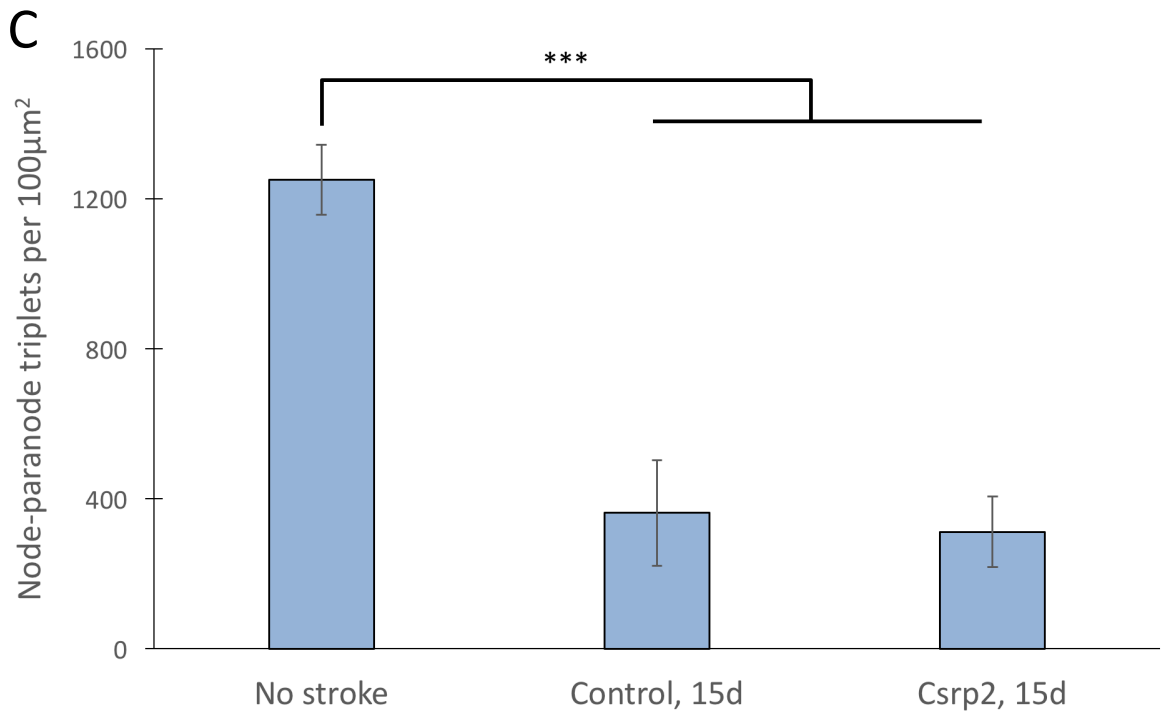

Figure 4-9. Quantification of node-paranode triplets as evidence of remyelination
(A) Schematic showing organization of Caspr (green) and βIV-spectrin (red) in triplets along nodes of Ranvier. **(B)** Stain for these markers in control (no stroke) tissue. Number of intact triplets per 50 µm square are counted to provide a readout of successful remyelination at concentric zones outside the infarct core providing the ability to determine extent of injury within different groups after WMS. **(C)** Quantification of node-paranode triplets per 2500 μm^2 image are shown. A clear deficit is seen in stroke, but no significant differences are seen between control virus and *Csrp2*-overexpressed post-WMS animals. Statistics were performed in Graphpad Prism using one-way ANOVA with Tukey's correction for multiple comparisons. $n = 3$ animals per group. Error bars show SEM. * $P < 0.05$, ** $P < 0.01$, *** $P < 0.001$.

Figure 4-10

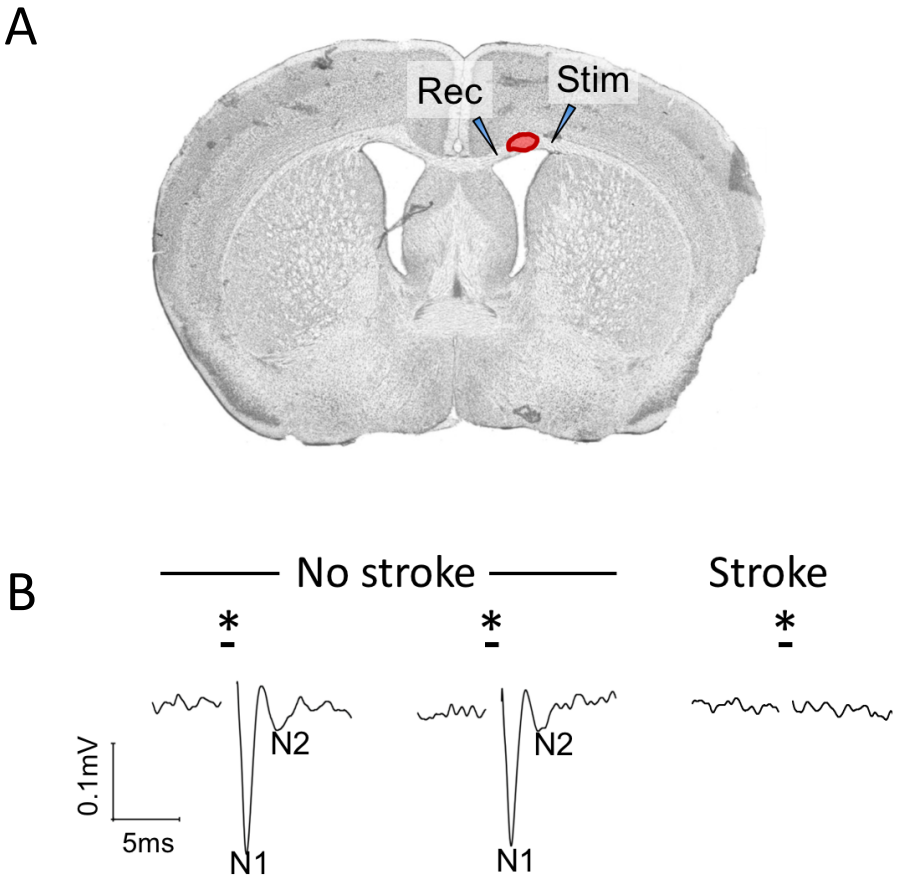

Figure 4-10. Compound action potential (CAP) recordings demonstrate loss of axon functionality in white matter stroke

(A) Schematic showing setup of field recordings. Recording and stimulation were ~1 mm apart for these experiments. **(B)** CAP recordings were obtained from 350µm slices and a 3 mA stimulus was delivered through the stimulating electode (Stim) for the period indicated by (*). N1 and N2 peaks correspond to varying levels of myelinated fiber bundles. CAP recordings were not detected in stroke tissue despite repeated attempts across multiple animals. *n* = 3 per condition.

4.6 References

Bakker, H. (2014). Carbohydrate sulfotransferase 10 (CHST10). In N. Taniguchi, K. Honke, M. Fukuda, H. Narimatsu, Y. Yamaguchi, & T. Angata (Eds.), *Handbook of Glycosyltransferases and Related Genes* (2nd ed., Vol. 1–2, pp. 1–1707). Japan: Springer. https://doi.org/10.1007/978-4-431-54240-7

Barratt, H. E., Lanman, T. a, & Carmichael, S. T. (2014). Mouse intracerebral hemorrhage models produce different degrees of initial and delayed damage, axonal sprouting, and recovery. *Journal of Cerebral Blood Flow and Metabolism*, *34*(May), 1–9. https://doi.org/10.1038/jcbfm.2014.107

Bhattacharya, R., Devi, M. S., Dhople, V. M., & Jesudasan, R. a. (2013). A mouse protein that localizes to acrosome and sperm tail is regulated by Y-chromosome. *BMC Cell Biology*, *14*, 50. https://doi.org/10.1186/1471-2121-14-50

Buga, A. M., Di Napoli, M., & Popa-Wagner, A. (2013). Preclinical models of stroke in aged animals with or without comorbidities: Role of neuroinflammation. *Biogerontology*, *14*(6), 651–662. https://doi.org/10.1007/s10522-013-9465-0

Crawford, D. K., Mangiardi, M., Song, B., Patel, R., Du, S., Sofroniew, M. V., … Tiwari-Woodruff, S. K. (2010). Oestrogen receptor beta ligand: A novel treatment to enhance endogenous functional remyelination. *Brain*, *133*(10), 2999–3016. https://doi.org/10.1093/brain/awq237

Crawford, D. K., Mangiardi, M., & Tiwari-Woodruff, S. K. (2009). Assaying the functional effects of demyelination and remyelination: Revisiting field potential recordings. *Journal of Neuroscience Methods*, *182*(1), 25–33. https://doi.org/10.1016/j.jneumeth.2009.05.013

Crawford, D. K., Mangiardi, M., Xia, X., López-Valdés, H. E., & Tiwari-Woodruff, S. K.

(2009). Functional recovery of callosal axons following demyelination: a critical window. *Neuroscience*, *164*(4), 1407–1421. https://doi.org/10.1016/j.neuroscience.2009.09.069

Dai, J., Bercury, K. K., Ahrendsen, J. T., & Macklin, W. B. (2015). Olig1 Function Is Required for Oligodendrocyte Differentiation in the Mouse Brain. *Journal of Neuroscience*, *35*(10), 4386–4402. https://doi.org/10.1523/JNEUROSCI.4962-14.2015

De Biase, L. M., Nishiyama, A., & Bergles, D. E. (2010). Excitability and Synaptic Communication within the Oligodendrocyte Lineage. *Journal of Neuroscience*, *30*(10), 3600–3611. https://doi.org/10.1523/JNEUROSCI.6000-09.2010

Dull, T., Zufferey, R., Kelly, M., Mandel, R. J., Nguyen, M., Trono, D., & Naldini, L. (1998). A third-generation lentivirus vector with a conditional packaging system. *Journal of Virology*, *72*(11), 8463–71. https://doi.org/98440501

Geller, S. F., Ge, P. S., Visel, M., & Flannery, J. G. (2008). In vitro analysis of promoter activity in Müller cells. *Molecular Vision*, *14*(August 2007), 691–705. Retrieved from http://www.pubmedcentral.nih.gov/articlerender.fcgi?artid=2330062&tool=pmcentrez&rendertype=abstract

Gitlin, A. D., Shulman, Z., & Nussenzweig, M. C. (2014). Clonal selection in the germinal centre by regulated proliferation and hypermutation. *Nature*, *509*(7502), 637–640. https://doi.org/10.1038/nature13300

Gleich, G. J., Frigas, E., Loegering, D. a, Wassom, D. L., & Steinmuller, D. (1979). Cytotoxic properties of the eosinophil major basic protein. *Journal of Immunology (Baltimore, Md. : 1950)*, *123*(6), 2925–7. Retrieved from http://www.ncbi.nlm.nih.gov/pubmed/501097

Hinman, J. D., Lee, M. D., Tung, S., Vinters, H. V., & Carmichael, S. T. (2015). Molecular disorganization of axons adjacent to human lacunar infarcts. *Brain*, 1–10.

https://doi.org/10.1093/brain/awu398

Hinman, J. D., Rasband, M. N., & Carmichael, S. T. (2013). Remodeling of the axon initial segment after focal cortical and white matter stroke. *Stroke; a Journal of Cerebral Circulation*, *44*(1), 182–9. https://doi.org/10.1161/STROKEAHA.112.668749

Lois, C., Hong, E. J., Pease, S., Brown, E. J., & Baltimore, D. (2002). Germline Transmission and Tissue-Specific Expression of Transgenes Delivered by Lentiviral Vectors. *Science*, *295*(5556), 868–872. https://doi.org/10.1126/science.1067081

McGarry, R. C., Helfand, S. L., Quarles, R. H., & Roder, J. C. (1983). Recognition of myelin-associated glycoprotein by the monoclonal antibody HNK-1. *Nature*, *306*, 376–378.

Overman, J. J., Clarkson, A. N., Wanner, I. B., Overman, W. T., Eckstein, I., Maguire, J. L., … Carmichael, S. T. (2012). A role for ephrin-A5 in axonal sprouting, recovery, and activity-dependent plasticity after stroke. *Proceedings of the National Academy of Sciences of the United States of America*, *109*(33), E2230-9. https://doi.org/10.1073/pnas.1204386109

Ransohoff, R. M. (2012). Animal models of multiple sclerosis: the good, the bad and the bottom line. *Nature Neuroscience*, *15*(8), 1074–1077. https://doi.org/10.1038/nn.3168

Remaud, S., Ortiz, F. C., Perret-Jeanneret, M., Aigrot, M.-S., Gothié, J.-D., Fekete, C., … Demeneix, B. (2017). Transient hypothyroidism favors oligodendrocyte generation providing functional remyelination in the adult mouse brain. *eLife*, *6*, e29996. https://doi.org/10.7554/eLife.29996

Rosenzweig, S., & Carmichael, S. T. (2013). Age-dependent exacerbation of white matter stroke outcomes: a role for oxidative damage and inflammatory mediators. *Stroke; a Journal of Cerebral Circulation*, *44*(9), 2579–86. https://doi.org/10.1161/STROKEAHA.113.001796

Saab, A. S., Tzvetavona, I. D., Trevisiol, A., Baltan, S., Dibaj, P., Kusch, K., … Nave, K. A.

(2016). Oligodendroglial NMDA Receptors Regulate Glucose Import and Axonal Energy Metabolism. *Neuron*, *91*(1), 119–132. https://doi.org/10.1016/j.neuron.2016.05.016

Sagave, J. F., Moser, M., Ehler, E., Weiskirchen, S., Stoll, D., Günther, K., … Weiskirchen, R. (2008). Targeted disruption of the mouse Csrp2 gene encoding the cysteine- and glycine-rich LIM domain protein CRP2 result in subtle alteration of cardiac ultrastructure. *BMC Developmental Biology*, *8*, 80. https://doi.org/10.1186/1471-213X-8-80

Shamamian, P., Schwartz, J. D., Pocock, B. J. Z., Monea, S., Whiting, D., Marcus, S. G., & Mignatti, P. (2001). Activation of progelatinase A (MMP-2) by neutrophil elastase, cathepsin G, and proteinase-3: A role for inflammatory cells in tumor invasion and angiogenesis. *Journal of Cellular Physiology*, *189*(2), 197–206. https://doi.org/10.1002/jcp.10014

Sozmen, E. G., Rosenzweig, S., Llorente, I. L., DiTullio, D. J., Machnicki, M., Vinters, H. V., … Carmichael, S. T. (2016). Nogo receptor blockade overcomes remyelination failure after white matter stroke and stimulates functional recovery in aged mice. *Proceedings of the National Academy of Sciences*, *113*(52), E8453–E8462. https://doi.org/10.1073/pnas.1615322113

Stauber, M., Weidemann, M., Dittrich-Breiholz, O., Lobschat, K., Alten, L., Mai, M., … Gossler, A. (2017). Identification of FOXJ1 effectors during ciliogenesis in the foetal respiratory epithelium and embryonic left-right organiser of the mouse. *Developmental Biology*, *423*(2), 170–188. https://doi.org/10.1016/j.ydbio.2016.11.019

Szymczak-Workman, A. L., Vignali, K. M., & Vignali, D. A. A. (2012). Design and construction of 2A peptide-linked multicistronic vectors. *Cold Spring Harbor Protocols*, *7*(2), 199–204. https://doi.org/10.1101/pdb.ip067876

Temkin, V., Aingorn, H., Puxeddu, I., Goldshmidt, O., Zcharia, E., Gleich, G. J., … Levi-Schaffer, F. (2004). Eosinophil major basic protein: First identified natural heparanase-inhibiting protein. *Journal of Allergy and Clinical Immunology*, *113*(4), 703–709. https://doi.org/10.1016/j.jaci.2003.11.038

Tennant, K. A., & Jones, T. A. (2009). Sensorimotor behavioral effects of endothelin-1 induced small cortical infarcts in C57BL/6 mice. *Journal of Neuroscience Methods*, *181*(1), 18–26. https://doi.org/10.1016/j.jneumeth.2009.04.009

Zhao, X., He, X., Han, X., Yu, Y., Ye, F., Chen, Y., … Lu, Q. R. (2010). MicroRNA-Mediated Control of Oligodendrocyte Differentiation. *Neuron*, *65*(5), 612–626. https://doi.org/10.1016/j.neuron.2010.02.018

Zuchero, J. B., Fu, M., Sloan, S. A., Ibrahim, A., Olson, A., Zaremba, A., … Barres, B. A. (2015). CNS Myelin Wrapping Is Driven by Actin Disassembly. *Developmental Cell*, *34*(2), 152–167. https://doi.org/10.1016/j.devcel.2015.06.011

Chapter 5

Approaches to further characterization of candidate genes: Mechanistic studies and small-molecule screens

5.1 Introduction

The studies conducted in Chapter 4 highlight Csrp2 as a protein with potential to induce oligodendrocyte differentiation in both post-ischemic and normal brain. This makes it a promising new candidate for promoting myelination. However, examination of a role in the mouse WMS model is only a small first step towards gaining a mechanistic understanding of this novel protein. In order to begin to consider possible applications of this discovery, an understanding of the role of Csrp2 must be ascertained. For example, Csrp2 is a transcription factor binding protein likely localized to the nucleus (Sagave et al., 2008; UniProt, 2017). Thus, exogenous application of a treatment to manipulate this pathway would require identifying protein interactors and thus potential receptors that facilitate external signals to induce Csrp2 activity.

These questions are challenging but necessary: given the number of reports of genes that impact oligodendrocyte differentiation, few have led to small molecule treatments that show clinical potential (for reviews see, for example, Franklin & ffrench-Constant, 2017; Nishiyama et al., 2009; Simons & Nave, 2016). Thus, this final chapter seeks to explore potential methodologies that may be able to address both of these questions. First, proximity biotinylation is applied to the study of Csrp2 in an attempt to identify binding partners within the nucleus, which would provide context that may assist in placing Csrp2 within existing pathways known to

impact oligodendrocyte differentiation. One hypothesis would be that Csrp2 could complex with and help to activate a known transcription factor like Olig1, which is known to be required to initiate oligodendrocyte differentiation (Dai et al., 2015).

Second, opportunities are explored to revisit the OPC stroke transcriptome in order to identify potential external regulators of genes of interest within the dataset. By comparing the stroke transcriptomic data to existing databases, it is possible to generate a list of small molecule candidates that are predicted to interact with each candidate gene.

The studies in this chapter both bring this work back to where it began – founded on a powerful and disease-specific gene expression dataset – while also extending it beyond the gene-by-gene approach initially planned for this dissertation. With the approaches and tools explored in this chapter, our hope is to provide avenues for continued discovery of new pathways important for recovery after white matter stroke, as well as beyond, to shed light on the many remaining mysteries of oligodendrocytes themselves.

5.2 Results

Proximity biotinylation of Csrp2

Csrp2 was shown to have a pro-differentiation effect through both *in vitro* (Chapter 3) and *in vivo* (Chapter 4) experiments. However, little is known about this protein, and thus it is difficult to interpret these encouraging results in a context relevant to understanding the implications for white matter stroke or oligodendrocyte biology more generally. To attempt to identify direct interactors of Csrp2, we turned to the BioID2 proximity biotinylation approach developed by the Kyle J. Roux (Kim et al., 2016; Roux et al., 2013). In this approach, a schematic of which is presented in **Figure 5-1**, a biotin ligase derived from the bacterium *A.*

aeolicus is modified such that biotinylation becomes promiscuous. Upon joining this protein, termed BioID2, to a protein of interest and treatment with biotin at micromolar concentrations, it the enzyme releases large quantities of activated biotin in the local vicinity of the protein of interest. Later, streptavidin bead purification of biotinylated proteins, Western blotting, and mass spectrometry allows for identification of novel proteins present within 10-20 nm of the chimeric protein (Lambert et al., 2015; Roux et al., 2012).

The BioID expression plasmid was obtained from Addgene, and Csrp2 was cloned in to the appropriate cassette to express BioID2 joined to the N-terminus of Csrp2, along with a myc tag for verification of expression via Western blotting. As a control, several options were considered, and use of a nuclear localization signal (NLS) sequence was chosen in an attempt to localize control BioID2 to the same subcellular compartment as the BioID2-Csrp2 construct. In fact, UniProt identifies a putative NLS within the Csrp2 sequence (UniProt, 2017). We also included a well-known NLS as an additional control (Pouton, 1998; Schmidt et al., 2015).

After expressing all constructs in the 293T cell line, pulldown of biotinylated proteins was analyzed using Western blotting, which verified both biotinylation of proteins selectively upon addition of biotin, as well as successful pulldown of those proteins (**Figure 5-2A**). Pilot samples were submitted for mass spectrometry in the laboratory of James Wohlschlegel at UCLA, and initial run successfully identified Csrp2, validating expression and experimental design (**Fig. 5-2B**). At this time, finalized samples have been submitted and awaiting results.

Bioinformatics analysis of upstream and small molecule regulators

Concurrently with proximity biotinylation as a biochemical approach to understanding the mechanism of promising candidate genes, we returned to the OPC stroke transcriptome

dataset for deeper analysis of our genes of interest. Data were imported into the Ingenuity Pathway Analysis software (QIAGEN Bioinformatics), which provides a curated database of protein-protein and protein-molecule interactions.

This software was used for two reasons. First, it allows for identification of small molecules, both endogenous and exogenous, that are predicted to interact with the gene of interest. This could provide a set of readily available molecules that could be tested in primary OPC culture and/or *in vivo* to assess whether it (1) affects Csrp2 expression, and (2) recapitulates the recovery response seen in previous studies.

This process was carried out with two molecules: *Csrp2*, as noted, as well as the extracellular matrix protein matrilin-2 (*Matn2*), which has been studied alongside these genes as part of a separate series of experiments derived from the OPC stroke transcriptome. It was selected due to interest in gaining a deeper understanding of the Matn2 functional network of proteins and potential pathways by which its expression could be manipulated *in vitro* or *in vivo*.

Results of Ingenuity Pathway Analysis investigation of these two genes are shown in **Figure 5-3**. A number of extracellular molecules were predicted to interact with Matn2, perhaps not surprising given its role as an extracellular matrix protein. A number of promising molecules, including CREB, IL-8 and TFG-β, were identified for Csrp2. In the interest of directly testing small molecules in a straightforward system, *Matn2* was selected for further investigation.

A number of the small molecules were available from commercial vendors, and thus were obtained for testing directly on oligodendrocytes. The same primary OPC culture system was used for these studies, along with qPCR, as a well-validated readout of oligodendrocyte differentiation of candidate molecules. The results of the initial screen are shown in **Figure 5-4.** Here, rifampin has a robust effect on both OPC differentiation as well as *Matn2* induction. Given

that previous results suggest Matn2 induces OPC differentiation itself, this result is consistent with previous results (data not shown). This highlights rifampin as a potential regulator of oligodendrocyte differentiation.

Rifampin treatment of post-stroke animals and effect on OPC differentiation

Based on the results *in vitro* suggesting a pro-differentiation effect of rifampin mediated by or in concert with matrilin-2 expression, additional studies were conducted to assess whether a similar effect on OPC differentiation is seen *in vivo*. As shown in **Figure 5-5**, animals received white matter stroke, and were treated with daily injections of rifampin or vehicle for ten days. Upon sacrifice, mRNA was extracted from white matter infarct and peri-infarct tissue. This was then submitted to for gene expression analysis using the Nanostring platform. In this system, a pre-defined set or sets of genes is analyzed for each sample, and an absolute number of reads per gene is quantified. After normalization to a set of five housekeeping genes, ratios of expression can be calculated for each gene between vehicle- and rifampin-treated animals.

As shown in **Fig. 5-5B**, 120 test genes were analyzed, divided into three groups: OPC, new oligodendrocyte (new OL), and myelinating oligodendrocyte (mOL). This was based on the Zhang dataset for the top 40 most enriched genes per cell type (Zhang et al., 2014). Enrichment of specific groups of genes can be used to identify trends in differentiation of OPC lineage cells. Results indicate that the mOL gene set is significantly enriched (ratio > 1) in rifampin-treated animals as compared to vehicle, and this enrichment is significantly higher than either OPC or new OL enrichment. Thus, rifampin treatment has a pro-differentiation effect *in vivo*, after white matter stroke, matching the results seen *in vitro*.

Electron microscopy analysis of matrilin-2 treatment

Finally, in Chapter 4 a number of attempts to quantify remyelination proved unsuccessful. In this study of matrilin-2, electron microscopy (EM) was used to assess remyelination, as has been done previously by our group and others (He et al., 2016; Sozmen et al., 2016). This directly assesses remyelination by quantifying the *g*-ratio of each axon within a field: that is, the ratio of axon diameter to the diameter of the axon + myelin. Thus, a lower *g*-ratio indicates a higher degree of myelination.

Aged animals were subjected to white matter stroke and then injected with soluble matrilin-2 protein or vehicle. After 30 days, tissue was prepared and imaged by EM. Quantification of remyelination is shown in **Figure 5-6**. Analysis of *g*-ratios shows a significant decrease in matrilin-2 treated animals (**Fig 5-6A** and **5-6B**). In addition, comparing the proportion of myelinated vs. unmyelinated axons in each section indicates that a higher proportion of axons are myelinated in animals treated with matrilin-2. Together, this suggests that matrilin-2 has a pro-myelination effect after WMS, and provides evidence of a well-validated technique in our hands to assess remyelination in this animal model.

5.3 Discussion

Proximity biotinylation offers a window into Csrp2 function in vivo

In this section, additional studies are presented that seek to deepen our understanding of the novel genes discovered through studies of the OPC stroke transcriptome. Csrp2, a novel transcription factor binding protein, is investigated using proximity biotinylation, with results ultimately derived from mass spectrometry. The benefits of this biochemical approach to the study of this protein pathway is that it is unbiased, meaning other novel proteins that come up

through this analysis may be identified as totally new binding partners to Csrp2, and potentially to novel actors in oligodendrocyte differentiation.

There were some notable limitations with this approach, however. First, due to time and resource constrains, experiments using BioID2-Csrp2 were performed in human-derived HEK cells; these cells are, in addition to being derived from a different organism, are not CNS-derived, and thus the biology may differ. Two reasons make us hopeful that this will not be an issue. First, the protein sequences between human and mouse Csrp2 are 99% identical (192/193 amino acids). Second, Csrp2 has been identified to play a role in differentiation and cell growth in cardiomyocytes as well, suggesting that this is perhaps a function not wholly specific to oligodendrocytes (Sagave et al., 2008).

Ingenuity pathway analysis identifies rifampin as a potential regulator of myelination

Ingenuity pathway analysis allowed us to identify putative regulators of candidate genes, including *Csrp2* but also the extracellular matrix protein *Matn2*. Analysis of small molecule interactors in particular suggested promising avenues of further study. When these small molecules were tested *in vitro*, several had significant effects on oligodendrocyte differentiation, but in particular, rifampin demonstrated a robust effect both on OPCs and on *Matn2* expression. Rifampin, an anti-tuberculosis drug, is FDA approved, making it especially promising is a candidate for remyelination after white matter stroke.

Use of NanoString analysis to study rifampin's effect on OPC differentiation *in vivo* represents application of a novel, and complementary, technique similar to the *in vitro* qPCR studies, but in a disease-relevant animal model. Combining assessments of OPC, new OL, and mOL gene sets within the tissue allows for a multi-point lineage analysis of oligodendrocyte

after injury. Most importantly, the significant results shown in this study further highlight rifampin as a readily-available drug to examine post-WMS. It also validates an additional technique that could be used to assess other small molecules identified through a similar process for *Csrp2*, *Chst10*, or other candidate genes that arise from this dataset or future transcriptomic datasets using a similar analysis pipeline.

Matrilin-2 electron microscopy analysis

Finally, results of EM analyses of matrilin-2 treatment in aged animals validates this molecule, the initiator of studies that led to the identification of rifampin, as a promyelinating factor after WMS. In this case, the *g*-ratio decreased upon matrilin-2 treatment, and a higher proportion of axons were myelinated, both of which indicate matrilin-2 is enhancing myelination after injury.

These studies are also relevant to this dissertation because they represent a methodology, often used in the glial biology field, that allows for measurement of remyelination. As seen in Chapter 4, a number of methods were explored to assess this, including compound action potential recordings and node-paranode quantification, each led to technical issues or did not demonstrate significant results. In some regard, EM analysis is more limited than those two techniques, as it does not analyze functionality of remyelination; still, it does provide evidence of successful outcomes of oligodendrocyte differentiation beyond expression of markers such as CC1 in tissue sections.

Future directions

This chapter chronicles experiments that aim to deepend our understanding of the genes we have identified in previous chapters as impacting OPC differentiation using a number of novel techniques. Initially, these highlight the potential of rifampin as a small-molecule treatment that enhances oligodendrocyte differentiation. Initial follow-up studies should investigate the effect of rifampin treatment on the tissue level, using a similar experimental design as outlined in Chapter 4. Additionally, a similar small-molecule screen could focus on identifying regulators of *Csrp2* and *Chst10* expression, which would, in combination with proximity biotinylation studies, help to put these in a broader context within the cell and could elucidate potential mechanisms for their impact on OPC differentiation.

On the whole, the results shown in this chapter help to reimagine the process of this dissertation, from the initial linear path of bioinformatics to cell culture to tissue studies, instead as a multi-faceted toolset in which techniques within each domain work together throughout the course of a study. In this way, we have been able to delve more deeply into the biologies and pathologies of a key disease process, both to uncover new cellular pathways, but also identify promising small molecules with the potential to impact treatment of these diseases.

5.4 Methods

BioID construct expression

BioID constructs were obtained from Addgene (74223 and 74224). Csrp2-ORF (mouse) was obtained from Origene (MC200815). NLS sequences were: Csrp2, KKYGPK; control, PKKKRKV and were tagged to the C-terminus of BioID2 (the same location as Csrp2 in the test construct).

BioID2 plasmids were expressed in HEK 293T cells (ATCC CRL-1573). To culture, cells were grown in DMEM as base media (Invitrogen 11995073). This was supplemented with 10% FBS (Invitrogen 10082147). To transfect BioID constructs, we used Mirus TransIT 293 (MIR 2700) according to manufacturer protocol. Cells were then grown for 72 hours post-transfection to ensure expression and correct localization of chimeric proteins or NLS-tagged controls. At that time, media was changed to prewarmed fresh media supplemented with 50 μM biotin (Sigma B4501). After 18 hours, cells were lysed as described below.

Streptavidin pulldown of biotinylated proteins

The following protocol was generously provided by Dr. James Wohlschlegel and Shima Rayatpisheh.

All steps involving exposure of sample were performed in a cell culture hood to limit keratin contamination. Cells were lysed in buffer containing 8M urea, 5% NP40, 30 mM NaCl, and 100 mM Tris-Hcl (pH 8), with 5 ml added to a total of six T75 flasks per condition. After resuspension, 2μl benzonase (Sigma E1014) and rotated for 30 min at room temperature. Samples were divided into DNase/RNase free 2 ml tubes and spun at 20,000 *g* for 15 min. Supernatant was collected, avoiding pellet and top milky layer, and added to pre-washed

Dynabeads MyOne Streptavidin C1 beads (Thermo Fisher 65001). Beads were rotated for 2 hours at room temperature, then put through a total of 8 wash steps, with each step involving 1 ml buffer per tube with 5 minutes rotation followed by application of tubes to a ThermoFisher MagnaRack (CS15000). Washes were: 4x lysis buffer, 2x wash buffer (lysis without NP40), and 2x digestion buffer (8M urea in 100 mM Tris-HCl pH 8.5). Following the final wash, all excess buffer was removed, and beads were combined within conditions in a total of 100µl digestion buffer and delivered to Dr. Wohlschlegel's lab for processing and mass spectrometry.

Western blot

Western blot was carried out with NuPage Bis-Tris 12% gels (Thermo Fisher NP034C) according to manufacturer instructions. Denaturing NuPAGE electrophoresis (Novex) was conducted prior to Western blotting, with a dual-component ladder containing 5 µl MagicMark XP Western Protein Standard and 5 µl Novex Sharp Pre-Stained Protein Standard (Thermo Fisher Scientific). Prior to gel loading, samples containing loading buffer, reducing agent, and deionized water were heated at 95°C for 10 minutes to facilitate denaturation.

Gels were subjected to Western blotting using the Abcam Western Blotting protocol (Abcam). Membranes were blocked for 1 hour in PBS with 5% reconstituted milk and 0.1% Tween. Membranes were incubated with Pierce high sensitivity Streptavidin-HRP (ThermoFisher 21130) according to manufacturer instructions. Signals were developed using Luminata Crescendo Western HRP Substrate (EMD Millipore).

Small molecule qPCR testing

Primary OPC cultures were carried out as described in Chapter 3 with the following change: after 1 day in culture to stabilize cells after immunopanning, media was changed to prewarmed DMEM-Sato proliferation media containing one of the following supplements: 2.5 μM rifampin (Sigma R3501), 1 μM methaneselenenic acid (Sigma 541281), 100 nM vitamin K2 (Sigma V9378). 100 ng/ml BMP6 (R&D 6325-BM-020). After 4 days in culture, changing media every other day, cells were prepared for qPCR as previously described.

NanoString analysis

WMS was induced in a total of 12 animals as previously described (6 per group). One day after WMS, animals began daily injections of rifampin (Sigma R3501, 50 mg/kg, in 10% DMSO) or vehicle. After 10 days, animals were sacrificed, and white matter tissue was isolated (3-5 mg per animal, from white matter ipsilateral to and including the stroke tissue). mRNA was isolated using the RNeasy kit described previously. Samples were submitted for NanoString analysis to the UCLA IMT core/Center for Systems Biomedicine, supported by CURE/P30 DK041301. Results were analyzed using nSolver Analysis Software 3.0. Briefly, after normalizing to housekeeping genes, ratios of expression in rifampin-treated animals to vehicle-treated animals were calculated for each test gene. The list of genes used is shown in **Table 5-1**.

For statistical analyses, one-way ANOVA was run comparing the ratios of each of the probe sets to each other, using the Dunnett multiple comparison correction. One-sample *t*-tests were used to test for difference in ratios in each probe set from a hypothetical mean of 1.

Electron microscopy analysis

Aged animals (18-22 months) were given WMS as described previously, but with DV coordinates of -2.0, -1.95, and -1.9 to account for smaller brain volume. Six days after WMS, animals received a total of 1 μg of recombinant mouse matrilin-2 (R&D Systems 3234-MN-050/CF; 2 μg/μl in PBS) or PBS only for the vehicle group. One month after treatment, animals were perfused with 2% PFA, 2.5% glutaraldehyde and sent to the UC Denver Electron Microscopy core for processing and electron microscopy.

For analysis, two 100 μm^2 sections were analyzed per animal, each within 200 μm of the infarct core as judged by Iba1 staining of remaining tissue not sent for EM. Images were analyzed for *g*-ratios and % myelinated using Fiji. To assess *g*-ratio, borders around the axon and myelin were drawn and diameter was calculated by approximating each as a circle, then calculating *g*-ratio as (diameter axon) / (diameter axon + myelin). Statistical analysis was performed in GraphPad Prism 6 using unpaired, two-way student *t* tests between animal-level averages in *g*-ratio and % myelinated axons between stroke + matrilin-2 and stroke + vehicle.

5.5 Figures

Figure 5-1

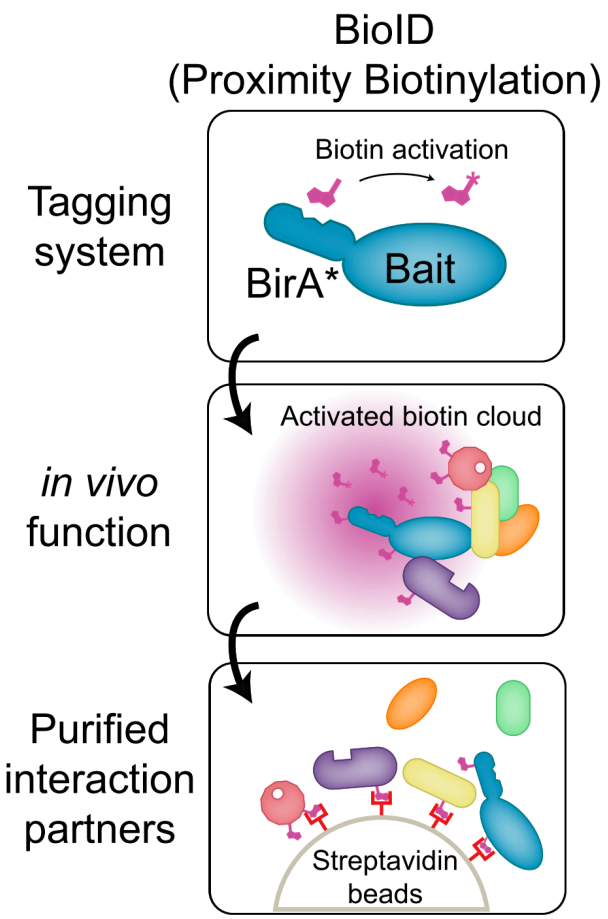

Figure 5-1. Schematic of proximity biotinylation
Proximity biotinylation like BioID and BioID2 rely on biotin ligases, such as BirA*, which are mutated such that they activate biotin in preparation for covalent binding to proteins, but release it prior to catalyzing the reaction. Thus, any proteins in a small area around the BirA* protein-GOI complex are biotinylated and can be purified with standard techniques, such as streptavidin bead pulldown, and analyzed through Western blot or mass spectrometry.

Figure 5-2

A

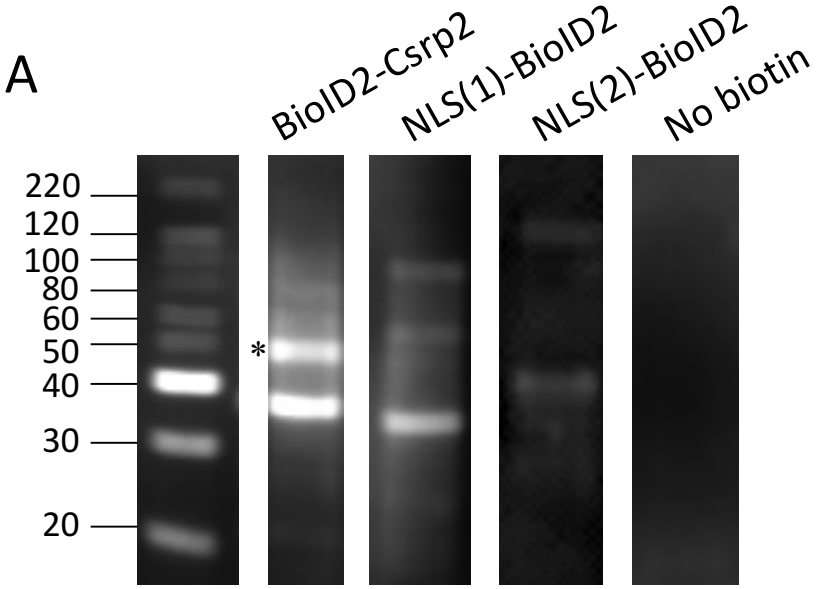

B

1.9648314 Cysteine and glycine-rich protein 2 OS=Homo sapiens GN=CSRP2 PE=1 SV=3

XCorr	DeltCN	Conf%	ObsM+H+	CalcM+H+	PPM	SpR	Prob Score	pI	Ion%	#	Sequence
3.8966	0.8427	100.0%	1563.688	1563.6857	1.5	1	21.891893	4.72	81.0%	3	R.TVYHAEEVQCDGR.S
3.8996	0.6739	100.0%	1563.69	1563.6857	2.7	1	14.764684	4.72	57.5%	9	R.TVYHAEEVQCDGR.S
3.9991	0.5192	100.0%	2136.039	2136.0278	5.3	1	10.350706	4.89	31.1%	2	R.KNLDSTTVAIHDEEIYCK.S
4.6758	0.7405	100.0%	2007.936	2007.9327	1.6	1	21.092209	4.4	43.3%	3	K.NLDSTTVAIHDEEIYCK.S
4.2378	0.6675	100.0%	2007.94	2007.9327	3.6	1	14.394843	4.4	29.0%	4	K.NLDSTTVAIHDEEIYCK.S
4.2228	0.7602	100.0%	1559.693	1559.6907	1.5	1	17.793507	6.56	76.0%	5	K.GYGYGQGAGTLNMDR.G
2.0437	0.5704	100.0%	1901.859	1901.8558	1.7	1	11.11154	6.56	24.0%	1	K.GYGYGQGAGTLNMDRGER.L
3.2814	0.5376	100.0%	1099.475	1099.4724	2.3	1	9.747417	4.46	76.5%	1	R.CGDSVYAAEK.I
2.4782	0.5171	100.0%	1108.576	1108.5731	2.6	1	10.990236	4.46	64.7%	2	K.SLESTTLTEK.E
2.3408	0.5214	99.2%	1987.959	1987.9528	3.1	1	11.7823925	4.4	20.0%	1	K.SLESTTLTEKEGEIYCK.G
4.8372	0.4931	100.0%	1987.963	1987.9528	5.2	1	13.531498	4.4	33.3%	7	K.SLESTTLTEKEGEIYCK.G
3.952	0.6608	100.0%	1432.7	1432.6968	2.2	1	18.073122	7.33	76.0%	6	K.GFGYGQGAGALVHAQ.-

Figure 5-2. Western blot confirms biotinylation
(A) Western blots run on eluates from the chimeric BioID2-Csrp2 construct in comparison to the Csrp2-NLS sequence (NLS[1]) or control NLS (NLS[2]) demonstrate biotinylation of unique proteins in the BioID2-Csrp2 condition as compared to control sequences. No protein appears with addition of chimeric enzyme but no biotin ("No biotin"). Expected band sizes of BioID2-Csrp2, 48.9 kDa; NLS(1)-BioID2, 28.7 kDa; NLS(2)-BioID2, 28.7 kDa. BioID2-Csrp2, visible on the gel, is marked with (*). **(B)** Csrp2 was detected on mass spectrometry on a Coomassie gel band isolate, confirming successful expression of gene construct and validating preparation techniques for mass spectrometry.

Figure 5-3

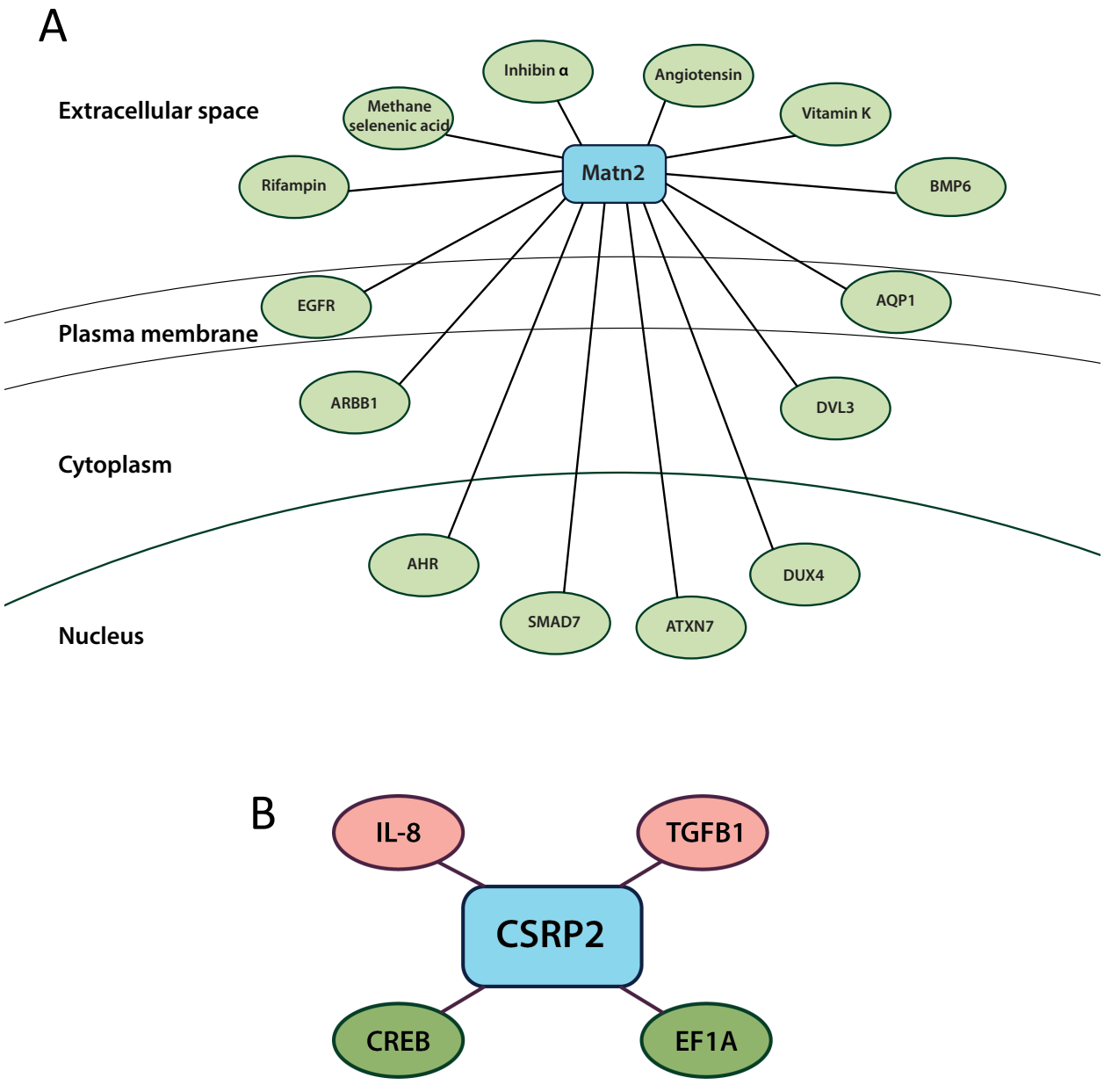

Figure 5-3. Upstream analysis of candidate genes using Ingenuity Pathway Analysis
(A) *Csrp2* and **(B)** *Matn2* are investigated using pathway analysis software to identify potential regulators of gene expression and thus, interactors within the large oligodendrocyte differentiation regulation network. In (A), molecules are arranged by cellular location, while in (B) they are identified based on predicted inhibition (red) or activation (green) of Csrp2. Of note, a number of extracellular and small molecule genes were identified as potential regulators of Matn2.

Figure 5-4

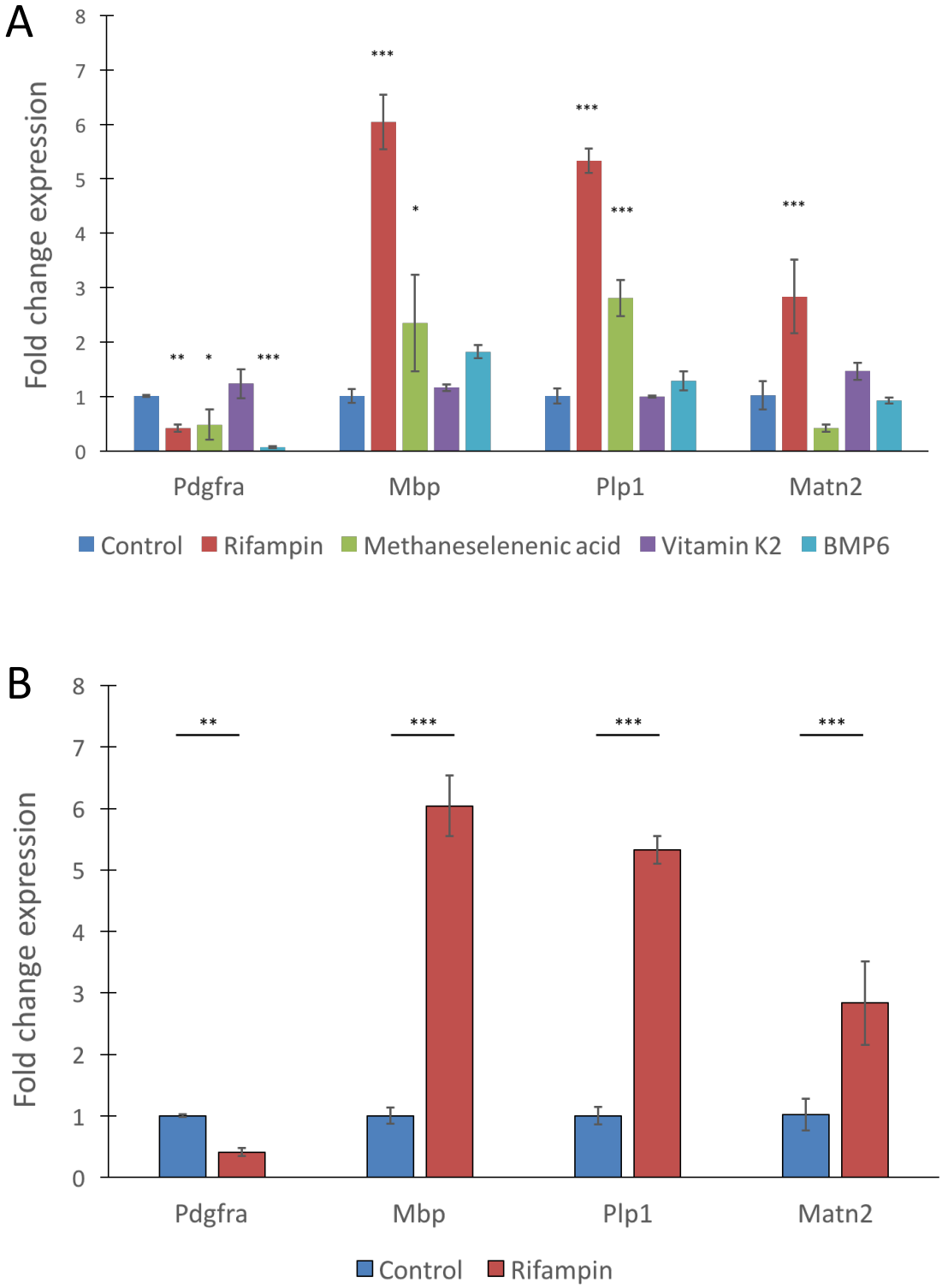
A
Fold change expression
8
7
6
5
4
3
2
1
0
**
*
***
***
*
***
***
***
Pdgfra
Mbp
Plp1
Matn2
Control
Rifampin
Methaneselenenic acid
Vitamin K2
BMP6
B
Fold change expression
8
7
6
5
4
3
2
1
0
**
***
***
***
Pdgfra
Mbp
Plp1
Matn2
Control
Rifampin

Figure 5-4. Assays of small molecule impact on OPC cultures and *Matn2* expression
(A) Primary OPC cultures were treated with small molecules predicted to interact with Matn2, and impact on gene expression of *Matn2* as well as target genes to assess OPC differentiation, outlined in Chapter 3, is assessed using qPCR. **(B)** Expanded view of the effect of rifampin on OPC cultures shows that there is a robust, pro-differentiation effect, corresponding to induction of *Matn2* mRNA expression in oligodendrocytes. Statistics were performed in Graphpad Prism using one-way ANOVA with Tukey's correction for multiple comparisons. Error bars show standard deviation. * $P < 0.05$, ** $P < 0.01$, *** $P < 0.001$.

Figure 5-5

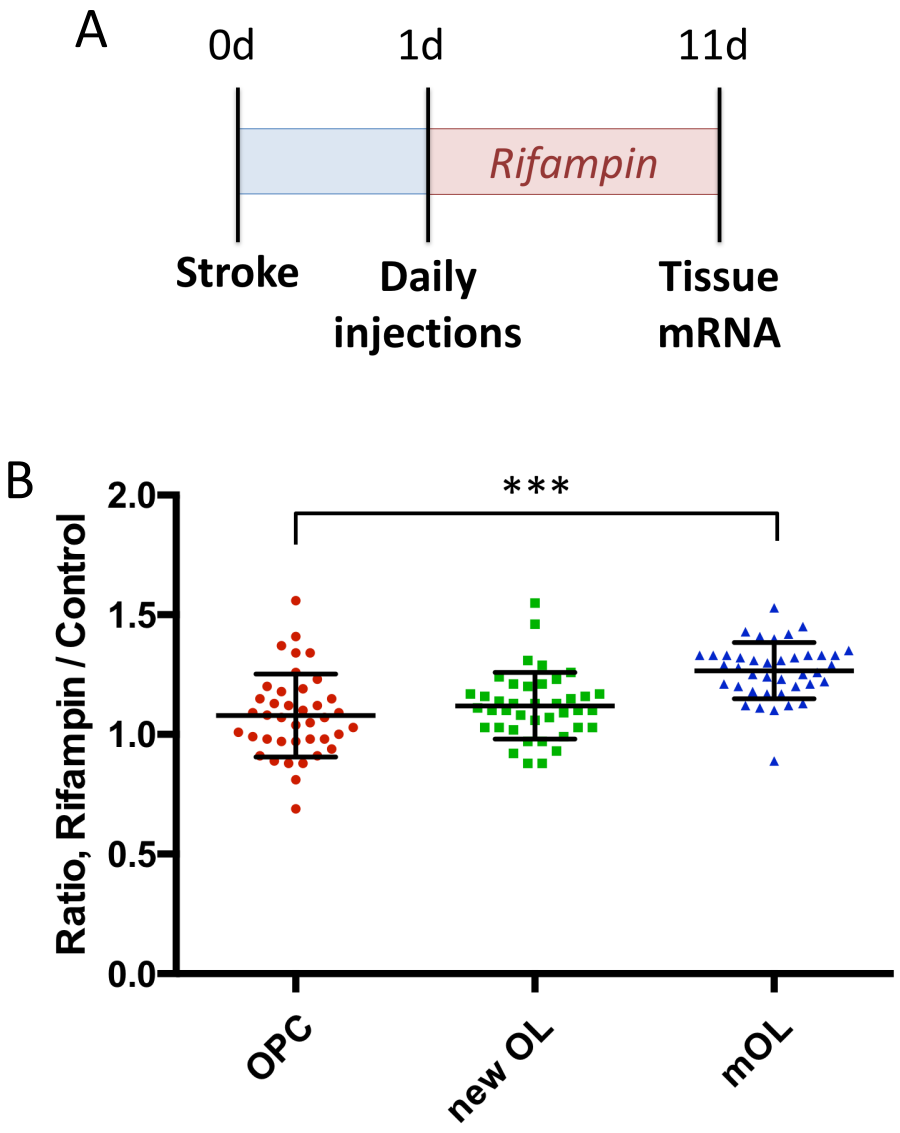

Figure 5-5. Study of rifampin's effect on OPC differentiation after WMS *in vivo*
(A) Outline of experiment. WMS was induced in animals at day 0, and daily injections of rifampin (50 mg/kg) were administered daily for 10 days following, beginning at 1 day post-WMS. At day 11, animals were sacrificed and mRNA was extracted from infarct and peri-infarct tissue and submitted for Nanostring analysis. **(B)** Analysis was performed on three groups of genes, as identified by the Zhang dataset: OPC-specific genes; newly differentiated oligodendrocytes (new OLs), and myelinating oligodendrocytes (mOLs). Fold change expression of each gene between vehicle and rifampin-treated animals are shown. Statistics were performed in Graphpad Prism using one-way ANOVA with the Dunnett correction for multiple comparisons. $n = 6$ per group. Mean ± SD. * $P < 0.05$, ** $P < 0.01$, *** $P < 0.001$.

Figure 5-6

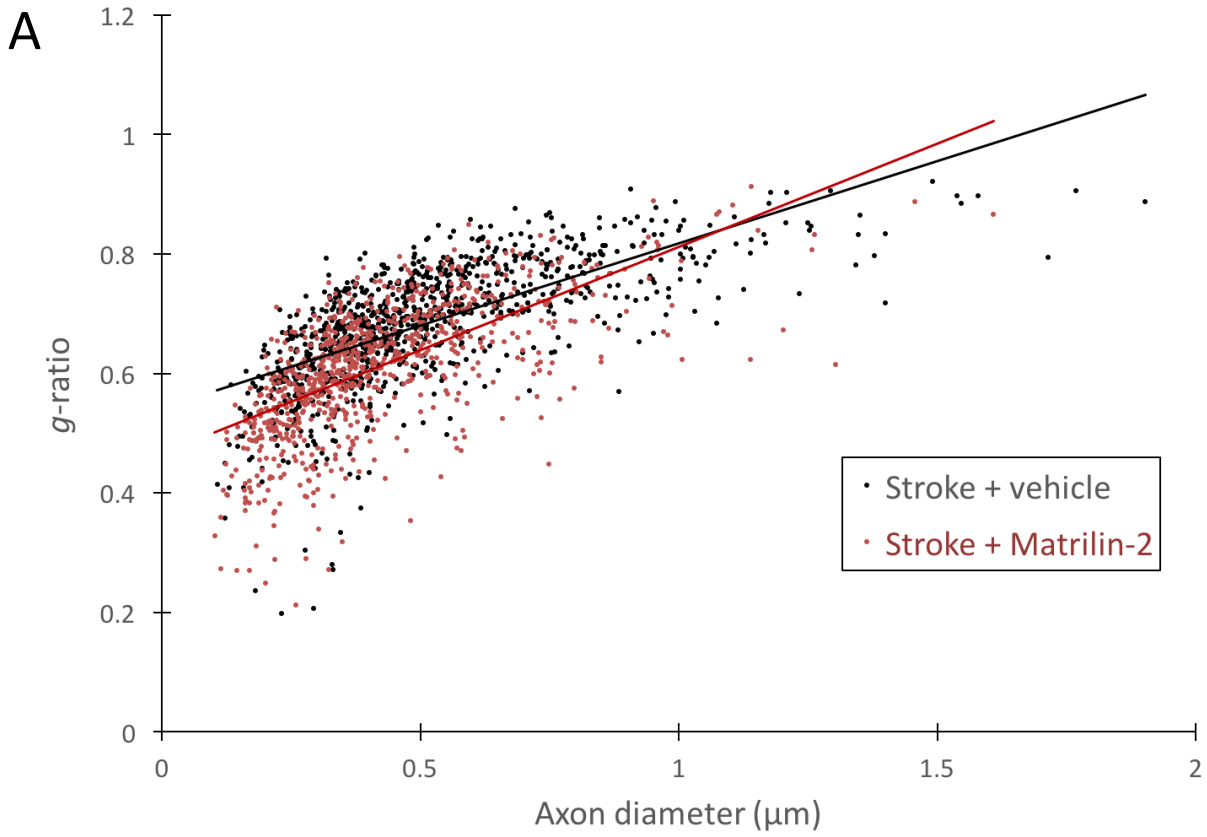
A
1.2
1
0.8
0.6
0.4
0.2
0
g-ratio
0
0.5
1
1.5
2
Axon diameter (µm)
Stroke + vehicle
Stroke + Matrilin-2

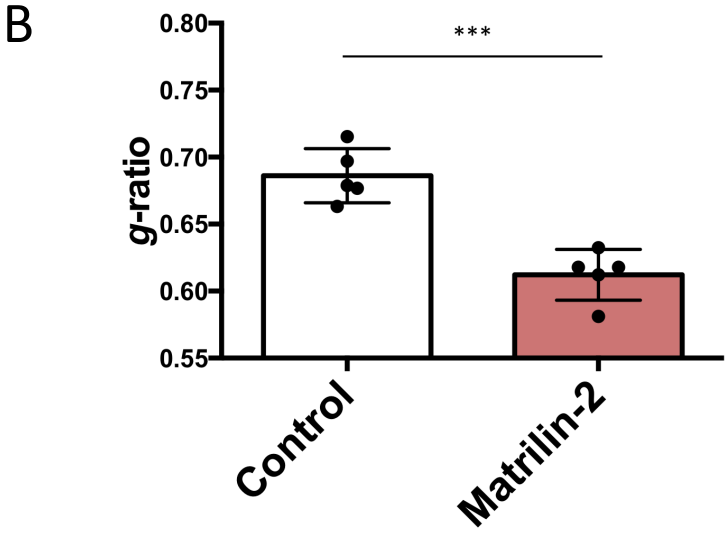
B
***
0.80
0.75
0.70
0.65
0.60
0.55
g-ratio
Control
Matrilin-2

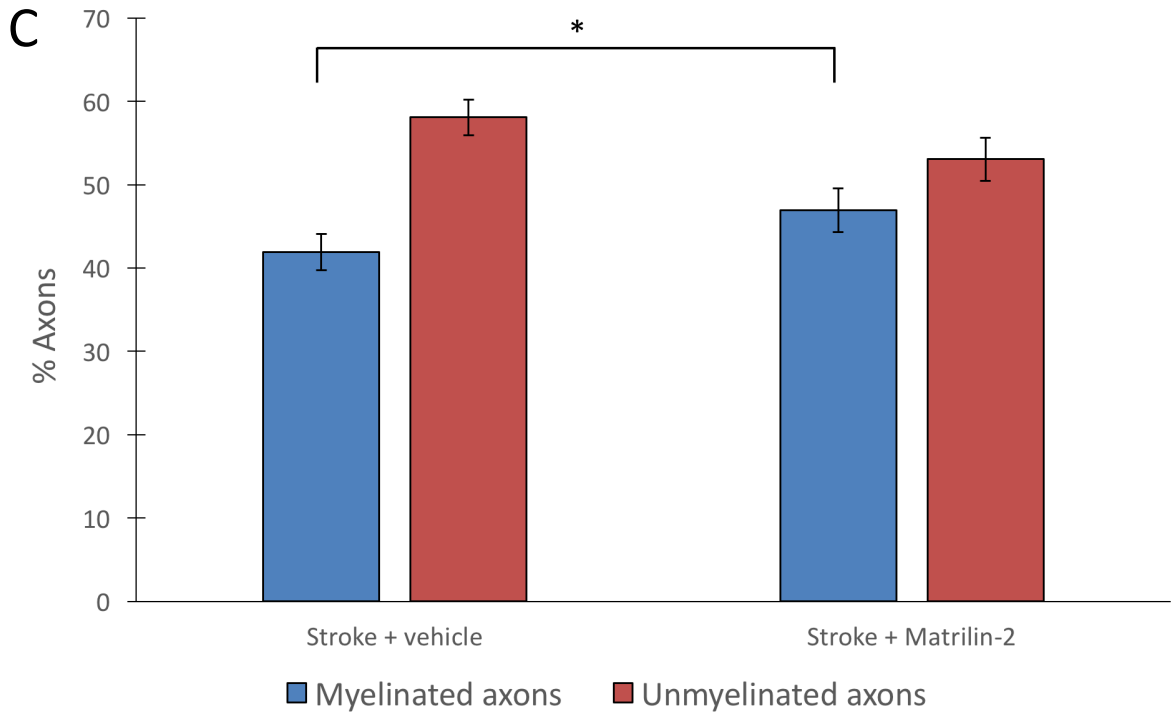

Figure 5-6. Electron microscopy analysis of matrilin-2 induced remyelination
(A) Aged animals were treated with matrilin-2 protein 6 days after WMS and g-ratios were analyzed 30 days later. A linear regression trendline is shown for vehicle (black) and matrilin-2 (red) treated animals. **(B)** Average *g*-ratios per animal are plotted and compared using student *t*-test, indicating significant decrease in *g*-ratio in matrilin-2 treated animals. **(C)** Analysis of proportion of myelinated vs. unmyelinated fibers shows that matrilin-2 treatment increases the proportion of axons that are myelinated. Statistics were performed in Graphpad Prism using unpaired two-way student *t*-tests (B and C). $n = 5$ animals per group. Mean ± SD. * $P < 0.05$, ** $P < 0.01$, *** $P < 0.001$.

Table 5-1

Genes included in each probe set in NanoString analysis

Gene Name	Set[1]	Accession #		Gene Name	Set[1]	Accession #
C1ql1	OPC	NM_011795.2		1810041L15Rik	PMO	NM_001163145.1
Cacng4	OPC	NM_019431.2		9630013A20Rik	PMO	NR_015539.1
Cdo1	OPC	NM_033037.3		Atrn	PMO	NM_009730.2
Chrna4	OPC	NM_015730.5		Bmp4	PMO	NM_007554.2
Col1a2	OPC	NM_007743.2		Cdc37l1	PMO	NM_025950.2
Cspg4	OPC	NM_139001.2		Cdv3	PMO	NM_175833.2
Dcaf12l1	OPC	NM_001190718.1		Chn2	PMO	NM_001163640.1
Dcn	OPC	NM_001190451.2		Cnksr3	PMO	NM_172546.2
Dll3	OPC	NM_007866.2		Cyfip2	PMO	NM_001252459.1
Emid1	OPC	NM_080595.2		Elovl6	PMO	NM_130450.2
Fam5c	OPC	NM_153539.3		Enpp6	PMO	NM_177304.3
Fam70b	OPC	NM_001143671.1		Fam3c	PMO	NM_138587.4
Gria3	OPC	NM_016886.3		Fam73a	PMO	NM_001162375.1
Grin3a	OPC	NM_001033351.1		Fmnl2	PMO	NM_172409.2
Kcnk1	OPC	NM_008430.2		Frmd4a	PMO	NM_001177843.1
Lhfpl3	OPC	NM_029990.1		Fyn	PMO	NM_008054.2
Lnx1	OPC	NM_010727.4		Glrb	PMO	NM_010298.5
Lppr1	OPC	NM_178756.4		Gp1bb	PMO	NM_010327.2
Lypd6	OPC	NM_177139.5		Itpr2	PMO	NM_010586.1
Megf11	OPC	NM_001134399.1		Kif19a	PMO	NM_001102615.1
Mmp15	OPC	NM_008609.3		Lims2	PMO	NM_144862.3
Myt1	OPC	NM_008665.4		Mical3	PMO	NM_001270475.1
Ncald	OPC	NM_134094.3		Mycl1	PMO	NM_008506.2
Nxph1	OPC	NM_008751.5		Nfasc	PMO	NM_001160316.1
Pcdh15	OPC	NM_001142741.1		Pik3r3	PMO	NM_181585.5
Pdgfra	OPC	NM_001083316.1		Ppp2r3a	PMO	NM_001161362.3
Pid1	OPC	NM_001003948.2		Rap2a	PMO	NM_029519.3
Pnlip	OPC	NM_026925.3		Rnf122	PMO	NM_175136.2
Ppapdc1a	OPC	NM_001080963.1		Rras2	PMO	NM_025846.2
Rasgrf1	OPC	NM_011245.2		Samd4b	PMO	NM_175021.3
Rlbp1	OPC	NM_001173483.1		Sema5a	PMO	NM_009154.2
Rprm	OPC	NM_023396.5		Slc12a2	PMO	NM_009194.3
Sapcd2	OPC	NM_001081085.1		Ssh3	PMO	NM_198113.2
Sdc3	OPC	NM_011520.3		Strn	PMO	NM_011500.2
Shc4	OPC	NM_199022.2		Tmem108	PMO	NM_178638.4
Slitrk1	OPC	NM_199065.2		Tmem163	PMO	NM_028135.2
Smoc1	OPC	NM_001146217.1		Tmem2_tv1	PMO	NM_031997.4
Sstr1	OPC	NM_009216.3		Tmem2_tv2	PMO	NM_001033759.2
Tmem179	OPC	NM_178915.3		Tns3	PMO	NM_001083587.1
Ugdh	OPC	NM_009466.2		Ust	PMO	NM_177387.3

Gene Name	Set[1]	Accession #		Gene Name	Set[1]	Accession #
Acy3	MO	NM_027857.3		actb	House	NM_007393.1
Adap1	MO	NM_172723.4		b2m	House	NM_009735.3
Adssl1	MO	NM_007421.2		gapdh	House	NM_001001303.1
Apod	MO	XM_003689301.1		pgk1	House	NM_008828.2
Arsg	MO	NM_028710.3		rpl19	House	NM_009078.1
Aspa	MO	NM_023113.5				
Carns1	MO	NM_134148.2				
Cdc42ep2	MO	NM_026772.2				
Cenpb	MO	NM_007682.2				
Cldn11	MO	NM_008770.3				
Cryab	MO	NM_009964.2				
Efhd1	MO	NM_028889.2				
Gjb1	MO	NM_008124.2				
Gsn	MO	NM_146120.3				
Hapln2	MO	NM_022031.2				
Hcn2	MO	NM_008226.2				
Inf2	MO	NM_198411.2				
Insc	MO	NM_173767.3				
Itgb4	MO	NM_001005608.2				
Kif5a	MO	NM_008447.4				
Mal	MO	NM_001171187.1				
Mog	MO	NM_010814.2				
Ndrg1	MO	NM_008681.2				
Nmra1	MO	NM_026393.1				
Nol3	MO	NM_030152.4				
Opalin	MO	NM_153520.1				
Pdlim2	MO	NM_145978.1				
Pla2g16	MO	NM_139269.2				
Plekhb1	MO	NM_001163184.1				
Ppp1r14a	MO	NM_026731.3				
Prr18	MO	NR_028280.1				
Rftn1	MO	NM_181397.2				
Slc45a3	MO	NM_145977.1				
Slco3a1	MO	NM_001038643.1				
Tbc1d9b	MO	NM_029745.2				
Tppp3	MO	NM_026481.3				
Trak2	MO	NM_172406.3				
Trf	MO	NM_133977.2				
Trp53inp2	MO	NM_178111.3				
mbp	MO	NM_010777.3				

[1] OPC, oligodendrocyte progenitor cell; PMO, premyelinating oligodendrocyte; MO, myelinating oligodendrocyte; House, housekeeping

5.6 References

Dai, J., Bercury, K. K., Ahrendsen, J. T., & Macklin, W. B. (2015). Olig1 Function Is Required for Oligodendrocyte Differentiation in the Mouse Brain. *Journal of Neuroscience*, *35*(10), 4386–4402. https://doi.org/10.1523/JNEUROSCI.4962-14.2015

Franklin, R. J. M., & ffrench-Constant, C. (2017). Regenerating CNS myelin — from mechanisms to experimental medicines. *Nature Reviews Neuroscience*, *18*(12), 753–769. https://doi.org/10.1038/nrn.2017.136

He, D., Wang, J., Lu, Y., Deng, Y., Zhao, C., Xu, L., … Lu, Q. R. (2016). lncRNA Functional Networks in Oligodendrocytes Reveal Stage-Specific Myelination Control by an lncOL1/Suz12 Complex in the CNS. *Neuron*, 1–17. https://doi.org/10.1016/j.neuron.2016.11.044

Kim, D. I., Jensen, S. C., Noble, K. A., KC, B., Roux, K. H., Motamedchaboki, K., & Roux, K. J. (2016). An improved smaller biotin ligase for BioID proximity labeling Dae. *Molecular Biology of the Cell*, *27*(8), 1188–1196. https://doi.org/10.1017/CBO9781107415324.004

Lambert, J. P., Tucholska, M., Go, C., Knight, J. D. R., & Gingras, A. C. (2015). Proximity biotinylation and affinity purification are complementary approaches for the interactome mapping of chromatin-associated protein complexes. *Journal of Proteomics*, *118*, 81–94. https://doi.org/10.1016/j.jprot.2014.09.011

Nishiyama, A., Komitova, M., Suzuki, R., & Zhu, X. (2009). Polydendrocytes (NG2 cells): multifunctional cells with lineage plasticity. *Nature Reviews Neuroscience*, *10*(1), 9–22. https://doi.org/10.1038/nrn2495

Pouton, C. W. (1998). Nuclear import of polypeptides, polynucleotides and supramolecular complexes. *Advanced Drug Delivery Reviews*, *34*(1), 51–64. https://doi.org/10.1016/S0169-

409X(98)00050-7

Roux, K. J., Kim, D. I., & Burke, B. (2013). BioID: A screen for protein-protein interactions. *Current Protocols in Protein Science*, (SUPPL.74), 1–14. https://doi.org/10.1002/0471140864.ps1923s74

Roux, K. J., Kim, D. I., Raida, M., & Burke, B. (2012). A promiscuous biotin ligase fusion protein identifies proximal and interacting proteins in mammalian cells. *Journal of Cell Biology*, *196*(6), 801–810. https://doi.org/10.1083/jcb.201112098

Sagave, J. F., Moser, M., Ehler, E., Weiskirchen, S., Stoll, D., Günther, K., … Weiskirchen, R. (2008). Targeted disruption of the mouse Csrp2 gene encoding the cysteine- and glycine-rich LIM domain protein CRP2 result in subtle alteration of cardiac ultrastructure. *BMC Developmental Biology*, *8*, 80. https://doi.org/10.1186/1471-213X-8-80

Schmidt, N. W., Jin, F., Lande, R., Curk, T., Xian, W., Lee, C., … Wong, G. C. L. (2015). Liquid-crystalline ordering of antimicrobial peptide–DNA complexes controls TLR9 activation. *Nature Materials*, *14*(June), 696–701. https://doi.org/10.1038/nmat4298

Simons, M., & Nave, K.-A. (2016). Oligodendrocytes: Myelination and axonal support. *Cold Spring Harbor Perspectives in Biology*, *8*(a020479), 1–16. https://doi.org/10.1101/cshperspect.a020479

Sozmen, E. G., Rosenzweig, S., Llorente, I. L., DiTullio, D. J., Machnicki, M., Vinters, H. V., … Carmichael, S. T. (2016). Nogo receptor blockade overcomes remyelination failure after white matter stroke and stimulates functional recovery in aged mice. *Proceedings of the National Academy of Sciences*, *113*(52), E8453–E8462. https://doi.org/10.1073/pnas.1615322113

UniProt. (2017). UniProtKB - P97314 (CSRP2_MOUSE). Retrieved November 19, 2017, from

http://www.uniprot.org/uniprot/P97314

Zhang, Y., Chen, K., Sloan, S. A., Bennett, M. L., Scholze, A. R., Keeffe, S. O., … Wu, X. J. Q. (2014). An RNA-Sequencing Transcriptome and Splicing Database of Glia, Neurons, and Vascular Cells of the Cerebral Cortex. *The Journal of Neuroscience : The Official Journal of the Society for Neuroscience*, *34*(36), 1–19. https://doi.org/10.1523/JNEUROSCI.1860-14.2014

Chapter 6

Integration of findings

This dissertation arose from the realization that white matter stroke affects millions of people each year, with devastating effect, and yet we have very little understanding of its pathology much less any idea of how to effectively treat it (Benjamin et al., 2017; Prins & Scheltens, 2015). Furthermore, much of the research focused on white matter pathology is founded on models of multiple sclerosis or other demyelinating diseases (Franklin & ffrench-Constant, 2017). Thus, white matter stroke was clearly a topic about which specific investigation was necessary, to identify unique pathologic features that made it unique, as well as any barriers preventing the development of practicable treatments.

This project began on the heels of our development of a transcriptomic dataset of OPCs, individually isolated from per-infarct tissue at experimentally-derived, pathologically-relevant post-injury time points. At that time, no major RNA-seq datasets of OPCs had been described, making this our first window into cell-specific tissue biology, with the added bonus that it provided insight into a major disease process as well. By all accounts, it represented the ideal opportunity for a dissertation project.

As the project has progressed, this project has lived up to those initial expectations, albiet in unexpected ways. While is many cases, transcriptome analysis is the culmination of a major research project, founded on a long-developed understanding of cell biology through tissue or cell culture studies, this analysis formed the foundation of the thesis work, and all subsequent

experiments were guided by initial analyses. In some cases, then, promising opportunities were sidestepped; or perhaps some paths were taken too readily.

The transcriptomic analyses described in Chapter 2, though presented as the first experimental step of the process, in fact were refined over the life of this dissertation. Although some candidate genes were selected early on, supplementation of the analysis with FPKM in 2014 added a further level of scrutiny to the analysis, prompting addition of a handful of new genes that stood up to increasingly stringent statistical standards. Rather than undermining the approach, however, this iteration deepened our understanding of the dataset by forcing us to become familiar with each facet of the analysis and its effect on the data. Lessons learned throughout these studies will now inform each similar dataset generated in the laboratory; and at a time many studies incorporate RNA-seq and its sibling approaches, this will no doubt prove useful.

Even after our candidate gene selection methodology came into final focus, a new resource became available that has undeniably shifted the field of glial biology: the cell-specific transcriptome data of Zhang et al. (2014). Their publication of complete gene lists for each major cell type, including three phases of oligodendrocyte lineage cells, has become a staple for discussion and evaluation of work presented in all major meetings within the field since. Certainly, it gave us a new tool to evaluate our own data, and to ask the questions more confidently: is our data OPC specific, or did the laser microscopy approach lead to significant off-target cell contamination? Is it stroke specific, or did our area of focus stray too far from the pathologically-relevant areas of damage?

The analyses presented in Chapter 2 are represent only just begin to answer these questions. In fact, as valuable as the Zhang dataset has been for the field—and it has been

instrumental by, at the least, establishing a baseline against which future similar approaches can be evaluated—it has key limitations. First, cells were isolated from P7 animals, and from whole- or near-whole brain tissue extracts. This ignores several recent studies that have established key region-specific differences in gene expression, even among cell types previously determined by consensus within the field to be well-defined (Chai et al., 2017; Marques et al., 2016). Second, the cells were processed through several platings and purification steps prior to analysis, and cells that spend even hours *ex vivo* are known to substantially alter gene expression patterns (Gosselin et al., 2017).

In other words, the heavily reliance on the analyses presented in Chapter 2 on the Zhang dataset to some extent overlook the ways in which this resource may not accurately reflect adult, white matter OPCs. To address this, we must consider additional methods of transcriptome analysis, such as making equivalent comparisons to classic markers of each glial cell type, and even tissue-mRNA driven qPCR confirmation of these results. Still, for the purposes of this study, the method used to selecting candidate genes did not rely on any external datasets, so no major alterations to experimental design were made based on these comparisons. Furthermore, the process of making these comparisons itself proved educational and may present a methodology that is useful more broadly as additional transcriptomic datasets become available, including multiple ongoing studies within our own laboratory. So, as an initial characterization, the studies in Chapter 2 were in many ways valuable.

One final decision had to be made prior to moving beyond the transcriptome and into cell culture studies of candidate genes: which of the three pairwise comparisons (5 day, 15 day, or 15 vs. 5 day) should be the focus of future study? We decided to focus on one set only, as this allowed us to both limit the scope of the project, as well as compare candidate genes more

directly moving forward. Although arguments could be made for any subset, the 15 vs. 5 day group was selected. This was the result of particular interest into the shifting biology of the OPC response. The proliferative response activated in the acute phase is intact at 5 days, but by 15 days, cell proliferation has stalled, while differentiation remains limited (Sozmen et al., 2016). Rather than compare 15 day post-WMS OPCs to their stroke-naïve counterparts, by comparing them to early-responding OPCs, we hypothesized that this would help us to focus specifically on genes involved in this behavioral switch. The transcriptomic characteristics support this hypothesis: while 1695 genes were differentially regulated between 15 day and control OPCs, only 389 genes were differentially regulated between 15 day and 5 day OPCs (**Fig. 2-3**). On the other hand, further analysis of other time points, in particular the 15 day vs. control set, should be considered in order to more fully assess OPC biology specific to stroke. The upcoming availability of additional transcriptomic data post-WMS within our laboratory may also provide additional metrics against which to assess our data and thus focus on a smaller set of interesting genes from this time point.

In any case, having selected candidate genes with our chosen metrics, cell culture studies were begun to analyze their biology within OPCs. This chapter chronicles a number of studies that did not ultimately prove usable as a screening tool as initially hoped. The first of these was the CG-4 cell line. Though this line has been successfully used elsewhere as a tool to study OPC biology, in our hands, they did not provide reproducible data across multiple analysis techniques (Ueno et al., 2012, and **Fig. 3-4 to Fig. 3-6**). Though the reason for this is not immediately clear, it is possible that genetic changes that accumulated in the clonally-derived cell line over time led to diminished OPC-like behavior.

Fortunately, primary OPC cultures were initiated through collaboration with Brad Zuchero in the Barres lab. These cultures, while more time-consuming to work with than CG-4 cells, were still remarkably straightforward to isolate, and qPCR analysis provided strong and reproducible evidence for a pro-differentiation effect of multiple candidate genes (**Fig. 3-9**). This ultimately provided a basis on which to identify genes for study *in vivo* in Chapter 4 (**Table 4-1**). Still, even with primary OPC cultures, some studies proved challenging. Knockdown studies of each candidate gene were initially planned to complement overexpression studies, with the idea that these would demonstrate whether candidate genes were necessary for OPC differentiation. The major problem encountered here was likely one of timing: OPCs in culture are easily maintained for about one week after plating, but given many of the candidate genes were unstudied, information on the protein half-life, and the time necessary to induce substantial knockdown, was not known. Thus, it was difficult to set up an experiment that sufficiently reduced candidate gene expression to a degree that provided the necessary power for qPCR analysis. Alternate approaches are still being explored, but one promising avenue is the use of siRNAs. Unlike microRNA plasmid constructs, these do not require harsh transfection protocols, and can exert an effect more rapidly upon treatment. Studies using siRNAs will be initiated to attempt to revisit the knockdown approach.

After identifying a rank order differentiation effect for each candidate gene (**Table 4-1**), three genes were chosen for *in vivo* study. As discussed in Chapter 4, however, we did not select the three genes ranked highest. In this case, two of the highly ranked genes, *Prg2* and *Ctsg*, had demonstrated roles in inflammation in eosinophils and neutrophils, respectively (Shamamian et al., 2001; Temkin et al., 2004). In contrast, the next two highly ranked candidate genes, which showed a similar degree of response in qPCR studies, were *C9orf9* and *Csrp2*, two novel genes

with few established functions in the literature (Bhattacharya et al., 2013; Sagave et al., 2008). Based on these observations, we chose to focus on the latter set of genes, in addition to *Chst10* as the top ranked gene based on qPCR studies. As with previous decision points within the study, this does not preclude *Ctsg* and *Prg2* from playing biologically interesting roles in OPC biology post-stroke. In fact, if at a later time, additional bioinformatics analyses or future transcriptomic datasets continue to identify these genes, the data presented in this dissertation provide strong evidence in support of their further study.

Chapter 4 extends our analysis of these three candidate genes into tissue studies using a mouse model of WMS. The studies outlined focus on two major phases of the OPC response to injury: first, the proliferative response, which is not significantly affected by overexpression of any of the three candidate genes as evidenced by EdU and BrdU labeling (**Fig. 4-5**). Next, OPC differentiation was assessed. The main goal of this experiment was to identify whether candidate genes promoted differentiation of OPCs, and so a method was developed to quantify cells at various stages along the oligodendrocyte lineage. Through this method, we identified *Csrp2* and *Chst10* as significantly promoting oligodendrocyte differentiation both after stroke, and in stroke-naïve animals (**Fig. 4-6**), further supporting the results seen in Chapter 3 after overexpression of candidate genes in culture.

However, two main questions remain in this arm of studies. The first is whether any OPCs overexpressing candidate genes are differentiating into other cell types, such as astrocytes, as previous studies have suggested that such alternate cell fates may be possible in early-stage OPCs (Sozmen et al., 2016; L. Zhang et al., 2016). In addition, assessing other glial cell types within the stroke area could identify off-target transduction, or changes in overall cellular response to stroke upon candidate gene overexpression. It should be noted that these studies are

ongoing, with GFAP and Iba1 used as markers of key glial cell types known to play a role in the WMS pathologic response (Rosenzweig & Carmichael, 2013; Sozmen et al., 2016).

Another question that arises from these *in vivo* studies is whether the observation that OPC differentiation is enhanced in stroke-naïve animals suggests that these pathways are not specific to WMS, but rather general pro-differentiation factors at play in OPC biology. Indeed, this cannot be ruled out from these studies alone. However, that these genes were identified as differentially regulated after stroke suggests that they do play some role in the post-stroke response; and even if they do impact differentiation when artificially overexpressed *in vivo* in non-stroke animals, this does not imply that this is a normal physiological function. Still, additional studies could also seek to answer this question, perhaps by studying OPC biology in development, or in other disease models such as multiple sclerosis, to understand whether these genes are involved in multiple processes beyond WMS.

A third goal of *in vivo* studies was to investigate whether gene overexpression led to remyelination, and here again, we encountered challenges. One approach was to measure node-paranode triads to quantify organization of intact nodes of Ranvier (**Fig. 4-9**). Initial quantifications, however, did not show significant increases in node density in candidate gene-overexpressed animals post-stroke. Expanding the analysis to a larger tissue area, or analyzing a larger proportion of tissue, will enable us to more completely analyze nodal organization within the peri-infarct area, including adding parameters such as the distance from infarct core at which nodes of Ranvier are found, which may provide more insight. The second approach to assessing remyelination was an electrophysiological approach, through compound action potentials (CAPs). These have been used to study remyelination in MS and in development (Crawford et al., 2009). However, though deficits were seen in stroke, the technique was so challenging as to

be beyond the scope of this dissertation. The technique certainly has potential, and we hope to revisit the technique as an additional set of experiments at a future date, perhaps in collaboration with experts in the area of slice electrophysiology.

Of note, the challenges faced in assessing remyelination outlined in Chapter 4 are to some extent addressed by another experiment described in the Chapter 5. As part of a study of an additional pro-differentiation candidate gene, *Matn2*, which is the subject of a different set of studies, electron microscopy was used to quantify myelination of axons after WMS in the peri-infarct area (**Fig 5-6**). The results suggested locally delivered matrilin-2 treatment enhances remyelination after WMS, and importantly, also establishes this as a workable technique in our hands. If other assays of remyelination after candidate gene overexpression do not demonstrate significance, electron microscopy studies should be strongly considered as a tissue-level measure that can be used to specifically focus on micron-scale peri-infarct tissue.

Building on the three major stages of investigations presented in Chapters 2 through 4, it is Chapter 5 that asks the question: "What next?" Though we have provided evidence that two novel genes, *Csrp2* and *Chst10*, promote oligodendrocyte differentiation in white matter OPCs, the applicability of this knowledge is limited without context. To approach this, we took a two-pronged approach. In the first, we used proximity biotinylation to interrogate the biochemistry of *Csrp2* binding within the nucleus. Mass spectrometry results are pending, but identification of protein interactors of *Csrp2*, if successful, could enable us to identify a pathway directly impacted by *Csrp2* overexpression. Whether this pathway is well-known within OPCs, or is itself novel, will help shape follow-up experiments, but either result would deepen our understanding of OPC biology both in normal and post-ischemic white matter.

The second, and perhaps most exciting, follow-up experiment further builds on the transcriptome dataset by identifying potential small molecule regulators of candidate genes. One in particular, rifampin, showed a significant impact on OPC differentiation both *in vitro* and *in vivo* (**Fig. 5-4** and **Fig. 5-5**). Of note, the use of Nanostring technology to assess differentiation based on gene expression in tissue is a first for the lab, and also demonstrates that this technique can be useful to assess OPC differentiation after WMS. Furthermore, the effect of rifampin, as an FDA-approved drug to treat tuberculosis, is promising and warrants follow-up tissue studies to assess differentiation at the cellular level, similar to the process followed in Chapter 4. Based on those results, additional behavioral testing may be of interest.

The studies outlined in the previous four chapters and discussed above brought new insights into oligodendrocyte biology after white matter stroke, but also many lessons learned. First, regarding the design and execution of a large-scale set of experiments based on a single biological question, this journey has highlighted the power of developing a toolset of techniques across several domains. The initial plan for this dissertation was to sequentially move from one set of studies to the next, each time moving deeper into the biology of oligodendrocytes in white matter and in stroke. Bioinformatic analysis of the transcriptome led to an *in vitro* screen, which led to more in depth studies *in vivo* (**Figure 6-1**). However, as the project developed and these techniques were established, the approach evolved. The studies in Chapter 5 begin to illustrate the power of move back and forth between techniques, and in particular, rifampin and other small molecules would not have been identified without the return to bioinformatics to more carefully analyze candidate genes and their predicted interactors. Certainly, this has highlighted the power of bioinformatics, both as a support for cellular biological studies, but also in its own

right, as a field that can carefully analyze disease- or even patient-specific data to uncover trends that may not be visible in more directed animal model-based studies.

In this dissertation, not only have we identified a new protein predicted to promote oligodendrocyte differentiation *in vitro* and *in vivo*, but we have gone beyond the original dataset and investigated new and even more fruitful avenues for additional studies based on these results. The studies contained herein thus make a strong argument not only for taking time and energy to fully investigate large gene expression datasets as seen here, but also of collaborating across disciplines, making use of new techniques and model systems to explore challenging questions from new angles. In this spirit of collaboration, these studies were undoubtedly made more powerful and fruitful from the generosity of scientists in the glial biology community who have worked diligently to broaden our understanding of these unknown but powerful cell types. As our understanding of the complex milieu of the brain deepens and our technical prowess continues to grow, redoubling our efforts to work together, collaborate, and communicate openly and collegially is sure to strengthen us all, and speed our path towards finding new and better treatments to address the ever-present burden of disease on society.

6.1 Figures

Figure 6-1

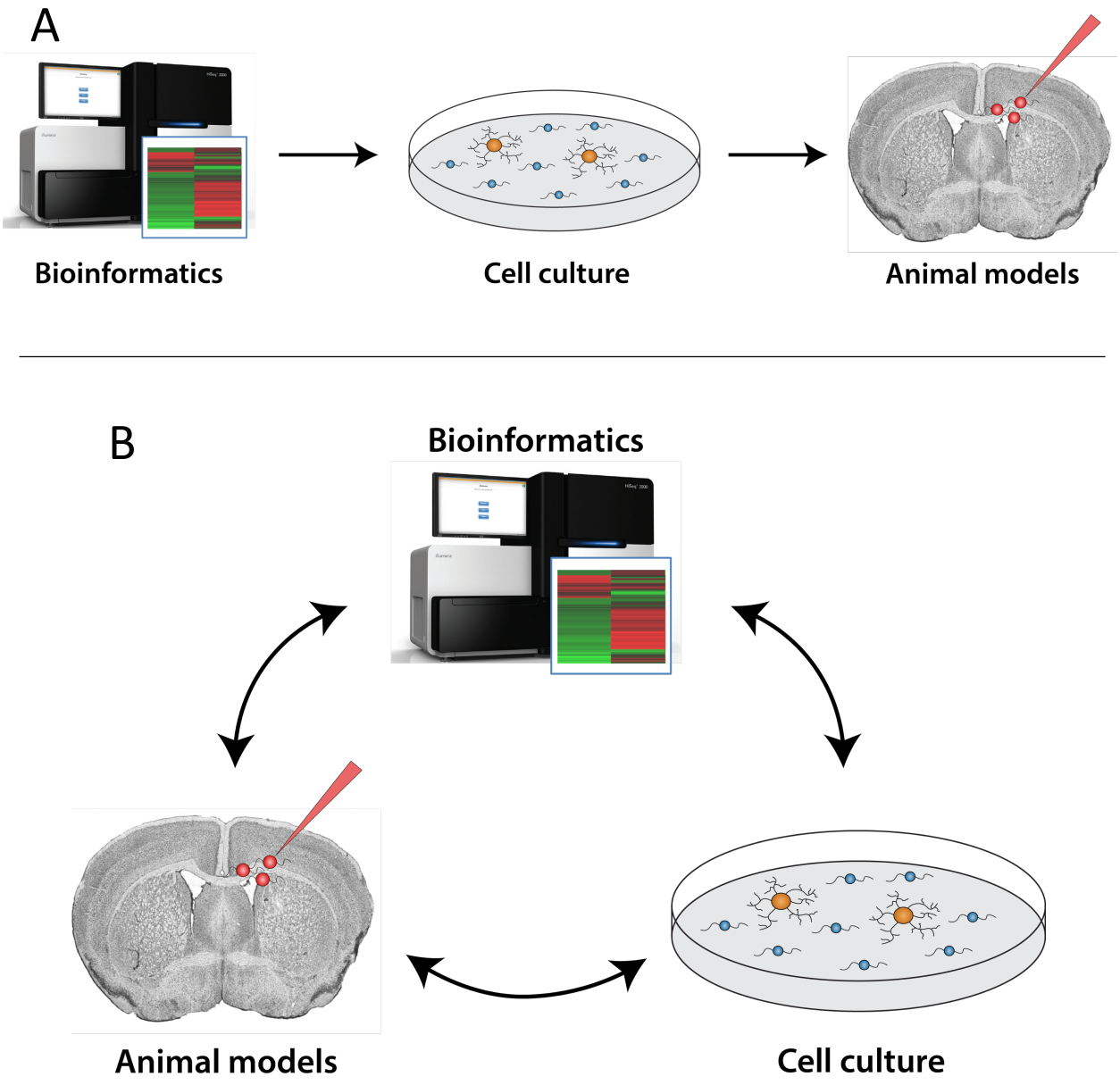

Figure 6-1. Reimagined model of studies spanning multiple platforms
(A) Initial experimental design focused on moving from bioinformatics analysis, to cell culture experiments, and finally to *in vivo* work in a mouse model. This linear approach moved sequentially to increasingly complex biological systems. **(B)** An alternate approach involves regular coordination of techniques across disciplines, a system adopted in the later stages of the study, which allowed for more rapid and informed design of new experiments.

6.2 References

Benjamin, E. J., Blaha, M. J., Chiuve, S. E., Cushman, M., Das, S. R., Deo, R., … Muntner, P. (2017). *Heart Disease and Stroke Statistics—2017 Update: A Report from the American Heart Association*. *Circulation* (Vol. 135). https://doi.org/10.1161/CIR.0000000000000485

Bhattacharya, R., Devi, M. S., Dhople, V. M., & Jesudasan, R. a. (2013). A mouse protein that localizes to acrosome and sperm tail is regulated by Y-chromosome. *BMC Cell Biology*, *14*, 50. https://doi.org/10.1186/1471-2121-14-50

Chai, H., Diaz-Castro, B., Shigetomi, E., Monte, E., Octeau, J. C., Yu, X., … Khakh, B. S. (2017). Neural Circuit-Specialized Astrocytes: Transcriptomic, Proteomic, Morphological, and Functional Evidence. *Neuron*, *95*(3), 531–549.e9. https://doi.org/10.1016/j.neuron.2017.06.029

Crawford, D. K., Mangiardi, M., & Tiwari-Woodruff, S. K. (2009). Assaying the functional effects of demyelination and remyelination: Revisiting field potential recordings. *Journal of Neuroscience Methods*, *182*(1), 25–33. https://doi.org/10.1016/j.jneumeth.2009.05.013

Franklin, R. J. M., & ffrench-Constant, C. (2017). Regenerating CNS myelin — from mechanisms to experimental medicines. *Nature Reviews Neuroscience*, *18*(12), 753–769. https://doi.org/10.1038/nrn.2017.136

Gosselin, D., Skola, D., Coufal, N. G., Holtman, I. R., Schlachetzki, J. C. M., Sajti, E., … Glass, C. K. (2017). An environment-dependent transcriptional network specifies human microglia identity. *Science*, *356*(eaal3222). https://doi.org/10.1126/science.aal3222

Marques, S., Zeisel, A., Codeluppi, S., Bruggen, D. Van, Falcão, A. M., Xiao, L., … Castelo-branco, G. (2016). Oligodendrocyte heterogeneity in the mouse juvenile and adult central

nervous system. *Science*, *352*(6291), 1326–9.

Prins, N. D., & Scheltens, P. (2015). White matter hyperintensities, cognitive impairment and dementia: an update. *Nature Reviews Neurology*, *11*(3), 157–165. https://doi.org/10.1038/nrneurol.2015.10

Rosenzweig, S., & Carmichael, S. T. (2013). Age-dependent exacerbation of white matter stroke outcomes: a role for oxidative damage and inflammatory mediators. *Stroke; a Journal of Cerebral Circulation*, *44*(9), 2579–86. https://doi.org/10.1161/STROKEAHA.113.001796

Sagave, J. F., Moser, M., Ehler, E., Weiskirchen, S., Stoll, D., Günther, K., … Weiskirchen, R. (2008). Targeted disruption of the mouse Csrp2 gene encoding the cysteine- and glycine-rich LIM domain protein CRP2 result in subtle alteration of cardiac ultrastructure. *BMC Developmental Biology*, *8*, 80. https://doi.org/10.1186/1471-213X-8-80

Shamamian, P., Schwartz, J. D., Pocock, B. J. Z., Monea, S., Whiting, D., Marcus, S. G., & Mignatti, P. (2001). Activation of progelatinase A (MMP-2) by neutrophil elastase, cathepsin G, and proteinase-3: A role for inflammatory cells in tumor invasion and angiogenesis. *Journal of Cellular Physiology*, *189*(2), 197–206. https://doi.org/10.1002/jcp.10014

Sozmen, E. G., Rosenzweig, S., Llorente, I. L., DiTullio, D. J., Machnicki, M., Vinters, H. V., … Carmichael, S. T. (2016). Nogo receptor blockade overcomes remyelination failure after white matter stroke and stimulates functional recovery in aged mice. *Proceedings of the National Academy of Sciences*, *113*(52), E8453–E8462. https://doi.org/10.1073/pnas.1615322113

Temkin, V., Aingorn, H., Puxeddu, I., Goldshmidt, O., Zcharia, E., Gleich, G. J., … Levi-Schaffer, F. (2004). Eosinophil major basic protein: First identified natural heparanase-

inhibiting protein. *Journal of Allergy and Clinical Immunology*, *113*(4), 703–709. https://doi.org/10.1016/j.jaci.2003.11.038

Ueno, T., Ito, J., Hoshikawa, S., Ohori, Y., Fujiwara, S., Yamamoto, S., … Ogata, T. (2012). The identification of transcriptional targets of Ascl1 in oligodendrocyte development. *Glia*, *60*(10), 1495–505. https://doi.org/10.1002/glia.22369

Zhang, L., He, X., Liu, L., Jiang, M., Zhao, C., Wang, H., … Lu, Q. R. (2016). Hdac3 interaction with p300 histone acetyltransferase regulates the oligodendrocyte and astrocyte lineage fate switch. *Developmental Cell*, *36*, 316–330. https://doi.org/10.1016/j.devcel.2016.06.004

Zhang, Y., Chen, K., Sloan, S. A., Bennett, M. L., Scholze, A. R., Keeffe, S. O., … Wu, X. J. Q. (2014). An RNA-Sequencing Transcriptome and Splicing Database of Glia, Neurons, and Vascular Cells of the Cerebral Cortex. *The Journal of Neuroscience : The Official Journal of the Society for Neuroscience*, *34*(36), 1–19. https://doi.org/10.1523/JNEUROSCI.1860-14.2014